Determination of Selenium in Selenium enriched yeast.

Kenneth Michael Kennedy B.Sc (Hons).

Submitted for the award of Masters of Science.

Galway-Mayo Institute of Technology

Supervisor: Dr. Joseph Scanlan

Submitted to the National Council of Educational Awards July 1999.

Acknowledgements:

In the completion of the enclosed thesis I would like to take time to thank a few people. Firstly to Dr. Joseph Scanlan who initially set up this project. He gave all his technical and academic support at any time. With out his help and expertise, this project would never have been finished. Thanks to the Department of Physical Sciences Galway-Mayo Institute of Technology (Dr Brian Place Head of School and Dr. Tom Gillen Head of Department.) To the Technical Support Staff who never minded if I borrowed a piece of equipment for an extended period of time. To the secretaries of the department who helped with all enquires mundane or otherwise that I threw at them, they were always willing to help. My thanks to the Administration Staff of the G.M.I.T especially to Phil Lydon who ploughed through red tape to make my life easier. To Tom Conlon in the Industrial Liaison Office for all his work. To Ann Joyce and the gang up in the Library who helped so many times in getting literature and waived a fine or two for over-due books. To all the Academic staff in the Life Sciences and Computers especially to Dr. Myles Keogh who was a great man for a chat and who was always on call to have his brain picked. To my fellow insomniacs and coffee pals Steven, Marrion, Steve and Iridia "ye kept me sane - God bless ye!" To Dr. Ronan Power of Altech for the samples which the thesis was based upon. To Dr. Michael J. Hynes of N.U.I.G. To Forbairt for financial support under the Graduate Training Programme. Thanks to my parents Owen and Teresa, it was your constant encouragement and support that helped me get this far. I will never be able to repay the debt. And finally to Ursula Owens who proof read the thesis, who corrected all my grammar mistakes and made me look good before it went to Joe for the final proof read. You have been a Godsend. Always and ever – and then some.

Chapter 1

1.1 Distribution of Selenium in nature.

Selenium, although a rare mineral, is widely distributed in minute amounts in virtually all materials of the earth's crust, its average abundance is approximately ~0.09ppm. Selenium is rarely found in its native state i.e. in elemental form, instead it is usually found as an oxide as selenite and selenate or in sulphur or porphyry copper deposits. The greatest abundance of selenium is found in igneous rocks, in hydrothermal deposits, and in the massive sulphide and porphyry copper deposits that are mentioned above. Known deposits of selenium are insufficient to permit their mining for the element alone and consequently it would be far too expensive to mine for its own commercial benefit. Virtually all production of selenium is via its extraction from copper refinery slimes along with the recovery of precious metals. (National Research Council, 1976b) Selenium is obtained commercially by treatment of anode slimes produced during the electrolytic refining of copper. The principal sources of selenium are the sulphidic copper ores in Canada, the United States and in Russia as a result the majority of literature dealing with selenium is from these non-European countries. This is not to say that there is no selenium outside these countries, some of the soils of Ireland contain reasonable amounts of selenium.

High concentrations of selenium are found in sedimentary rocks such as shale, sandstone, limestone and phosphorite rocks. The average concentration in shales has ranged from 0.24ppm for Palaeozoic shales of Japan to 277ppm for black shales of Permian age from Wyoming (Lakin and Davidson, 1967). Shales are also the principal sources of selenium–toxic soils in Ireland, Australia and several other

countries of the world (Johnson 1975). In Ireland these shales can be found around Sligo, Carrick-on-Shannon, and Enniskillen. The soil type is gleys which is Shale-Old Red Sandstone Till and due to the Ice Age, the soils have been sculpted into drumlins by the glaciers: see *Appendix.1.1* (Supplied by the Geological Survey of Ireland)

In general, the selenium content of limestone derived soils is generally low as found by Lakin and Davidson in 1967. Here in Ireland these limestone derived soils can be found around Limerick, south west of Kilkenny, south of Wexford and a large area west of Roscommon. The parent material is limestone-sandstone –shale till. The soil type is gleys dominantly influenced by surface water impendence see *Appendix 1.1* (Geological Survey of Ireland). Phosphate rocks contain, relatively high concentrations of selenium; this could lead to an increase in the Se in soils because of the wide use of phosphate fertilisers made from these deposits. Seleniferous sulphur is a source of selenium in phosphate fertilisers and sulphur containing inorganic salts included in livestock diets. The selenium content of Japanese and Hawaiian volcanic sulphur ranged from 67 to 206ppm and 1,026 to 2,000ppm respectively (Lakin and Davidson, 1967), Ireland is not an island created from volcanic activity, so no comparative study can be done with respect to these islands. Although selenium has also been found to occur in fossil fuels, Irish fossil fuels are relatively low in selenium content. Exact concentrations have not been calculated, as the economic importance of selenium in fossil fuels is negligible.

Uses of selenium in history

In the early Stone Age and through to the Pre-Iron Age selenium, in the form of sodium selenite crystals (Na_2SeO_3), was used by the inhabitants of Montana, Oregon and Wyoming (North America) as powerful talismans and in religious ceremonies.

This is evidenced from caves recently discovered (1980's) in these states. The caves are over twelve miles in length and entirely devoid of light. Many questions arise from this, why did people dig out the selenium as selenite crystals? And how did they travel such great lengths in total darkness? Answers to these questions have been given by archaeologists. Shaman or religious leaders used the element in ancient ceremonies because in appearance they are very much like quartz crystals, they refract the light within its many prisms producing beautiful colours within the crystal. These people dug the crystals out with primitive tools such as bone picks. Archaeologists have figured out how these ancient people travelled the great distances in pitch-blackness. Using cane-reed, which were in ample abundance around the cave area, the reeds were gathered into bundles to form rough lamps, which archaeologists used when trying to recreate the method of illumination used by these people. The cane lamps were lit at the entrance to the cave, then a group of archaeologists travelled for over three days in these caves, using the cane lamps as the only source of light. They found charcoal marks on the low roofs of the caves where the cane was scratched to mark the path or to scratch off the spent cane to keep the lamp rejuvenated.

Present day uses for selenium

Today selenium and its compounds have a multitude of uses such as, in the manufacturing of glass to make ruby coloured glass and enamels or to decolourise glass, in xerography as a photographic toner and as a pigment when mixed with a cadmium compound. It is used as conductors, rectifiers, electron emitters, and insulators, as reagents in remedies for eczema and fungus infections in pets, in antidandruff agents for humans, and in veterinary therapeutic agents. In agriculture, early uses for selenium compounds involved control of mites and insects. Nowadays sodium selenite and sodium selenate are presently used in agriculture as injectables

and feed additives to control selenium related deficiency disorders such as Keshans disease etc., these will be discussed later in **Section 1.3**.

In the following sections the role of selenium will be discussed in:

1. Selenium cycle
2. Bioavailability of selenium
3. Selenium in soils
4. Selenium in plants
5. Selenium in animal feedstuffs
6. Selenium in water
7. Selenium in human foods
8. Dairy products and eggs

1.1.1 Selenium Cycle

Although quantitative information on the selenium cycle in nature is sketchy, it is possible to make generalisations on the cycle. Selenium initially is brought to the surface from the earth's core by igneous extrusions and volcanic gases. Soils are produced be the weathering of these rocks and as a result selenium enters into the soil initially by this pathway. More and more however, man is playing a role in the cycle as the selenium found in commercial fertilisers and industrial airborne waste also enters the soil. Geological processes such as wind erosion, glaciation, water erosion and leaching all effect the selenium content. Selenium in sedimentary soil is unavailable for the uptake by plants, but due to the pH of the soil, chemical weathering and bacterial oxidation the selenium is altered into a form that is available to plants and thus enters the animal food chain. The atmosphere is supplied with

Selenium via soil dust, volcanoes, burning of fossil fuels, industrial emissions and volatile products produced by plants and animals (Selenium in Nutrition (1983)).

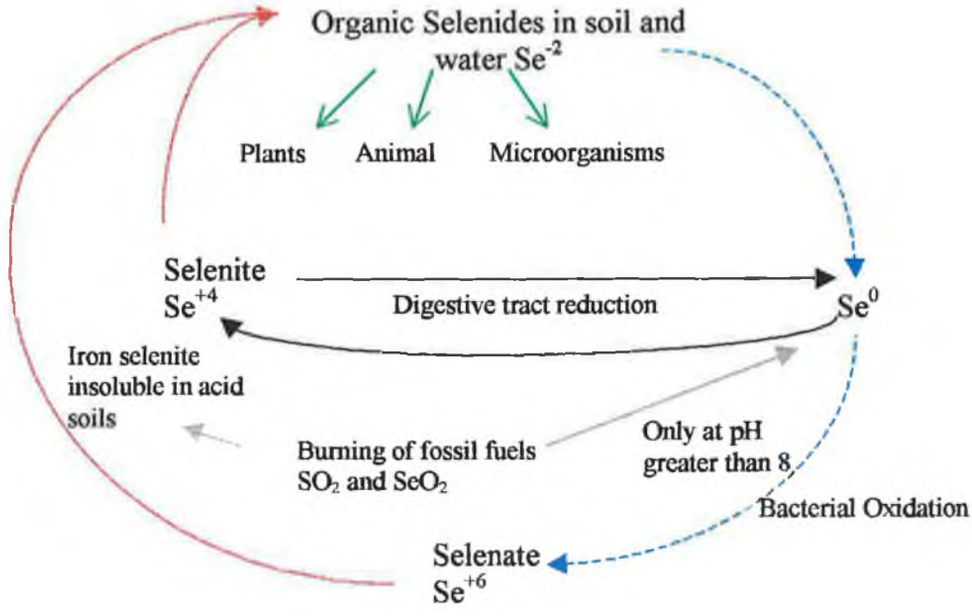

Fig 1.1

Taken from Selenium in Nutrition (1983) and Frost (1973)

1.1.2 Bioavailability

"Bioavailability" is the term coined that refers to the availability of any element to the body for absorption. There have been several published studies illustrating differences in the biological availability of selenium occurring in various feedstuffs. Miller et al., (1972) reported a study in which selenium retention by chicks was compared when the element was derived from four different media: fishmeal, fish solubles, selenite, or selenomethionine. Se from selenomethionine was retained better than that from selenite, and compared to selenomethionine, the fishery products were only about 31% as effective. A bioavailability trial conducted on Finnish men of selenium deficient diets, who were supplemented with different forms of selenium, indicated that a comprehensive assessment of selenium bioavailability requires the determination of several parameters. These include a short term platelet glutathione

peroxidase activity measurement to determine immediate availability, a medium term plasma selenium measurement to estimate retention, and a long term platelet glutathione peroxidase measurement after discontinuation of supplements to determine the convertibility of tissue selenium stores to biological active selenium (Levander, 1983)

1.1.3 Selenium in soils

The overall relationships among the concentrations of selenium in rocks, soils, and plants have been summarised as follows (NRC, 1971)

- When rocks with a **high selenium content** weather and decompose and form well drained soils in *subhumid areas* (less than 8cm of annual rainfall), the selenides and other insoluble forms of selenium will be converted to selenates and organic selenium compounds. These compounds will be available to plants, and vegetables containing potentially toxic levels of selenium, could be produced on these soils.
- When rocks with a **high selenium content** weather and decompose and form soils in *humid areas*, slightly soluble complexes of ferric oxide or hydroxide and selenite ions will be formed. These soils will range from slightly acidic to strongly acidic, and the plants produced on them will not contain toxic concentrations of selenium. However, they may contain sufficient selenium to protect livestock consuming them from selenium deficiency.
- When rocks with a **high selenium content** weather and decompose and form *poorly drained soils* or where selenium from higher lying areas is deposited in poorly drained areas by alluvial action, and the soils are alkaline, plants containing toxic levels of selenium are likely to be produced. This will be most likely to happen if the aeration of these soils is improved by artificial drainage. The more

acid the soils in an area, the less the likelihood of vegetation containing toxic levels of selenium.

- When rocks which have **low selenium content** weather and decompose to form soils under either *humid* or *dry conditions*, the plants are likely to contain insufficient selenium to protect animals from selenium deficiency. The more humid the area and the more acid the soil, the greater the likelihood of extremely low selenium concentrations in the plants. (Selenium in Nutrition Revised Ed, 1983).

This range of relationships between selenium concentrations and soil type is more clearly illustrated in diagram **Fig 1.2**.

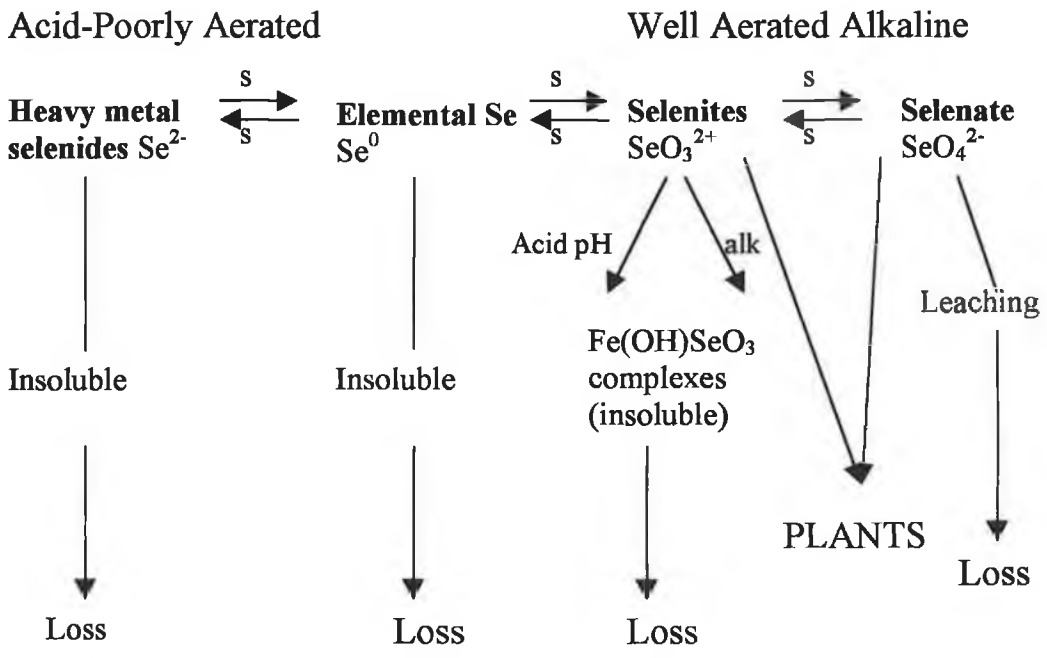

s: slow reaction
Loss: Process leading to loss of "Biologically active" Se

Fig 1.2

Taken from Selenium in Nutrition Revised Ed, 1983 (Allaway 1973)

Soil management practices

While selenium deficiency can result directly from a specific combination of rock type, soil type, drainage and weather conditions, there are in addition a number of aggravating factors e.g. the addition of gypsum to soils. According to studies carried out by Muth (1955) and Schubert et al.,(1961) the application of gypsum to soils causes the exaggerated deficiency of selenium from the soil. Conversely, the concentration of selenium in some seleniferous soils has been markedly reduced, both by leaching during the soil development process (Moxon et al., 1939) and by irrigation water (Larkin, 1961). This is of relevance to farmers who are interested in future crops and deficiency levels. Rivers are transporting selenium from their upper watersheds. It appears, however, that selenium is being removed from the surface layers of the seleniferous areas and not from the lower profiles where deep rooted plants can still accumulate toxic amounts of selenium (Johnson 1975). Good soil management practices therefore impact greatly on selenium deficiency and selenium content.

1.1.4 Selenium in plants

Plants can be divided into three groups on the basis of their ability to accumulate selenium when grown on high-selenium soils (Rosenfeld and Beath 1964). The first two groups are referred to as selenium accumulator or indicator plants. These grow well on soil containing high levels of selenium and thereby assist in the location of seleniferous areas.

Group 1. This includes *Astragalus*, *Machaerathera*, *Crucifera*, *Happlopappus*, and *Stanleya*. These are called primary indicators. Normally they accumulate selenium at very high levels, often several thousand parts per million.

Group 2. Secondary selenium absorbers include *Aster*, *Atriplex*, *Castelleja*, *Grindelia*, *Gutierrezia* and *Mentzelia*. Their selenium levels can be as high as 200ppm.

Group 3. This includes grains, grasses and many weeds, plants which do not normally accumulate selenium in excess of 50ppm when grown on seleniferous soil.

The *Crucifera* genus in Group 1 contains the subgroup of mustard, cabbage, broccoli and cauliflower. However, in general many of the plants in the Groups 1 and 2 probably add very little to the selenium content of feeds because they normally grow in dry non-agricultural areas. Any types of crop grown on neutral or acid soils absorb very little selenium (Ehlig et al., 1968). This demonstrates that there is more than one factor alone that contributes to the overall concentration of selenium in crops.

Shrift (1973) studied the metabolism of plants and stated that selenium metabolites identified in plants are analogues of sulphur compounds. Although they found the sulphur analogues the process by which these analogues are derived is still relatively unknown, as they do not follow the same pathways already know for the sulphur mechanisms.

1.1.5 Selenium in animal feedstuffs

As can be expected, the amount of selenium that is in animal feed stuffs is dependant on a wide variety of factors such as soil type, vegetation, agriculture practised in the area etc. In the seleniferous areas, accumulator plants frequently contain selenium at levels that are toxic to farm animals. However, the impact of these plants on the livestock industry in the seleniferous areas is small because of the widespread adoption of practical techniques for controlling the problem. The animals tend to eat these plants only in extreme conditions e.g. severe weather conditions that result in

the lack of growth of vegetation other than the hardier growing selenium accumulator plants. The concentration of selenium in feed ingredients varies widely depending on the area in which the feedstuff was produced.

1.1.6 Selenium in Water

The U.S. Department of Health, Education and Welfare (1962) has set the upper limit for selenium in drinking water to be 10μg/liter (10ppb). In drinking water, springs and wells this rarely reached but there have a few known documented cases that have had 5,800 ppb and above. Rivers average at 1 ppb and oceans 0.09 ppb.

1.1.7 Selenium in Human Foods

The amount of selenium in a "plant derived" food varies largely depending on its protein content because most of the selenium that enters the human body is as amino acids that are selenium analogues of the sulphur compounds, as in selenomethionine or selenocystine. These are selenium analogues of the sulphur based compounds. The selenium content is also based on the area of the country in which it is grown. The concentration of selenium in the milk, eggs, and meat of animals is influenced by the level of selenium in the plant material they consume (Allaway 1978). In N. American diets cereals are the dominant food of plant origin for supplying selenium, with much of the cereal consumption in the form of bread. Bread appears to be a relatively good source of selenium ranging from 0.28 to 0.68ppm in various reports, with whole-wheat dread containing more than white bread (Levander 1976a).

Meat and fish also are good sources of selenium for humans. It is apparent from the results of many studies that levels in animal tissue tend to be reflections of the concentrations of available "natural" selenium in the diets (Hoffman et al., 1973;

Jenkins et al., 1974). Kidneys were found by Morris and Levander (1970) to contain the highest concentration of selenium (1.4 to 3ppm) in animal tissues, followed by the liver (0.2 to 0.85ppm). Fish and other seafood are good sources of selenium. While trout was reported to contain 0.36ppm and shrimp to contain 2ppm (Arthur 1972). Other workers in this field (Morris and Levander 1970) found an average value of 0.63ppm in cod and flounder fillets and 0.63ppm for various shellfish.

Most fruits and vegetables provide little selenium. Fruit and vegetables are recognised as poor dietary sources of selenium (Levander, 1976a) Many have less than 0.01ppm (Morris and Levander 1970; Arthur 1972; Ganapathy et al., 1977).

There are large differences in selenium levels reported for the same food item among different investigators. One of the main factors contributing to these differences is undoubtedly the use of a small number of samples from a few localised areas. Problems in analytical precision sometimes appear, particularly at low selenium levels below 0.01 ppm (Schroeder et al., 1970).

1.1.8 Dairy Products and Eggs

Levels of selenium in milk reflect the level of naturally occurring selenium in the diet. Values obtained in other countries for cows' milk. Germany 0.09ppm (dry basis, Kiermeier and Wigand 1969) Denmark 0.2ppm (dry basis, Bisbjerg et al., 1970) Japan 0.030ppm (Sakurai and Tsuchiya, 1975) Canada 0.015ppm (Arthur, 1972) Great Britain 0.010ppm (Thorn et al., 1978) New Zealand 0.006ppm (Millar and Sheppard, 1972)

There are no documented details for any selenium in dairy produce in Ireland.

1.2 Chemistry of Selenium

The chemistry of selenium is similar to that of sulphur. Selenium is recovered by roasting the muds with soda or sulphuric acid, or by smelting them with soda and nitre. Selenium exists in several allotropic forms. Three are generally recognised but as many as six have been claimed. Selenium can be prepared with either an amorphous or crystalline structure. The colour of amorphous selenium is red in powder form or black in vitreous form. Crystalline monoclinic selenium is deep red; crystalline hexagonal selenium the most stable is a metallic grey. A member of the sulphur family, it resembles sulphur both in its various forms and in its compounds. Selenium exhibits both *photovoltaic action*, a term to describe a process by which light is converted directly into electricity, and *photoconductive action*, a different process where the electrical resistance decreases with increased illumination. These properties make selenium useful in the production of photocells and exposure meters for photographic use, as well as solar cells. Selenium is also able to convert alternating current (a.c.) electricity to direct current (d.c.) and is extensively used in rectifiers. Below its melting point selenium is a p-type semiconductor and is finding many uses in electronic and solid-state applications. Selenium is also used as an additive to stainless steel. (Bock 1974)

Chemical Behaviour

Selenium has a complex redox chemistry. Natural selenium contains six stable isotopes. The oxidation of selenium to selenite (4^+) or selenate (6^+) ions does take place, although these reactions require more strongly oxidising conditions than the formation of sulphate. (Greenwood and Earnshaw. 1997)

While sulphur is a true insulator, (specific resistivity in $\mu\Omega$ cm^{-1} = $2x10^{23}$) selenium ($2x10^{11}$) and tellurium ($2x10^{5}$) are intermediate in their electrical conductivities, and the temperature coefficient of resistivity in all three cases in negative, which is usually considered characteristics of non metals.

Selenium reacts when heated with halogens, most metals, and non-metals. It is not affected by non-oxidising acids and reacts with many organic molecules e.g. saturated hydrocarbons are dehydrogenated.

Cationic compounds: Selenium will dissolve in olleums to give a green solution, which is unstable and changes colour when left undisturbed over a period of time or heated.

Selenium halides.

Selenium forms SeF_4,SeF_6, Se_2Cl_2, $SeCl_4$ (which dissociates in the vapour), Se_2Br_2 and $SeBr_2$ (both dissociate in the vapour) and $SeBr_4$.

Selenium fluorides SeF_4

$$EO_2 + 2SF_4 \rightarrow EF_4 + 2SOF_2 \qquad \textbf{Eqn 1.1}$$

The compound SeF_4 Selenium tetrafluoride (mp~ -39^0C, bp = 106^0C) resembles SF_4, but being a liquid and somewhat easier to handle, it has some advantages as a fluorinating agent. Selenium hexafluoride SeF_6 is a colourless gas somewhat more reactive than SF_6. SeF_6 though unreactive toward water is very toxic.

For selenium, these halides are mostly of marginal stability and the characterisation is incomplete; the most stable ones are $SeCl_2$ and Se_2Br_2 whose structure is known. The

two halides are known only in the vapour phase; attempts to isolate them as solids result only in disproportionations to yield Se, Se_2X_2 and SeX_4. The SeX_4 molecules themselves tend to decompose under most conditions, for example, $SeBr_2$, Br_2 and Se_2Br_2. In acetonitrile these are the following equilibria.

$$2SeBr_2 = Se_2Br_2 + Br_2 \quad K = 1x10^{-2} \qquad \textbf{Eqn 1.2.}$$

$$3SeCl_2 = Se_2Cl_2 + SeCl_4 \quad K = <2x10^{2} \qquad \textbf{Eqn 1.3.}$$

Oxides of Selenium.

These are forms of selenium which occur when the element is burnt in air giving SeO_2 in the case of selenium dioxide. Selenium dioxide is also obtained by treating the metal with hot nitric acid to form H_2SeO_3 then heating to drive off the water. SeO_2 is a white volatile solid.

Selenium trioxide SeO_3 is obtained as an anhydride of H_2SeO_4 by dehydration of H_2SeO_4 by P_2O_5 at 150 to 160 ^0C; it is a strong oxidant and is rapidly rehydrated by water. Selenium trioxide dissolves in liquid HF to give fluoroselenic acid ($FSeO_3H$; c.f. FSO_3H) a viscous fuming liquid. (Cotton and Wilkinson, 1988)

Oxygen stands apart in many physical and chemical properties, with close similarities among S, Se, and Te. A major difference is that third-period (and later) elements have d-orbitals available for pπd bonding or for the expansion of the valence shell beyond the octet. There are no oxygen counterparts of SF_4 and SF_6. Thus for groups 15-17 we have a big change in properties from the first member of each group to the next, but a very small change from the second member to the third. Within each main-group

family to the right of the transition series, the pairs Al and Ga, Si and Ge, P and As, S and Se, and Cl and Br display the greatest similarities, because of their equivalent sets of valence shell orbitals and similar radii.

Oxygen shows negative oxidation states except in combination with F. The oxide ion is a hard Lewis base, whereas S^{2-} and Se^{2-} are very soft bases. Metal oxides commonly have typical ionic-type lattice structures, whereas metal sulphides and selenides more likely have layer-type structures or other structures. These structures are encountered only where polarisation effects are great. Family trends are quite regular for S, Se and Te, but with greater importance of positive oxidation states and an increasing similarity to metals.

Selenium and tellurium occur in nature as metal selenides and tellurides, usually accompanying metal sulphides. Se and Te, as the dioxides, concentrate in fly ash from the roasting of sulphide ores.

Chemistry of Selenium Compounds

As previously stated the chemistry of Se is very similar to that of S. Both differ greatly from oxygen although they are from the same group. Chalcogen Cations: S, Se and Te dissolve in oleum (H_2SO_4 / SO_3) to form coloured cyclic cations. All three elements form square-planar cyclic X_4^{2+} cations, but S also gives S_8^{2+} (C_{2h}, blue) and S_{16}^{2+} (red), and Se gives Se_8^{2+} (green). The X_8^{2+} rings are folded with one short transannular distance, suggesting a weak bond to give a bicyclic ion.

Hydrogen Compounds of Se.

H_2Se selenium hydride burns with a blue flame to give the dioxide. The hydrides H_2X can be obtained from the elements at elevated temperature or by reaction of metal selenides with acid. They are highly toxic, and the odour of H_2Se is even worse than that of H_2S. The strengths of the acids H_2X increase in the order $H_2S < H_2Se < H_2Te$. The other method by which the hydride of selenium can be made is by reacting the selenate with sodium borohydride $NaBH_4$. [This is dealt with in more detail later in **Chapter 4**.] The compound H_2Se is a volatile material and is particularly dangerous, the maximum permissible limit for air-borne concentration is 0.1mg m^{-3}. The kidneys, spleen and liver take up the Se, with a result that even minute concentrations cause headaches, nausea and irritation of the mucous membrane.

Oxoacids of Selenium

Selenium and tellurium do not form extensive series of oxoacids; those containing Se-Se or Te-Te bonds are unknown. Selenium dioxide dissolves in H_2O to form selenous acid (H_2SeO_3) which can be obtained as colourless crystals by evaporation of the solution. H_2SeO_3 (s) decomposes into SeO_2 and water on warming. Selenous acid is reduced easily to Se by mild reducing agents such as HI, SO_2, or N_2H_4. Concentrated solutions of $HSeO_3^-$ contain the $Se_2O_5^{2-}$ ion, with a symmetrical structure, unlike $S_2O_5^{2-}$, with Se-O-Se bonding. Very strong oxidising agents (O_3, MnO_4^-, and H_2O_2) oxidise H_2SeO_3 to H_2SeO_4. Selenic acid is a strong acid and a rather strong oxidising agent.

$$SeO_4^{2-} + 4H^+ + 2e^- \longrightarrow H_2SeO_3 + H_2O \qquad E^0 = 1.15V \qquad \textbf{Eqn 1.4}$$

Redox chemistry of Selenium

E_A^0 $\quad SeO_4^{2-} \rightarrow^{1.1} H_2SeO_3 \rightarrow^{0.74} Se \rightarrow^{-0.11} H_2Se$ **Eqn 1.5**

E_B^0 $\quad SeO_4^{2-} \rightarrow^{0.03} SeO_3^{2-} \rightarrow^{-0.36} Se \rightarrow^{-0.67} Se^{2-}$ **Eqn 1.6**

The Pourbaix (E/pH) diagram for Se is more complex than that for S. H_2SeO_3 and its salts are stable, and elemental Se has a wide range of stability. A dashed line represents the reduction of H_2SeO_3 to H_2Se, because this is within the region of stability for Se and H_2SeO_3 will oxidise to Se. H_2Se is a strong enough reducing agent to reduce water, but the reaction is slow, because of the H_2 over-voltage. The Pourbaix diagram can be found on *Appendix 1.3*.

(Douglas, McDaniel, and Alexander 1985.)

Oxidation of H_2SeO_3 with H_2O_2, $KMnO_4$ or $HClO_3$

(i) $H_2SeO_3 + H_2O_2 \longrightarrow H_2SeO_4 + H_2O$ **Eqn 1.7**

$Na_2SeO_3 + H_2O_2 \longrightarrow Na_2SeO_4 + H_2O$ **Eqn 1.8**

(ii) $8H_2SeO_3 + 2KMnO_4 \longrightarrow 5HSeO_4 + K_2SeO_3 + 2MnSeO_3 + 3H_2O$ **Eqn 1.9**

(iii) $5H_2SeO_3 + 2HClO_3 \longrightarrow 5H_2SeO_4 + Cl_2 + H_2O$ **Eqn 1.10**

Oxidation of Se with chlorine or bromine water

(i) $Se + 3Cl_2 + 4H_2O \longrightarrow H_2SeO_4 + 6HCl$ **Eqn 1.11**

Action of bromine water on a suspension of silver selenite

(ii) $Ag_2SeO_3 + Br_2 + H_2O \longrightarrow H_2SeO_4 + 2AgBr$ **Eqn 1.12**

(Greenwood and Earnshaw1997)

Organoselenium compounds if ingested are slowly released over prolonged periods resulting in foul-smelling breath and perspiration. Se in 1957 was found to play an essential role in metabolism in the formation of the enzyme glutathione peroxidase, which is involved in fat metabolism. It was found that in incidence of kwashiorkor (severe protein malnutrition) in children is associated with inadequate uptake of Se, and it may be involved in protection against certain cancers. The average U.S. daily intake ~150μg. (Shamberger. 1983.)

1.3 Biochemistry of Selenium.

The discussion of the biochemistry of selenium will be dealt with in terms of the following:

1. Nutritional aspects of selenium.
2. Biochemical functions of selenium.
3. Metabolism of selenium.
4. Selenium in human health.

1.3.1 Nutritional aspects of selenium

Dietary requirements of animals for selenium

It is important to note that the need for Se in animals depends upon various interactions, in particular, upon the dietary supply of vitamin E as it appears to be an important complementary factor (Buchanan – Smith et al., 1969). Bioavailability is relevant in so far as the required concentration of selenium in the diet may need to be twice as great in a situation where bioavailability is only 50 percent than that of a more useful selenium source. The consequence of these considerations is to render doubtful a single statement of the selenium requirement for any single species. It is probable that selenium requirements for most of the animals studied fall in the range of 0.05 to 0.3ppm in the dry diet. Supplemental selenium levels approved by the U.S. Food and Drug Administration are 0.1ppm for cattle, sheep, swine (0.3ppm in prestarter and starter diets) chickens, ducks and 0.1ppm for turkeys (U.S. Dept of

Health, Education and Welfare, Food and Drug Administration 1974,1979; U.S. Dept of Health and Human Services, Food and Drug Admin, 1981a, 1981b, 1982).

Meeting Selenium requirements for Animals

Selenium supplements that have proved satisfactory include sodium selenite or sodium selenate, the former being the one most commonly used. It may be incorporated in the complete diet or mixed at higher concentrations in free – choice supplements such as salt (Rotruck et al., 1969). To ensure continued bioavailability the carriers should have minimum reducing activity. If they do not, a significant proportion of selenite may be reduced to elemental selenium. This is detrimental as the bioavailability of elemental selenium is much lower than selenate or selenite. (Groce et al., 1973a). A selenium pellet (elemental selenium and powdered iron) of high specific gravity has been devised (Kuchel and Buckley, 1969) which is retained in the reticulum of ruminants and slowly release selenium in amounts consistent with daily needs (Handreck and Godwin, 1970;Whanger et al., 1978b)

Cattle and Sheep

The occurrence of selenium deficiency in the diets of domesticated ruminants is associated largely with muscular degeneration or weakness. Most prominent among the conditions is nutritional muscular dystrophy, a metabolic disease that has occurred most widely in sheep (Muth 1963), but also occurs in cattle. In addition, it appears that certain reproductive problems in cattle and sheep are related to the muscular incompetence, which results from selenium deficiency (Segerson et al., 1977).

Nutritional Myopathy

While there are other diseases associated with selenium deficiency none are as wide spread and common as nutritional associated muscle dystrophy. Nutritional Myopathy is a further effect of selenium deficiency. It is because that this disease is so common that there has been so much research in it understanding and hopefully its eventual cure. This condition first came to prominence in the "improved" grazing lands (fertilised lands) of the United States of America and Canada after the Second World War (Muth 1955,1963). The nutritional importance of selenium had just been discovered and now the effects of its deficiency were being brought to light. One of the factors in the growing incidence of myopathy or white muscle disease was identified as changes in grazing systems. The system of low-yielding hays and grasses for foraging, supplemented with grain and protein concentrates, was replaced with intensified high-yield-grass production. There are fewer studies on white muscular dystrophy disease in cattle than in sheep, possibly because the disease is not as common in the former. The predominant sign is muscular weakness. The lambs walk with a stiff gait and arched back if they walk at all, avoid movement, in general lose condition, and die. Skeletal muscles show dystrophy, but cardiac lesions are not always present.

The much higher levels of protein in the so called "improved" grasses meant protein concentrates, the normal carriers of organic sources of selenium, were eliminated from the feeding cycle of the grazing animal herds in this instance sheep (Muth 1963). In addition, a greater dependence on ruminal synthesis of protein, exposes plant proteins to the reducing action of rumen microflora (Cousins and Cairney. 1961; Whanger et al., 1945a), a problem enhanced by the longer residence time of grasses in the rumen (Van Soest 1965). Selenium deficiency had to be addressed, it appeared

that by maintaining the dietary selenium at 100ppb selenium in dry feed given to ewes the signs of muscular dystrophy in lambs would be eliminated. Less dietary selenium was found to be needed when it was contained in the natural proteins because a greater proportion is absorbed.

Selenium deficiency associated reproductive failure.

Selenium deficiency has been related to other reproductive failures in ruminants (Hartley and Grant 1961; Andrews et al., 1968; Buchanan – Smith et al., 1969). During the course of an experiment to develop improved laboratory methods for ova culture and transfer the impaired fertility of ova was noted in a group of cows after transferring them from Green County to Wayne County Ohio, America (Segerson et al., 1977). Chemical profiles of the diets consumed indicated that protein, energy, vitamin E, and selenium were below requirements. Subsequently, the effect of combined selenium and vitamin E injections upon the fertilisers of ova was evaluated in super-ovulated beef cows maintained on either adequate or inadequate plain nutrition. Optimum fertilisation [100% of ova] occurred in those taken from females being administered supplemental selenium and vitamin E and being maintained on adequate nutrition. Other groups were only 40% fertilised.

One of the most important selenium-responsive diseases in dairy cows is retained placenta. This disorder results from the failure of the foetal placenta to separate from the maternal crypts in the caruncles, a process that normally occurs within 2 to 8 hours postpartum. Retention refers to placenta that remains attached to the uterus for more than 2 hours. It occurs in about 10 percent of the nutritionally deficient dairy cows (Black et al., 1953). Placental retentions result in an increased incidence of uterine infections in 54 % of affected animals, compared to 10 % incidence in cows

with normal calving (Callahan 1969). Selenium deficiency has surfaced recently as a major factor in the onset of this disease. In Great Britain, Trinder et al., (1969) first observed higher retention rates for placentas in herds with corresponding greater problems of nutritional muscular dystrophy and were able to reduce incidence through supplementation of selenium and vitamin E (Trinder et al., 1973). The optimum time for dosing was between 1 and 3 weeks prepartum, since the biological half-life of selenium is about 10days and clearance is accelerated in the immediate postpartum period (Conrad and Moxon 1979). The importance of vitamin E in the etiology of retained placenta is not known, but the small amounts of tocopherol in many silages (Schingoethe et al., 1978) and its necessity, as a complement to selenium in other reproductive diseases suggests that its role needs to be determined.

Other Selenium-Related Diseases.

Having discussed the diseases caused by selenium deficiency it is interesting to note the number of instances in veterinary diseases, where selenium can have a role in finding a solution or cure. The addition of selenium can also be of benefit in a number of ways. Selenium additions 1ppm to diluted semen increased motility and oxygen consumption in 13 of 15 ejaculates of sperm, although this occurs prior to fertilisation, it increases the chance of fertilisation. If the sperm have poor motility, they stand a less likelihood of fertilising the ova (Julien and Murray 1977; Pratt 1978). Unthriftiness in both cattle and sheep (characterised by loss of condition and diarrhoea that can lead to death) has responded to selenium therapy (Andrews et al., 1968).

A possible mechanism by which selenium counters unthriftiness is through protection of the immune system. There is strong evidence to suggest that selenium functions

biochemically in the neutrophilis of steers (Boyne and Arthur, 1979). There was no detectable GSH-Px activity (associated in fat metabolism) in selenium-deficient neutrophilis, whereas activity was systematically detected in the selenium-adequate group. The deficiency of selenium does cause a significant reduction in the ability of the phagocytic neutrophilis to kill ingested bacteria. Periodontal disease or "camel-back" in ewes, pneumonia in lambs and non-specific diarrhoea in calves are diseases that respond to selenium therapy (Kendall 1960; Hamdy et al., 1963; Andrews et al., 1968; Mosier et al., 1978).

Selenium in Human Nutrition.

In 1957, the essential role of the enzyme glutathione peroxidase (GSH-Px) was first established. The stoichiometry of selenium in human erythrocyte GSH-Px is similar to that of the enzyme derived from various animal sources (Awasthi et al., 1975). Burk et al., in 1967 noted that blood selenium levels are low in children with kwashiorkor disease (also Levine and Olson 1970). Other specialists discovered that the administration of selenium had resulted in growth (Schwarz 1961) and reticulocyte responses in kwashiorkor patients (Hopkins and Majaj 1967). It appears that the growth of human fibroblasts in cell culture is enhanced by selenium (McKeehan et al., 1976). A recent balance study estimated that a daily Se intake of about 70μg was needed to replace excretory losses and maintain body stores of what in healthy young North American males (Levander et al., 1981). 20μg/day was needed to maintain a balance in young New Zealand women. The difference is probably due to the greater total body pool of selenium in Americans. One example of a 43 year old American is given. This person had been on TPN (Total Parenteral Nutrition) for two years, had poor selenium levels, as evidenced by low erythrocyte and heart (post-mortem)

selenium levels and depressed GSH-Px activities. The patient was diagnosed as having had a dilated cardiomyopathy similar to that of Keshan Disease. It was concluded that the patient suffered from Se deficiency due to long-term TPN complicated by a draining fistula and mal-absorption. The result was that organoselenium compounds were slowly being released over prolonged periods, causing foul-smelling breath and perspiration (Shamberger. 1983).

Keshan Disease.

This disease primarily affects children from 1 to 9 years of age and is characterised by galloping rhythm of the heart, heart failure, cardiogenic shock, abnormal electrocardiograms, and heart enlargement. The average selenium content in hair of children in affected areas, is generally below 0.12μg/g, compared with that of children in unaffected areas which was from 0.25 to 0.6 μg/g. This was in correlation with the Se content of several staple foods was found to be lower in affected than unaffected areas.

Although the positive prophylactic response obtained with Se and the multitude of relationships revealed between Se and Keshan disease indicate a role for Se in the disease, the Chinese workers who initiated the study interpreted their data cautiously and calculated that deficiency of Se was probably not the only cause of the disease. It was suggested that a lack of Se was only one component in the causality of the disease and that other predisposing environmental conditions would have to be met before Keshan disease would occur.

As the Chinese studies point out, infants and children appear to be most at risk with regard to Se deficiency, presumably because of their increased metabolic

requirements and faster growth rates. Most animal studies show that it is the young of any species that bear the most severe consequences of ingesting a Se deficient diet.

Another group of infants and children who might be especially prone to developing a Se deficiency are those who suffer from certain metabolic diseases such as phenylketonuria (PKU) and maple syrup urine disease (MUD). As a consequence of their diseases, these children must consume only special synthetic diets that are very low in Se. McKenzie et al., 1978 described one such case of a 13 year old child in New Zealand whose whole blood and plasma Se levels were 0.016 and 0.009μg/ml respectively, and yet the child was clinically in good health.

1.3.2 Biochemical functions

It was Klaus Schwarz 1965, in whose laboratory the essentiality of selenium in animals was discovered (Schwarz and Foltz 1957), who first postulated that selenium functioned as an essential cofactor at specific sites of intermediary metabolism. Currently, the known biochemical functions of selenium are as a component of the enzyme glutathione peroxidase which can be found in animals and as a component of several bacterial enzymes. The selenium deficiency signs observed in animals can be partially explained by a lack of glutathione peroxidase [GSH-Px] (Hoekstra 1975).

In animals, GSH-Px is presently the only known selenoenzyme, and thus knowledge of the chemistry and biochemistry of GSH-Px is an important part of our current understanding of the biochemical function of selenium in animals.

In contrast to animals, micro-organisms generally grow and reproduce well in the absence of selenium, a lack of certain selenium-containing enzymes being the only sign of selenium deficiency in bacteria. Two bacterial enzyme activities, nicotinic acid hydroxylase (Inhoff and Andreesen, 1979) and xanthine dehydrogenase (Wagner and Andreesen 1979) have been reported recently to require the presence of selenium.

Nature and Properties of Glutathione Peroxidase.

Glutathionine peroxidase enzyme in the presence of reduced glutathione would protect erythrocytes against H_2O_2 - induced and ascorbate–induced haemoglobin oxidation and hemolysis. Rotruck et al. 1971, 1972a demonstrated that dietary selenium protected erythrocytes from ascorbic acid-induced hemolysis only if glucose was included in the incubation medium.

Glutathione Peroxidase Activity in animals.

In the selenium-adequate rat the highest GSH-Px activity is found in the liver and erythrocytes; moderate activity in the heart, kidney, lung and adrenal glands; and low activity in the brain and testis. (Lawrence et al., 1974) In the selenium adequate chick, GSH-Px activity is high in the liver and moderately low in erythrocytes (Omaye and Tappel, 1974). In the selenium adequate lamb, GSH-Px activity is very high in the erythrocytes and low in the liver (Oh et al., 1976a,b). These reports demonstrate that the tissue distribution of GSH-Px varies from species to species.

Function of Glutathione Peroxidase.

The discovery that hydroperoxides were substrates for GSH-Px (Little and O'Brien 1968) proved an important clue to the biochemical function of GSH-Px, and thus of selenium.

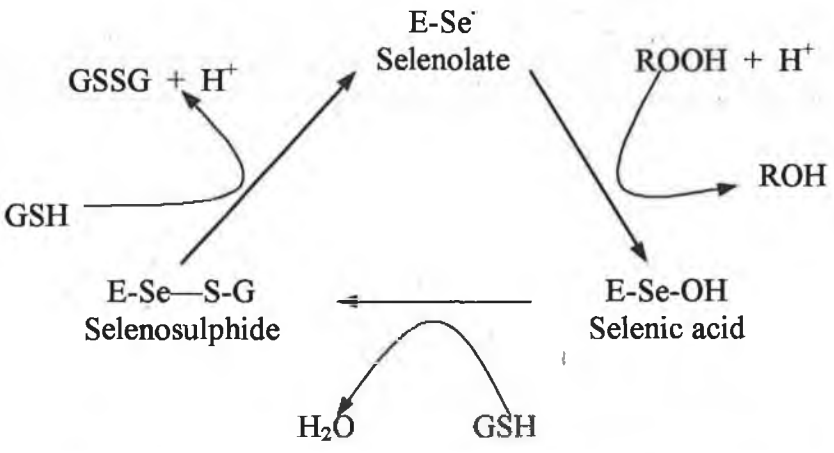

Proposed mechanism of catalysis of GSH-Px (Opp et al., 1983) M.D. Kelly 3109 Thesis U.C.G.

Fig 1.3

The erythrocyte possesses both catalase and GSH-Px activity. From kinetic data and GSH levels present in the erythrocyte, Flohé et al., 1972 have calculated that the rate of H_2O_2 reduction per heme or per selenium, respectively, is nearly identical for these

two enzymes in the erythrocyte. Catalase would therefore seem to be far more important than GSH-Px for H_2O_2 destruction because of the higher concentrations of catalase in the red blood cell. However, GSH-Px deficient erythrocytes are susceptible to hemolysis when exposed to oxidising agents, indicating that the ability to reduce hydroperoxides is of critical importance in the erythrocyte.

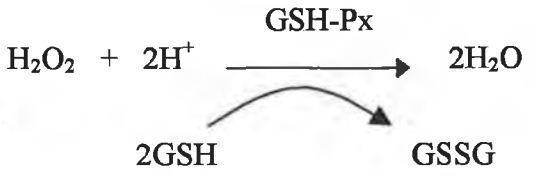

The catalytic degeneration of peroxidase by GSH-Px

Fig 1.4

Only in degenerate cells, like the mammalian erythrocyte, are the catalase and GSH-Px localised in the same compartment. Normally they are localised in distinctly defined compartments [i.e. catalase in the peroxisomes and GSH-Px in the cytosol and mitrochondrial matrix space] to ensure that there is little direct overlap in the competition for H_2O_2. In other words, the two protective enzymes are generally not in direct competition for H_2O_2. In weanling rats fed a selenium deficient diet at the time that liver necrosis develops, the GSH-Px activity falls to undetectable levels (Hafeman et al., 1974) while in chicks there is a relationship between exudarive diathesis development and depressed plasma GSH-Px activity (Noguchi et al., 1974). These diseases are prevented either by dietary selenium or by vitamin E. It can be deduced from this that selenium and vitamin E have overlapping or complementary roles in the protection of cells.

Liver perfusion experiments have helped to substantiate the role of GSH-Px in protecting the liver against peroxidation. Perfused rat liver has been shown to have the

ability to destroy H_2O_2 or organic hydroperoxides added to the perfusate and to release GSSG (Sies et al., 1972; Sies and Summer, 1975). Other experiments by Burk et al., 1978 and Chance et al., 1978 demonstrated that GSH-Px, vitamin E, and possibly GSH-Px transferase, can function in the cell to protect against peroxidation.

Other Functions of Selenium.

Selenium may have other biochemical functions in higher animals that are not a result of the ability of GSH-Px to serve as a biological antioxidant. A Mammalian selenium-binding protein, clearly different from GSH-Px, was reported to be present in selenium-adequate lambs but absent in lambs suffering from nutritional muscular dystrophy (Pederson et al., 1972). However, the protein has proved difficult to purify and characterise (Whanger et al., 1973; Black et al., 1978).

A selenium binding protein has been observed in bovine and rat spermatozoa. Calvin 1978 reported a selenium binding protein located in the midpiece of rat sperm. Spermatozoa from selenium deficient rats have been reported to show decreased mobility and increased midpiece breakage (Brown and Burk, 1973; Wu et al., 1973,1979). Thus, spermatozoa may possess a specific selenoprotein that serves as a mitrochondrial structural protein or as an enzyme. Selenium deficiency, in combination with vitamin E deficiency, has shown to decrease the ability of ducks to resist infection (Yarrington et al., 1973).

Nutritional and Metabolic Interrelationships

With the first demonstration of the essentiality of selenium, that selenium was the integral part of Factor 3 and prevented liver necrosis in rats, it was clear that the biochemistry of selenium is interrelated with other nutritional factors. Of these other

factors, the biochemical function of vitamin E seems most complementary with that of selenium.

Selenium and vitamin E deficiencies in animals cause degenerative lesions; the nature of the lesions and their tissue location depend on the species involved and the status of other nutritional factors. The effect of vitamin E and of selenium deficiency have been postulated to result from the destruction of cellular membranes or of critical cellular proteins and thus of cellular integrity.

Selenium has been shown to reduce the toxicity of cadmium, inorganic and methyl mercury, thallium, and silver. It apparently decreases the rate of excretion of these toxic substances and changes the distribution of these elements within the body (Parizek et al., 1974). Gasiewicz and Smith (1978) identified a specific protein in plasma that binds both cadmium and selenium; either element alone will not result in the formation of this relatively stable complex, suggesting that this complex is a possible biochemical mechanism for the decreased toxicity and metabolic changes observed within the body when selenium and cadmium are administered concurrently. Ganther et al., 1972 demonstrated that selenium also protects against methylmercury toxicity and suggested that the presence of selenium may lessen the toxicity of the mercury in tuna.

Reports that lead (Bell et al., 1978) and copper (Godwin et al., 1978) are more toxic to selenium-deficient animals and that copper pre-treatment will decrease the toxicity of selenium (Stowe and Brady 1978; Stowe 1980) suggest that the metabolism of several other elements is interrelated with that of selenium.

1.3.3 Metabolism

Dietary forms

There are various forms of dietary selenium selenocystine, selenocysteine, Se–methylselenocysteine, seleno homocystine, selenomethionine, Se-methyl-selenomethionine, selenomethionine selenoxide, selenocystathionine, and dimethyl diselenide (Shrift 1969). The selenium compounds found in seeds and forages most commonly consumed by livestock and thus in the human food chain, are divided into four major groups selenocystine, selenocysteine, selenomethionine and Se-methyl-selenomethionine (Peterson and Butler 1962;Shrift 1969; Olson et al., 1970).

Approval was given for the addition of inorganic selenium to feeds deficient in this element, and the most common forms used are sodium salts of selenite and selenate. Selenized yeast tablets, containing primarily organic selenium, are available as human supplements and have been shown to increase blood selenium levels (Schrauzer and White 1978).

Most of the absorption is done in the bottom half of the gastro intestinal tract. The transport of selenomethionine was inhibited by methionine, but the transport of selenite and selenocystine was not inhibited by their respective sulphur analogues.

In a short-term human study, selenite was almost as well absorbed as selenomethionine in young women (Thomson *et al*, 1978a). In a prolonged study, three individuals were given different treatments. One was given 100μg Se as selenomethionine, the second was given 10μg selenium as selenite, and the third was given 65μg selenium in mackerel, daily for 4 to 10 weeks (Robinson et al 1978a). Selenite was not absorbed (45%) as well as Selenomethionine (75%) or the fish

(66%). Thus different dietary forms of selenium may have an influence on its absorption in humans.

The importance of selenium in male reproduction is indicated by the incorporation of Se^{75} as SeO_3^{2-} in the reproductive organs. In contrast to other tissues, the maximum incorporation of selenium in testes and epididymis of rats was reached 2 to 3 weeks after injection (Brown and Burk 1973; McConnell et al., 1979b). As an indication of the accumulation of selenium in male reproductive organs, about 40 percent of the total body Se^{75} was found in the testes plus epididymis of rats 3 weeks after injection (Brown and Burk 1973). Within the sperm, Se^{75} became associated primarily with the midpiece of the sperm tail. Calvin (1978) extended these studies with rat sperm and found the selenium to be primarily in the sperm keratin, a disulphide – stabilised fraction, obtained by extracting isolated tails with sodium dodecyl sulphate. The name selenoflagellin (flagella = tail) was proposed for this selenium binding polypeptide in sperm. Calvin suggested that it may be essential for proper assembly of the rat sperm tail.

Inorganic Selenium

There is very little doubt concerning the ability of animal tissue to convert inorganic selenium to organic forms. This is demonstrated by the incorporation of Se^{75} from selenite into dimethlyselenide (Hsieh and Ganther., 1975) and into GSH-Px (Oh et al., 1974; Forstrom et al.,1978) and into selenoamino acids (Godwin and Fuss., 1972; Olson and Palmer, 1976) Although the pathways for reduction of selenite to selenide have been fairly well established (Ganther 1979), the pathways for conversion of selenide to selenoamino acids have not been fully delineated.

By a mechanism in tRNA (transfer ribonucleic acid), the selenocysteine could be incorporated during translation via the action of this tRNA and its changing enzymes. An alternative mechanism is that the selenocysteine is formed in situ from some serine, which would be susceptible to a post-translational modification.

Organic Selenium

In contrast to sulphur, selenium compounds tend to undergo reductive pathways in tissues. However, reduced selenium compounds can be metabolised by animal tissues. Feeding selenomethionine to hens resulted in more selenium in egg white than in egg yolk, whereas feeding selenite or selenocystine resulted in the reverse (Latshaw and Osman 1975). A higher concentration of selenium was found in the pancreas and breast muscle (Osman and Letshaw 1976) of chicks fed selenomethionine than when fed either selenite or selenocystine. These authors concluded that selenocystine is not incorporated into protein but is metabolised like inorganic selenium compounds.

Reduction of Selenium

Evidence has been obtained for the formation of hydrogen selenide from selenite in tissues (Diplock et al.,1973; Hsieh and Ganther 1975). There are some formidable problems, however involved in studying the production of hydrogen selenide. Oxygen must be rigorously excluded in order to prevent oxidation of H_2Se (Se^{-2}) to Se^0. Ganther (1979) has provided the basic information on the mechanism for reduction of selenite to selenide. A specific requirement for GSH, anaerobic conditions (for best activity), and NADPH are essential for the reduction. Reduction of selenite to selenide occurs by a series of reactions involving initially the nonenzymic reaction of selenite with GSH to form an intermediate in which selenium is joined to GSH in the S-Se-S

linkage (reaction 1). This is followed by NADPH to NADP linked reduction of this intermediate by GSH reductase to form H_2Se (reaction 2 and 3).

$$H_2SeO_3 + GSH \xrightarrow{(1)} GSSeSG \xrightarrow{(2)} GSSeH \xrightarrow{(3)} H_2Se$$

Eqn 1.13

McConnell and Portman 1952b reported that rodents tolerated large amounts of dimethyl selenide (the LD_{50} at 24 hours was 1.3g selenium or 1.8g dimethyl selenium / kg of body weight for rats) suggesting that it is a detoxification product of selenium metabolism. The degree to which the tissues have been previously saturated by dietary selenium greatly influences the retention of a subsequent dose.

Influence of Sulphur

The sulphur analogues of selenium compounds appear to have the greatest influence on selenium metabolism. This is demonstrated by nearly a three fold increase in urinary excretion of selenium following a parenteral dose of sodium selenate when rats were given sulphate either parenterally or in the diet. Sulphate had only slight effects on the urinary excretion of selenium that was administered in the form of selenite (Ganther and Baumann, 1962a)

Influence of other elements

The toxicity of selenium can be reversed by such metals as copper, mercury and cadmium when given at high dietary levels (Hill 1974) suggesting that metals can influence the metabolism of selenium.

1.3.4 Selenium in human health

There are relatively few studies that have specifically investigated any possible relationship between overexposure to selenium and the increased incidence of cancer in humans. However, Glover (1967) commented that the death rate, due to malignant neopasms observed among workers in a selenium rectifier plant in West England, was about the same as that expected for the general population of England and Wales. Moreover, studies that have compared death rates due to cancer in different geographical areas with blood selenium levels in the general population are not consistent with the concept that high selenium intakes contribute to an overall increased human cancer mortality.

It was concluded for regulatory purposes that selenium could cause hepatomes, but only in the presence of severe hepatotoxic phenomena. As a result it was felt that selenium could not properly be classified as carcinogenic because of its capacity to induce liver damage when abused by being consumed at high levels (Gardner 1973). However, this concept may have to be re-examined in light of the fact that selenium sulfide can cause liver cancer in rats without producing liver damage (NCI 1979). On the other hand, Van Houweling 1979 concluded that there must be a no-effect level for carcinogenicity for an essential trace nutrient such as selenium.

Dental Caries

Poor dental health was observed in persons living in seleniferous areas of South Dakota (Smith et al., 1937) or in children residing in seleniferous zones of Venezuela (Jaffe 1976). The conclusions drawn suggest that if high levels of Se were given during tooth development, some effect on dental caries be obtained.

Selenium treatment had no effect on the first permanent molars, which had already formed before the start of the experiment, but the second permanent molars had a yellow chalky appearance in the selenium treated monkeys and curious lesions developed more rapidly in these teeth in the selenium-exposed group. A recent evaluation of the relationship between dental caries and human selenium intake (NRC, 1976a) concluded that there seems no reason to suspect that selenium is important to cariogenesis in man, and the report by the subcommittee set up by the National Research Committee (1983) uncovered no new evidence to contradict that view.

Reproduction

Sodium selenite protected partially against the teratogenic effect of injected sodium arsenate or cadmium sulphate. On the other hand, selenium compounds have long been known to cause embryonic abnormalities when injected into the eggs of chickens. (Palmer et al., 1973). More recently, one probable and four certain pregnancies among six women formulating microbiological media containing sodium selenite were reported to terminate in abortions (Robertson, 1970). However, a survey of other laboratories doing similar work revealed no pattern of such trouble, and no difference in urinary selenium levels was noted between the affected group of women and a control group residing nearby.

Conclusions

Certain specific compounds containing selenium i.e. bis-4-acetamino-phenyl-selenium dihydroxide, selenium diethyldithiocarbamate, and selenium sulphide, are capable of causing cancer in rats when administrated at high levels for prolonged

periods. However, it is not possible on the basis of these results to generalise about the carcinogenicity of different selenium compounds.

A comparison of public health statistics from various parts of the United Sates reveals that, if anything, the cancer death rate is lower in those areas of the country in which consumption of locally produced foods could result in an increased dietary selenium intake. A limited number of observations on workers industrially exposed to selenium gives no indication that cancer rates are any higher in such workers than in the general population. Also there is no evidence to suggest that typical levels of exposure result in increased caries in humans.

Reproduction and Neonatal health

Cowgill (1976) found that the birth rate in the continental U.S. is lower in those regions where the selenium concentration in forage crop is low, than the rate in those where the concentration of selenium is high. Shamberger (1971) noted higher neonatal death rates on a population basis in low-selenium areas of the U.S. than in high-selenium areas, but Cowgill (1976) concerned that couples in low-selenium areas were taking Se to prevent neonatal death, pointed out that comparisons of neonatal death rates should be made on the basis of live births. When expressed on this basis, no differences in neonatal death rates were observed between high and low Selenium regions. Money (1970) suggested that selenium may play a role in the etiology of the sudden infant death syndrome (SIDS), but Rhead et al., (1972) found no difference in the blood or plasma selenium levels between normal infants and those that had died of SIDS. In a later paper, Money (1978) suggested that a somewhat elevated iron intake might precipitate SIDS in infants of marginal selenium

and vitamin E status, but no definitive role for any of these nutrients has been established in this condition

Infectious disease

Chen and Anderson (1979) reported that the selenium concentration in the sera of 17 patients acutely ill with Legionnaires disease were lower than in their paired convalescent –phase sera. Such a trend was not seen in 10 similarly matched samples of serum from control patients with pneumonia. Although the mechanism of this effect is not known, Jaquess et al., (1980) reported that rather high concentration of sodium selenate (50μg/ml) stimulated the growth of *Legionella pneumophila* when grown on agar cultures.

Cystic Fibrosis

Research on cystic fibrosis in humans has been hampered by the lack of a suitable animal model of the disease. The histopathology of the pancreatic lesions seen in selenium-deficient chickens in some ways resembles that of cystic fibrosis in humans, but the similarities are superficial and are not considered to be the result of the same underlying maladies. Wallach (1978) shows that the rate of Cystic Fibrosis in New Zealand is only one fifth to one half that in the U.S.; the rate in Sweden, another country thought to have rather low selenium-intakes; is only one-tenth to one-fifth that in the U.S. Further comparisons would be unwise.

Selenium Supplementation.

Some workers have called for an increase in dietary selenium intakes to protect against cancer, either by consuming selenium-rich foods or by taking selenium

supplements (Schrauzer and White 1978). Griffen (1979) in his research concluded that the supplementation of selenium in humans is not warranted at this time and that in fact there are reasonable doubts that selenium may have any practical value in the prevention of cancer in humans.

The amount of selenium needed to cause toxicity can be decreased in certain situations. Also, selenium has peculiar metabolic interactions with other compounds e.g. methylated selenium metabolites that occur naturally in the body have a pronounced synergistic toxicity with mercuric chloride and inorganic arsenic compounds. Jacobs and Griffin (1979) combined supplementation of 1,2, - dimethylhydrazine treated rats with Vitamin C in the diet and selenium in the drinking water, this led to an increased incidence of colon tumours as compared to unsupplemented rats or rats supplemented with selenium or Vitamin C alone. This observation is of importance to human health because those persons taking selenium supplements may also be taking Vitamin C supplements for other reasons.

In brief: experiments with rodents have shown under a wide variety of conditions that selenium has a protective effect against certain chemically induced and spontaneous, presumably virally induced, tumours. Animals deficient in both Vitamin E and selenium develop cardiomyopathy, but such a condition is not found in animals suffering from an uncomplicated selenium deficiency. There is no evidence to suggest that an inadequate selenium intake play any role in human reproductive failure. Selenium at levels in excess of nutritional requirements improves the immune response in mice, and selenium deficiency decreases the microbial activity of phagocytes in rat. However, there is no evidence indicating that suboptimal selenium intake contributes to impaired resistance to infectious disease in humans.

2.1 Polarography Introduction

Many elements have been analysed using the polarographic technique and Selenium is no exception, having been analysed by many researchers using this technique. Much of the research has been carried out using seawater matrix. Seawater is used because of the very low degree of humic substances it contains. This is relevant because humic substances can interfere with the analysis of selenium. The discovery of this fact lead to most of the research being directed into removing the humic material.

With the selenium enriched yeast that is under investigation in this thesis, the humic content is much higher than any other matrix investigated to date. This created the difficult problem of removing the humic content. In past analyses, the humic material was removed by passing the solution through an ion exchange resin or by adding another mineral to mask the humic effects [copper has been used to a good degree in this regard].

Voltammetry is a branch of electroanalytical chemistry that deals with the effect of the potential of an electrode in an electrolysis cell on the current that flows through it. *Polarography* is the branch of voltammetry in which a mercury drop electrode [MDE] is used as the working electrode. (Meites 1965) Jaroslav Heyrovský, a Czech chemist, first described this technique in 1922 (Heyrovský and Zuman 1968).

Mercury Drop Electrode

The main points in MDE electrolysis are:

1) The solution is not stirred, so electroactive material in solution can only reach the working electrode by diffusion.

2) Currents of only a few microamperes are passed.

3) The amount of material actually reduced during the course of analysis is only a small fraction of the total electroactive material present. (Meites 1965)

These will be discussed in detail in later sections.

Ordinarily, the dropping mercury working electrode is operated at negatively applied potentials, so that reduction occurs and cathodic (negative) waves are observed. At less negative or positively applied potentials, oxidation can occur at the working electrode, giving rise to an anodic (positive) wave.

The mercury drop electrode consists of, a reservoir of mercury that is pushed through a thin capillary by a sustained pressure. The mercury drops emerge in the solution and become the working electrode. There is also a reference electrode (Ag/AgCl) and an auxiliary electrode (platinum wire). A hammer at the top of the capillary controls the drop rate of the mercury drop precisely. As each drop grows, its surface area increases simultaneously. This increase in surface area in turn increases the rate of the electrochemical reaction and the current; the converse of this is also true, the decrease in surface area decreases both of these factors.

The working electrode is always kept very small to prevent the electrolysis from becoming significant enough to decrease the concentration of the electroactive material appreciably, as this can result in a nearly constant concentration of the solution. While the polarogram is being recorded, the applied voltage is gradually increased, so that the potential of the working electrode becomes progressively more negative.

When the applied potential becomes large enough that the applied emf (electro motive force) is greater than the back emf of the cell, an electrochemical reaction occurs at the working electrode and current begins to flow through the cell. At this point

$$i = f(E) \qquad \textbf{Eqn 2.1}$$

While the current ***i*** is small, the depletion of electroactive ions near the electrode is small and ***i*** responds dramatically to changes in E. This is reflected by the steep rise in the curve of the polarogram. The increase in ***i*** with applied E does not continue indefinitely. This is due to the fact that as the electrolysis rate becomes large enough, the supply of ions in the vicinity of the electrode becomes exhausted. Therefore, ***i*** becomes limited by the rate of *mass transport* i.e. by the rate at which additional ions are transported from the bulk of the solution to the vicinity of the electrode surface. This is significant, as the only way the reducible ions can reach the vicinity of the analytical electrode is by diffusion. The limiting current produced by diffusion and subsequent reaction at the analytical electrode is called the *diffusion current*.

The primary advantage of polarography is that by using a mercury drop electrode, each drop exactly duplicates the behaviour of the one that preceded it. Consequently, the currents are accurately reproducible from one drop to the next, and independent of the previous history of the experiment. Solid products cannot accumulate on the electrode surface, changing its properties, as can occur with solid electrodes. Therefore, there are only three important variables essential when using this technique. These are 1) electrode potential, 2) solution composition, and 3) current. Another advantage is that the high over-potential for the reduction of hydrogen ion or water on a mercury surface makes it possible to investigate processes that can occur only under extremely strong reducing conditions.

There are some disadvantages of the MDE technique however. Mercury is rather easily oxidised, so that very positive potentials cannot be secured. Another drawback is the continuous variation of electrode area which gives rise to significant currents even in the absence of a reducible or oxidisable substance (Pecsok *et al.*,1922) i.e a large

background noise. Mercury is also a toxic chemical and adequate precautions much be in place and employed each time the instrument is used.

However, in the situation like the premise under examination in this thesis, the advantages of the MDE outweigh its drawbacks it for this reason that the selenium yeast was chosen to be analysed for selenium by this method.

De-aeration of solution

It is essential for any electrolyte to be thoroughly de-aerated. Consider a 0.1M Potassium nitrate aqueous solution saturated with air. In such a solution, when a polarogram was generated, two cathodic waves are observed. The first wave represents a two-electron reduction of oxygen to hydrogen peroxide:

$$2H_2O + O_2 + 2e^- \longrightarrow H_2O_2 + 2OH^- \qquad \textbf{Eqn 2.2}$$

The second wave (at a more negative applied potential) is for the further reduction of hydrogen peroxide.

$$H_2O_2 + 2e^- \longrightarrow 2OH^- \qquad \textbf{Eqn 2.3}$$

Since the reduction of oxygen covers a large part of the available potential range and would mask any other reaction that is occurring simultaneously, most MDE polarograms are undertaken on low level concentrations. Thus if any dissolved oxygen is present in the electrolyte before the polarograph is undertaken then this causes a background signal, it is this that is superimposed on the polarographic wave that is being investigated. It is for this reason that it is almost always necessary to remove dissolved oxygen from water before making a polarographic determination (Meites 1965).

Polarographic Techniques

Over the years, various techniques have been developed for specific methods of determining the exact concentration of selenium in each sample and as you will see they are designed for certain environments but not for all. Stationary working electrodes use either Pt, Au, Cd or HMD electrodes. A rapid linear potential scan is used in the range of 20 to 400mV s^{-1}. In direct current polarography, there are two contributions to the total current, the Faradaic current and the residual current. With the latter being due to a capacitance effect at the mercury / solution interface. It is the magnitude of this capacitive current, which sets the detection limit for the d.c. method. At about 10^{-4} mol dm^{-3} of analyte the capacitive current becomes comparable with the Faradaic current and the wave shape disappears. A brief out line is given of the following techniques:

1. D.C. polarography
2. Normal Pulse Polarography
3. Differential Pulse Polarography
4. Stripping Voltammetry
    - Linear Sweep Stripping Voltammetry
    - Linear Cathodic Stripping Voltammetry
    - Linear Anodic Stripping Voltammetry
5. Differential Pulse Stripping Voltammetry
    - Differential Pulse Anodic Stripping Voltammetry
    - Differential Pulse Cathodic Stripping Voltammetry
6. Square wave Voltammetry
    - Square wave Anodic Stripping voltammetry

- Square wave Cathodic Stripping voltammetry

The first three techniques normally use a modern version of the dropping mercury electrode called the static mercury drop electrode [SMDE]. The last three techniques use a stationary electrode, normally a hanging mercury drop electrode [HMDE].

1. D.C. Polarography

This was the initial polarographic technique undertaken, using the Mercury Drop Electrode [MDE]. The applied voltage is gradually increased, so that the potential of the analytical electrode becomes progressively more negative (Riley. T. and A. Watson. 1987). A typical polarogram is given below in **Fig 2.1**. The half wave potential $E_{½}$ is characteristic of the species and the limiting diffusion current (i_l) is proportional to the concentration.

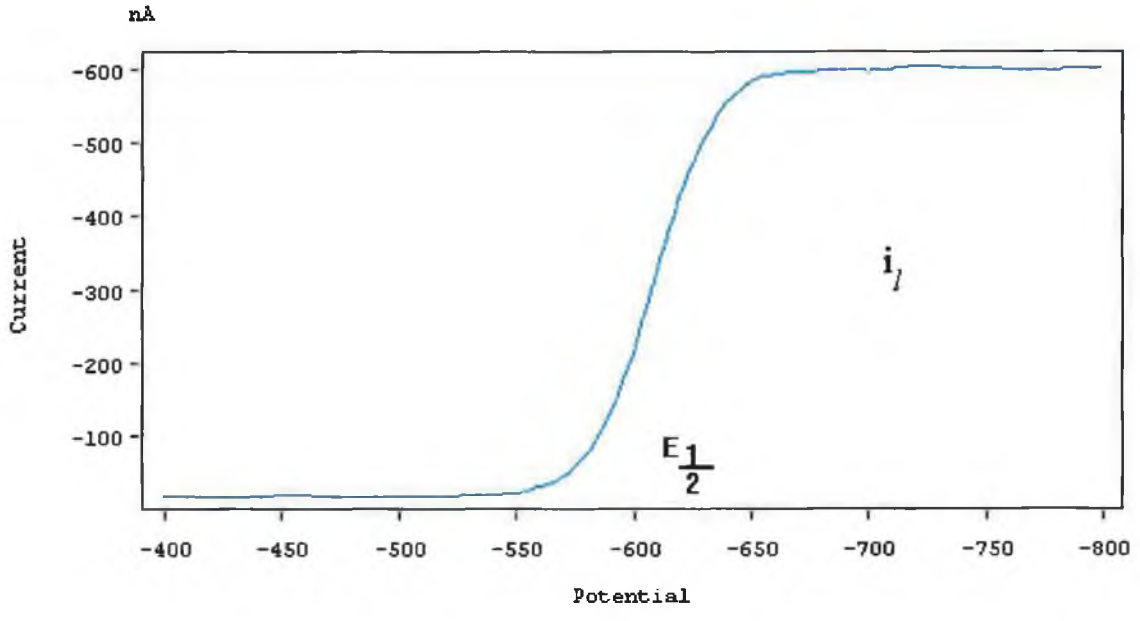

Fig 2.1

2. Normal Pulse Polarography (NPP)

Consider a cathodic [reduction] process. The working electrode is set just too positive to achieve any electrochemical reaction and is maintained at this value. A potential pulse of a few milli volts is superimposed on this base potential near the end of the drop lifetime. The current is sampled at the end of the pulse, which coincides with the end of the life of the drop. The additional potential, in the form of the pulse, is increased each time in a negative direction taking the total potential into the electroactive range of the analyte. Only the sampled current is recorded. The pulse enhances I_f relative to I_{cp} and sampling at the end of the drop lifetime discriminates against I_{cp}. The detection limit has now being lowered to about 10^{-6} to 10^{-7} mol dm^{-3}. Sensitivity could possibly be increased, if electrolysis could be prevented during most of the drop lifetime, i.e. if the potential was kept at a lower voltage until the moment of measurement. This is the basis of NPP. The potential is kept at a suitable constant base potential throughout the drop lifetime. The chosen potential signal is imposed as a very short pulse near the end of the drop lifetime. Thus very little electrolysis and depletion occurs. The overall form of the applied voltage signal is a series of potential pulses, one to each drop, rising in a linear ramp with a base potential maintained between the pulses. The current recorded at each pulse is recorded and plotted against the potential of the pulse. (Riley and Watson.1987)

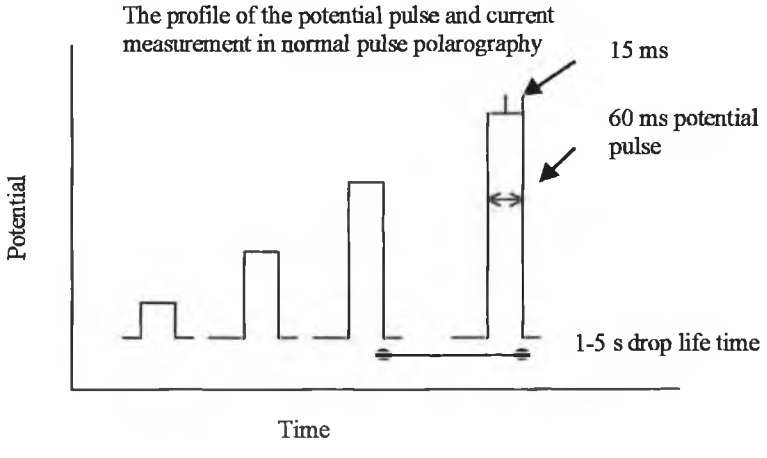

Fig 2.2

3. **Differential Pulse Polarography (DPP)**

A small fixed potential pulse [in the range of 10 to 100mV] is applied near the end of the drop lifetime. The current is sampled twice, once just before the pulse is applied and again at the end of the pulse (just before the drop falls). The electronic circuitry enables the difference to be calculated and plotted. The greater the pulse the greater the sensitivity but the broader the peak, lowering resolution between neighbouring peaks. The form of the result when plotted is a peak not a wave.

This differs from NPP in that after the potential pulse, the potential does not return to a constant base value. Instead the potential itself is a small constant amplitude and is superimposed on a conventional rising linear d.c. voltage ramp. And again as with the NPP, the pulse is imposed for a brief time near the end of the drop lifetime when the growth of the drop has almost ceased. The current is measured in two intervals of about 15ms, the first immediately prior to the potential pulse and the second towards the end of the potential pulse. The final current signal displayed is in fact the difference of these two current values.

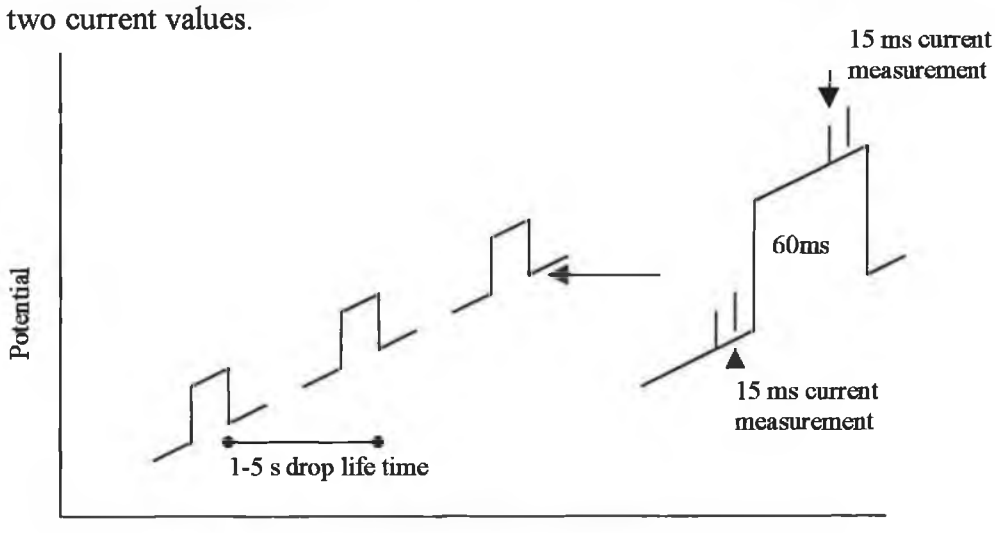

Fig 2.3

The two current values represent the current at two potential values separated by about 10-100mV (the pulse amplitude). This difference in current will be greatest on

time the analyte is oxidised (ASV) or reduced (CSV) back into the solution. This is termed the stripping step.

This technique is employed extensively in the analysis of very dilute solutions of metallic cations. The detection limit is about 10^{-8} mol dm^{-3} (0.001 ppm 1ppb) (Riley and Tomlinson 1987).

The following is a more detailed outline of the main steps in stripping voltammetry.

a) *The Deposition Step.*

The Hanging Mercury Drop Electrode (HMDE) and the Mercury Film Electrode (MFE) supported on a conducting electrode are the most popular electrodes. The advantage of using mercury when analysing metals is that they dissolve into the mercury forming an amalgam. This offered better reproducibility and sensitivity.

b) *Stirring*

If the solution is stirred during the deposition step, this increases the amount of analyte reaching the electrode, thus increasing the rate at which the analyte reaches the electrode. For this to work, control of the stirring is vital. If stirring is too vigorous, the drop could be dislodged and this can cause unpredictable eddy effects. If the stirring is too gentle, the result can be a loss of sensitivity. Deposition in a non-stirred solution offers a higher reproducibility but with a consequent loss of sensitivity and/or very much longer deposition times. To counteract this, differential pulse stripping is used because of its greater sensitivity.

c) *Choice of Deposition Time.*

The best sensitivity is achieved if all the analyte is deposited onto the electrode. However, this is not practical with anything other than a very small dilute sample. In general, only a small fraction of the analyte is ever deposited. Long deposition times can lead to complications and complex reactions on the electrode, so they are best avoided. Too much deposit can also cause problems with proportionality between concentration and signal received. Generally, a good guide is to choose a time which results in only 2% of the total analyte being depleted from the solution. This allows the nature of the solution to remain constant.

d) *The Stripping Step*

During the stripping step the various polarographic modes can all be employed. In D.C. or Linear Sweep Stripping Voltammetry the voltage increases or decreases at a constant unvarying rate with respect to time. A plot of potential (volts) against time would be a straight line. In D.C. anodic stripping a cathodic deposition potential (negative) is set for the deposition time reducing the ions to metals. Then the linear voltage scan is started moving to an anodic (positive) potential for the re-oxidation of the metal. (Aydin. and Yahaya. 1992). In D.C cathodic stripping the pre-electrolysis step oxidation is anodic or cathodic and the stripping step is to a cathodic potential (negative).

Differential Pulse Stripping Voltammetry [DPSV] offers a better differentiation of faradaic current signal and noise such as capacitive current. i.e. DPSV gives better signal to noise ratio by cutting out the background noise inherent in d.c. or linear sweep stripping voltammetry. In DPSV, increasing the pulse amplitude increases the peak height and sensitivity. However, increasing the pulse amplitude will decrease the ability to resolve close lying or overlapping peaks. (Wei Guang Lan, Ming Keong Wong and Yoke Min Sin, 1994)

Applications of stripping voltammetry.

a) *Anodic Stripping Voltammetry [DPASV].*

Formation of intermetallic compounds can cause problems. When metals such as copper and zinc are present in solution, there is a tendency to form a Zn/Cu intermetallic compound, resulting in a shift of the peak and signal depression even signal loss (Aydin. and Yahaya. 1992). Florence (1992) compared d.c. ASV to DPASV in the speciation of trace Cu, Cd, and Pb. The use of d.c. ASV in place of

DPASV for the speciation analysis was limited by the significantly lower sensitivity (about 5 fold), but d.c. measurement had the advantage that the kinetics of the stripping step had little effect on the determination. Fernando A. R. and J. A. Plambeck (1992) studied the DPASC for soil samples on Pb trace amounts. Adeloju. S.B., A.M. Bond, M.H.Briggs and H.C. Huges (1983) using d.c.ASV determined Se using a rotating gold disk electrode, which was found to be better than the gold-platted glassy carbon electrode. The DPASV Se determination was determined, by the above specialists, to be influenced by the deposition time, the rotating velocity, conditioning potential and the scan rate but the overall better sensitivity and the well resolved peaks gave the advantage to the DPASV technique.

b) *Cathodic Stripping Voltammetry [DPCSV].*

Judging from the amount of papers published on the determination of Selenium, CSV seems to be the preferred method for Se determination. The diversity within the CSV technique shows the difficulty of getting a single technique for the variety of samples both organic and inorganic, environmental and synthetic.

CSV of Se has been used since the early 1960's. The method has been recently described by Mattsson, Nyholm and Olin (1994). In the deposition step selenium (IV) is irreversibly reduced to mercuric selenide.

$$H_2SeO_3 + Hg + 4H^+ + 4e^- \rightarrow HgSe + 3H_2O. \qquad \textbf{Eqn 2.4}$$

In the cathodic stripping step the mercuric selenide is further reduced to hydrogen selenide and mercury

$$HgSe + 2H^+ + 2e^- \longrightarrow H_2Se + Hg \qquad \textbf{Eqn 2.5}$$

The supporting electrolyte employed was 0.1M $HClO_4$. The deposition potential was –350mV and the stripping step covered the range –350 to –800mV. They concluded that square wave voltammetry [SWV] or differential pulse voltammetry [DPV] is preferable as a stripping technique for routine analysis. For more accurate results linear sweep voltammetry [LSV] is preferable.

Mattsson, Nyholm *et al*, (1995) looked at the d.c. CSV and found that the high concentrations of Cl^- at low pH interfere with CSV so the sample was buffered to pH 9 and H_2O_2 was added in combination with UV photolytic digestion. By this method the recovery was 86%. As a result, a co-precipitation with Cu^{2+} in acidic media was investigated and gave less interference with better detection. Samples were analysed for total selenium by CSV after UV photolysis, and by HG-AAS after oxidative digestion followed by reduction with HCl. The results were in good agreement.

Filipovic-Kovacevic *et al*, (1996) looked at the simultaneous d.c.CSV of Cr, Ni, and Se. The pH chosen was 1.2 and the peak for Se was found to be at -0.45V. This study found that a decrease of hydrogen ion concentration caused a decrease in the peak height, because at pH over 2, the reduction of Se from selenite becomes irreversible.

Potin-Gautier et al., (1995) investigated the DPCSV of Se. They used the DPCSV method because of its high sensitivity and ease of use. This method is selective for Se(IV). Humic substances that are found in environmental samples, which are the main components of organic matter both in water and soils, give rise to disturbances at the surface of the mercury drop electrode during the metal analysis by ASV. These humic substances interfere with the Se measurements by DPCSV. There was found to

be a linear response between 25 – 4000 ng L^{-1}. A competition between the adsorption of Fulvic Acid (main constituent of humic substances) and the film formation of HgSe (s) occurs at the HMDE surface leading to non linear responses. Low FA concentrations < 0.25mg L^{-1} allow an decrease of the Se(IV) detection limit (125ng L^{-1}), but at high concentrations 5mg L^{-1} the Se(IV) signal is depressed causing a serious increase in the detection limit (750ng L^{-1}) but the linearity range is shifted to 25000ng L^{-1}. Samples were digested using a 2:1 ratio of HNO_3:H_2O_2 and reduced to Se(IV) using 6M HCl at 90^0 C for 45 minutes. The other parameters are summarised in the table below. **Table 2.1**

Deposition Potential	-200mV	Scan Range	-200mV to –700mV
Electrolyte	0.1M H_2SO_4	Pulse amplitude	50mV
Scan rate	$5mV^{-1}$	Deposition time	120 s
Se Peak	-450mV	Detection limit	25ng L^{-1}

Séby et al., (1995) studied the DPCSV technique on Se. The performance of DPCSV can be enhanced by the addition of Cu^{2+} ions or Rh^{3+} ions. These involve respectively the formation and dissolution of Cu_2Se (s) or Rh_2Se_3 (s). The advantage of the CSV method was the ability to concentrate and extract simultaneously Se (IV) from sample matrix. The advantage that the Adsorptive CSV and SWV offers is the quicker analysis but neither can improve on the sensitivity or detection limit of classic DPCSV. The chosen supporting electrolyte was 0.1M H_2SO_4 over HCl because they found the detection limit to be lower. The sample was digested using a combination of HNO_3:$HClO_4$:H_2O_2 in the ration 10:2:5 for 24 hours at 70^0 C. The reduction selenate was reduced to Se(IV) with 6M HCl at 90^0 C for 35-45 minutes. A summary of the conditions is given below.

Table 2.2

Deposition Potential	-200mV	Scan Range	-200mV to –700mV
Electrolyte	0.1M H_2SO_4	Pulse amplitude	50mV
Scan rate	$5mV^{-1}$	Deposition time	120 s
Se Peak	-450mV	Detection limit	$25ng\ L^{-1}$

Ishiyama and Tanaka, (1996) also investigated d.c.CSV and found that the anodic procedure usually requires troublesome and time consuming pre-treatment of the solid gold electrode. The stripping of the silver selenide was done on a rotating silver electrode and gave rise to a single well-defined peak without the addition of any metal ions to the solution as found with other studies. The selenide was deposited onto the electrode in an acidic electrolyte of 0.06M HCl-0.07M HNO_3, then the deposit was cathodically stripped in another solution (2M NaOH). The deposition time of 30 minutes was used. Tellurium (IV) and Bismuth(III) was found to cause interference.

Reduction

$$H_2SeO_3 + 2Ag + 4H^+ + 2e^- \rightarrow Ag_2Se + 3H_2O \qquad \textbf{Eqn 2.6}$$

In Acid $$Ag_2Se + 2H^+ + 2e^- \rightarrow H_2Se + 2Ag \qquad \textbf{Eqn 2.7}$$

In Base $$Ag_2Se + H_2O + 2e^- \rightarrow Hse^- + OH^- + 2Ag \qquad \textbf{Eqn 2.8}$$

bin Ahmad *et al*, (1983) studied Se determination by DPCSV. The parameters that were employed in the study are E_d = -0.05V, D_t = 120s. Scan rate = $5mVs^{-1}$. Pulse amplitude = 25mV. Temperature = above 20^0C. The selenium peak was located at –0.45V. It was found that at higher temperatures there was a less sensitivity, the reason since there is an apparent transformation into an electroinactive state that may be due to an increase in solubility of the HgSe with temperature. It was also found

that there is an enhanced peak when Cu^{2+} ions or As^{3+} ions are present but if there are Fe^{3+} ions the Se peak is depressed.

Elleouet *et al.*, (1996) described the DPCSV of Selenium they used a pre-treatment of a U.V. digestion. To separate the organic and the inorganic forms a rapid ion exchange method was employed. The UV digestion was done in alkaline media. The following parameters were used in the study. The electrolyte was 10ml . l^{-1} HCl which had a pH $\leq$ 2. The Scan rate was determined at $4mVs^{-1}$. The pulse amplitude was 50mV. Temperature 25 ± 0.5^0C. Deposition potential (E_d) was used as –0.2V with the deposition time (t_d) of 120-600s. The detection limit was $5ng.l^{-1}$ at 600 seconds.

Se (VI) can be reduced to Se(IV) by chloride ions in high acidic medium.

$$H_2SeO_4 + 2H^+ + 2Cl^- \longrightarrow H_2SeO_3 + Cl_2 + H_2O \qquad \textbf{Eqn 2.9}$$

while Se(-II) should be oxidised into Se(O) by H^+. Photochemical treatment is the elimination of the organic matter, which often produces adsorptive interference. The measurement of the three oxidation states [Se(VI), Se(IV), Se(-II)] needs their separation which can be realised on an anion exchange resin followed by the transformation step into Se(IV).

Prasada Rao et al., (1996) also studied the determination of Se by DPCSV. Prior pretreatment for the preconcentration step was the co-precipitation of Se with $Fe(II)OH_2$. The DPCSV was carried out in the presence of Cu^{2+} as this gave better linearity and better sensitivity. The detection limit was found to be 10ng $500mL^{-1}$.

Parameters:

Deposition potential = -0.45 Deposition time = 60s

Preparation of 1000 ppm Se as Sodium selenate

Na_2SeO_4 contains 41.8 % Se. Since 1000 ppm Se contains 1.000 g dm^{-3}, this is equivalent to 2.392 g dm^{-3} of Na_2SeO_4. Therefore 0.5986 g of Na_2SeO_4 was accurately weighed out and transferred to a clean 250 cm^3 volumetric flask. The volumetric flask was made up to the mark with distilled water. This stock solution was made up freshly every two weeks. Dilutions were made up in different media using this stock for the relevant experiments.

Preparation of 1000 ppm Se as Sodium Selenite

Na_2SeO_3 contains 45.67 % Se. Since 1000 ppm Se contains 1.000 g dm^{-3}, this is equivalent to 2.1896 g dm^{-3} of Na_2SeO_3. Therefore 0.5474 g of Na_2SeO_3 was accurately weighed out and transferred to a clean 250 cm^3 volumetric flask. The volumetric flask was made up to the mark with distilled water. This stock solution was made up freshly every two weeks. Dilutions were made up in different media using this stock for the relevant experiments.

HCl dilutions:

Concentrated HCl is 37% m/v and contains 36.46 g mol^{-1}. Dilutions were carried out using distilled water in clean dry volumetric flasks. 6M HCl was prepared by diluting 510 cm^3 of the concentrated acid to 1000cm^3 with distilled water. 1M HCl was prepared by diluting 85 cm^3 of the concentrated acid to 1000cm^3 with distilled water.

For any concentration of hydrochloric acid below 1M HCl this solution was diluted further.

Dilution of selenate and selenite solutions

10ppm Se (as sodium selenate) was prepared by pipetting $1cm^3$ of the 1000 ppm Se (as sodium selenate) into a clean $100cm^3$ volumetric flask. The $1cm^3$ pipette was washed at least 10 times with the selenate solution before the measured amount was taken. The volumetric flask was made up to the mark with distilled water or with 1M HCl or 0.1M HCl or 0.1M $HClO_4$ depending on the experiment. This was prepared daily. 10ppm Se as selenite was made up exactly the same way as the 10ppm Se (as sodium selenate) using 1000 ppm Se (as sodium selenite) for the stock solution.

2.3 Instrumentation

The instrument used was a Radiometer POL 150 Polarographic Analyser (Radiometer Copenhagen) with a Radiometer MDE 150 Polarographic Stand using Trace Master 5 Software. The system was enclosed in a fume hood (Chemical Systems Control Ltd. Ashbourne, Co Meath.). The instrument was controlled by a Dell Optiplex 466/Le (personnel computer Dell Ireland) and polarograms were printed on a Hewlett Packard DeskJet 520 (Printer: Hewlett Packard Ireland). All additions of samples and standards were made using a Micropipette: Research Eppendorf (100μL) (Unitech: Belgarde rd, Dublin) with disposable tips.

2.3.2 Methods of Digestion

A number of different acids have been suggested for the digestion of organic materials.

A). The first mixture investigated was H_2SO_4 (Conc.), HNO_3 (Conc.), and $HClO_4$ (70%) in the ratio 1:1:1 (Metrohm 199)

500mg of the yeast was boiled for 40 minutes with 12mL of the 1:1:1 acid mixture and then allowed to cool to room temperature. The solution was clear but viscous. There was a light scum on the top of the solution. This was then made up to $50cm^3$ with conc. HCl for the reduction step.

B). The next investigation was on the 5:5:4 $HClO_4/H_2SO_4/HNO_3$ acid mixture. The $HClO_4$ and the H_2SO_4 was increased in relation to the HNO_3 and this was hoped to clear the solution of the remaining organics. The mixture was boiled for 35 minutes before being made up to $50cm^3$ with 6M HCl.

C). The digestion acid ($HClO_4/H_2SO_4/HNO_3$) was reduced to 4:4:3 to reduce the time it took the sample to dissolve. So the boiling time that was used was 30 minutes.

D). H_2SO_4 and H_2O_2 (Bruttel and Schäfer 1990)

The procedure for this method is along the lines outlined by Metrohm. Originally this method had been designed for wet digestion of various cereals for the voltammetric determination of Cu and Zn but has been modified for our purposes. However, various changes were developed through the course of the experiment resulting in the following procedure.

- 500mg of the yeast was accurately weighed out and warmed in $5cm^3$ of H_2SO_4 at 70 ^0C for two minutes on the isomantle until the solution had turned a light brown colour and the yeast had adsorbed the solution.
- The solution was then taken off the direct heat.
- $5cm^3$ of 35% H_2O_2 was added using a pasteur pipette so the hydrogen peroxide could be added drop-wise and to avoid splashes.
- The reaction was allowed to subside before the next drop of peroxide was added. This was gently warmed and the solution went clear. This step was repeated until the whole 5 cm^3 of the hydrogen peroxide was used.
- The flask was then placed on to the isomantle at 110^0C and as the water resulting from the reaction was boiled off, the colour of the solution changed back to the brown colour once the sample had been dehydrated.
- Another $5cm^3$ addition of the 35% H_2O_2 was added and the procedure repeated again.
- A third addition of the hydrogen peroxide was made and this time the sample did not turn brown but stayed at a faint brown colour indicating that the organics had been destroyed.

A table giving the essential details of the various methods of digestion is given below (**Table 2.3**). It outlines the various acids that were used, along with their ratios and the duration of each digestion.

Table 2.3

Method	Reference	Ratio	Time
H_2SO_4/HNO_3 /$HClO_4$		1 : 1: 1	40 minutes
$HClO_4$ / H_2SO_4 / HNO_3		5 : 5 : 4	35 minutes
$HClO_4$ / H_2SO_4 / HNO_3		4 : 4 : 3	30 minutes
H_2SO_4 / H_2O_2	Metrohm (P. Bruttel and J. Schäfer)	5 : 20	40 minutes

Digestion D was chosen because it gave the best results for our yeast sample. The other methods were designed for digestion of low organic matter quantities and gave low results with spiked samples, indicating that the organic matrix was not sufficiently digested and complexing with the selenite and thus not allowing it to give the true Se concentration value.

2.4 The Polarographic procedure.

The theory of polarography has already been discussed (**Section 2.1**). A polarographic wave is a plot of current versus applied potential. The following diagram is an example of a typical polarographic scan obtained in this work, using the Differential Pulse Cathodic Stripping Voltammetry [DPCSV] with a solution of sodium selenite in 1M HCl as the electrolyte.

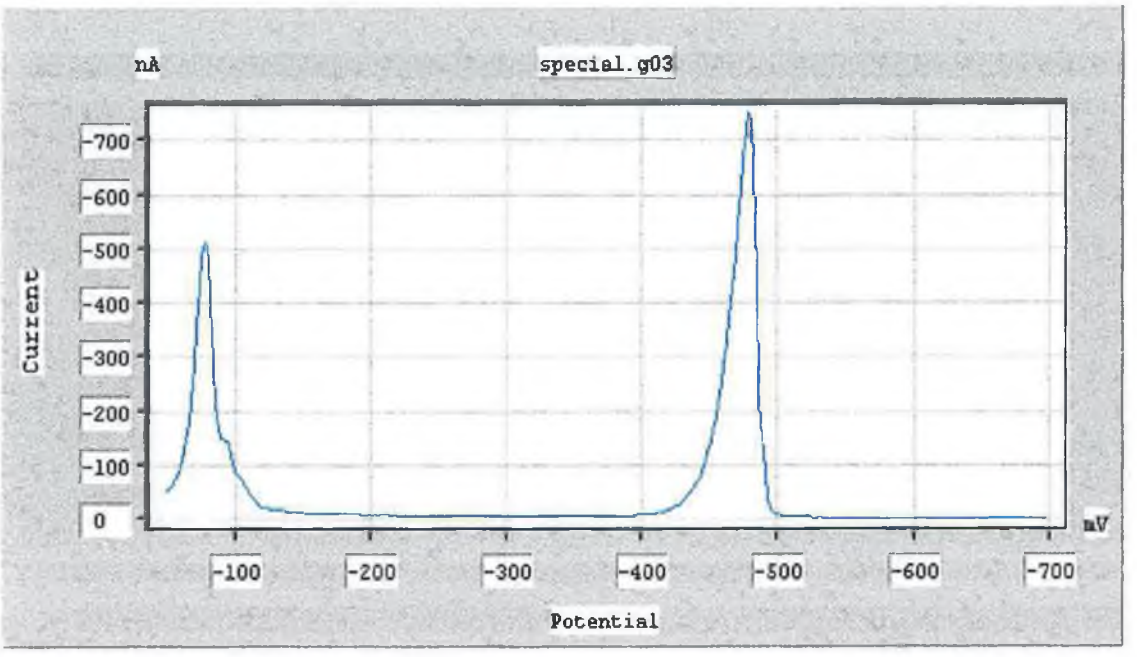

Fig 2.4

The following general procedure was followed. N_2 (oxygen free) (BOC gases Guildford Surrey) was bubbled through the supporting electrolyte (usually 10 cm^3 of 1M HCl) solution for 360 seconds to remove any dissolved oxygen. An aliquot of the 10ppm Se (as selenite) was then added using an automatic micro-pipette. The table below (**Table 2.4**) shows a typical set of operating parameters entered prior to running a scan.

The initial deposition potential (E_d) was set for a certain electrolysis time (t_e). The solution was stirred at 300 r.p.m. for the duration of the deposition time. During this time the selenite is reduced at the surface of the mercury drop.

$$Hg(0) + Se(IV) + 4e^- \rightarrow HgSe(s) \qquad \textbf{Eqn 2.10}$$

Table 2.4 Operating parameters for Se determination using DPCSV

Technique	DPCSV
Electrolysis Time	120s
Purge Time	360s
Waiting time	10s
No. of Drops	3
Drop Growth time	0.5s
Initial deposition potential	-50mV
Final potential	-700mV
Scan rate	12.5 mVs^{-1}
Pulse amplitude	-25mV
Pulse duration	0.4s
Step amplitude	2mV
Electrolyte	1M HCl
Standard	10ppm Se as selenite in 1M HCl

Stirring was stopped for a waiting time of 10 seconds during which the initial potential was still applied. The voltamogram was then recorded at a certain scan rate in a negative direction to a final potential. During the scan two peaks appeared. The peak at –480 mV was used in this work. This peak is due to the reduction of the mercuric selenide layer on the surface of the drop.

$$HgSe\ (s) + 2H^{+}\ (aq) + 2e^{-} \rightarrow Hg(s) + H_2Se \qquad \textbf{Eqn 2.11}$$

At the beginning of each stripping cycle, two mercury drops were discarded in order to give a fresh surface for each scan. The data was obtained at room temperature,

except where indicated. Using the software on the Trace Master 5, the peak height was measured and recorded for the selenium peak at approximately –480mV.

In developing the polarographic procedure the following experimental investigations were undertaken.

1. Effect of deposition potential.
2. Effect of pressure on the mercury drop.
3. Effect of deposition time.
4. Reproducibility of a measurement.
5. Determination of the linear calibration range.
6. Working calibration curve.
7. Effect of supporting electrolyte.
8. Effect of increasing acid concentration on linearity..
9. Effect of Cl^- on Selenite peak
10. Reduction of selenate solution.
11. Effect of stoppering the reduction flask.
12. Effect of the organic matrix on Se yeast.
13. Analysis of the Se enriched yeast.

2.5.1 Effect of the deposition potential on the Se signal.

In order to carry out reproducible, accurate and quantitative recordings the various parameters for the analysis must be investigated. A set of optimum parameters is needed. This section deals with the investigation of the parameters and their effect on the selenium peak (peak height, shape, resolution, sensitivity etc.).

The effect of the initial potential at which deposition of the HgSe was carried out was investigated. Adeloju (1983) investigated various initial potentials from -200mV to –400mV (v's Ag / AgCl) for determining selenium in samples containing relatively high concentrations of other metal ions. It was concluded that more negative potentials were superior to the more positive values around zero volts used by previous workers. The more negative the initial deposition potential the better the shape, resolution and height of the selenium peak to the selenium peak formed at much more positive potentials. In the work reported here, the initial potential was varied from zero to –350 mV in 25 mV increments (using a solution containing 60μL of 10 ppm Se (as selenite) in 1M HCl). The conditions for this experiment are as shown in **Table 2.4** except for the initial potential which is being varied.

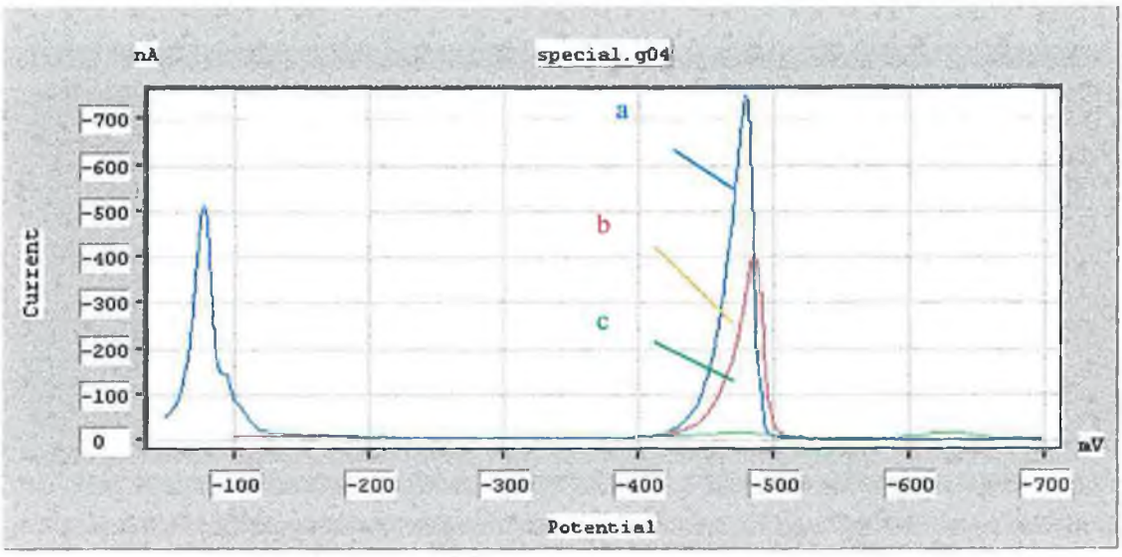

Fig 2.5

Fig 2.5 contains illustrative polarograms at initial deposition potentials of –50 mV (a), -100 mV (b) and –200 mV (c). More positive initial potentials gave rise to two peaks, due to selenium, at –480 mV and –80 mV. The second peak at –80mV is often unsymmetrical and was previously found not to correlate with Se concentration (Mattsson *et al.*1994). As the initial potential becomes more negative this peak falls outside the scan range. The peak at –480 mV, which has been confirmed as the HgSe peak (Mattsson *et al.*1994), shifts to slightly more negative values as the initial deposition becomes more negative (**Fig 2.5a and 2.5b**).

A Table of deposition potentials and the resulting peak currents is given in *Appendix Table 2.1* and shows any variation in parameters away from those in **Table 2.4**.

The results were plotted in **Fig 2.6** below, which shows the sensitivity to deposition potential.

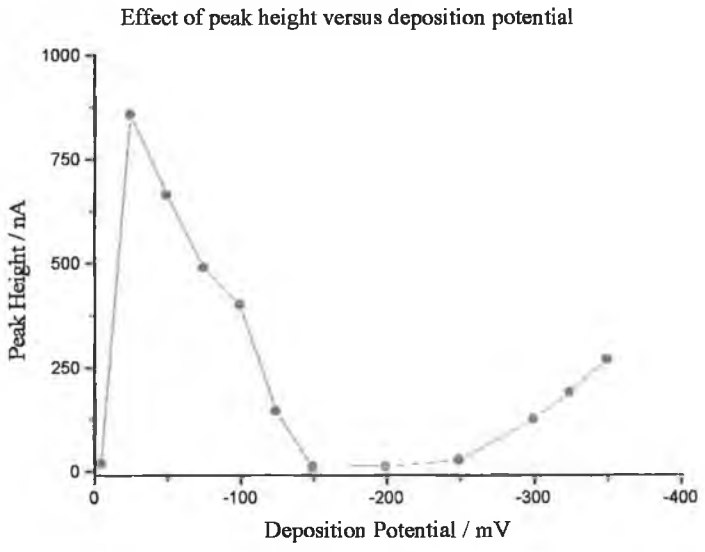

Fig 2.6

The results do not agree with those of Mattsson (1994). Therefore, an initial deposition potential of –50 mV was chosen as a standard operating parameter, as it gives the optimum combination of sensitivity, peak symmetry and peak height. This deposition potential was used subsequently.

2.5.2 Effect of increasing the nitrogen pressure on the mercury drop.

The recommended operating procedures for the Radiometer POL 150 Polarographic Analyser instrument specify a nitrogen pressure of 2 Bar, at the nitrogen cylinder, and 1.2 Bar at the MDE (mercury drop electrode). It was therefore deemed necessary to test the effect of pressure on the peak current to investigate if a slight decrease or increase in pressure would affect the selenium peak current. An increase in the pressure at the MDE, should increase the drop size, which in turn increases the drop surface and thus the reactive surface is increased. Consequently, the premise is that the

amount of Selenium that can be absorbed onto the surface has increased so the peak current should increase.

The electrolyte which was employed was 1M HCl, to which 60 μL of 10 ppm Se (as selenite) was added. The instrument parameters were identical to those given in **Table 2.4**. The pressure on the drop was increased in 0.1 bar increments, from 0.9 Bar to 1.4 Bar, and the resulting polarographic waves were recorded. The concentration of the solution stayed constant. The reason was that, the fraction of Se that is reduced at the drop is negligible, in relation to the total concentration of the solution in the polarographic cell.

The polarographic wave that resulted was similar to the example of the polarographic wave that is given in **Fig 2.4**. The peak at 80 mV was not symmetrical as it had a shoulder at 100mV. This peak was not sensitive to gas pressure, as with increasing pressure the peak height did not increase. The peak at 470mV was more symmetrical and peak height increased with pressure as expected. The peak current at each pressure was recorded and the results are given are given below (**Table 2.5**).

Table 2.5

Effect of nitrogen pressure at MDE	
Pressure / bar	Current / nA
0.9	177
1.0	196
1.1	207
1.2	219
1.3	235
1.4	247

These results were graphed as a plot of current versus pressure **Fig 2.7** below.

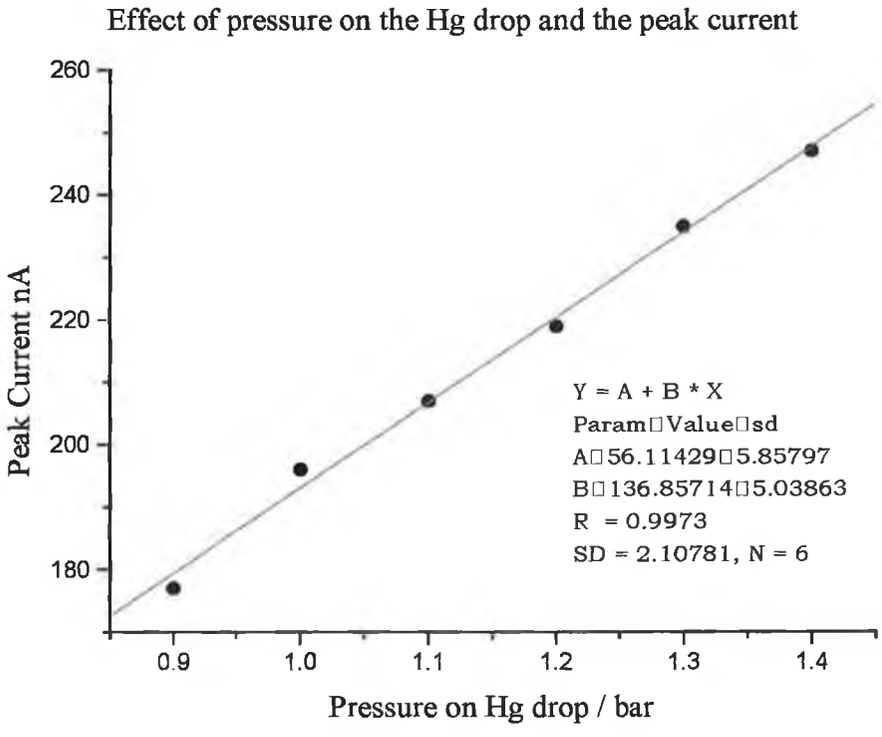

Fig 2.7

Using the linear regression results i.e. $Y = A + B*X$ we may write:

$$i = 136.9\,P + 56.11 \qquad \textbf{Eqn 2.12}$$

This equation may be used to correct for variation in pressure if required. **P** is the pressure (bar) at the time of the experiment and **i** is the current (nA) of the Se signal. For any given experiment if pressure is not constant then a correction factor can be made using the above equation. However, since samples and standards were normally measured on the same day, this correction was deemed unnecessary. If the pressure

drops from 1.2 Bar to 1.1 Bar during an experiment the current would drop from 220.4 nA to 206.7 nA an error of 6.0 %.

2.5.3 Effect of deposition time on the Se peak current.

Theoretically, the observed peak current should be directly proportional to the electrolysis or deposition time (t_e); however, this is not often the case in practice. The lower concentrations of selenium (IV) examined (2 and 10 ng/mL) obey this relationship for electrolysis time up to 240 seconds and 120 seconds, respectively, while the response for the high concentrations (above 10 ng/mL) was only linear with electrolysis time up to 60 seconds (Adeloju, 1983). It appeared that an equilibrium surface concentration is reached in the latter case, when longer deposition times are used. The use of an electrolysis time of 60 seconds enabled determination of selenium within a linear working range of 0-100 ng/mL and with a detection limit of 0.25 ng/mL. (Adeloju, 1983)

The following experiment was undertaken to establish the ideal length of time for the deposition potential for this specific project. Using Adeloju's (1983) work as a guide line, the deposition time was initial set at 20 seconds using all the other parameters as described in **Table 2.4**. 10cm^3 of the 1M HCl electrolyte was placed into the cell. 60µL of 10ppm Se (as selenite) made up in 0.1M HCl was added, using an automatic micro-pipette. The polarographic scan was then run and a selenium peak current recorded and plotted against time. The deposition time was increased in 20 seconds

intervals up to 200 seconds and the respective polarographic scans recorded. The following results were obtained.

Table 2.6

Deposition time / Seconds	Peak Current / nA
20	60.503
40	87.053
60	123
80	152
100	186
120	213
140	251
160	287
180	323
200	361

The plot shown is the peak current against deposition (electrolysis) time.

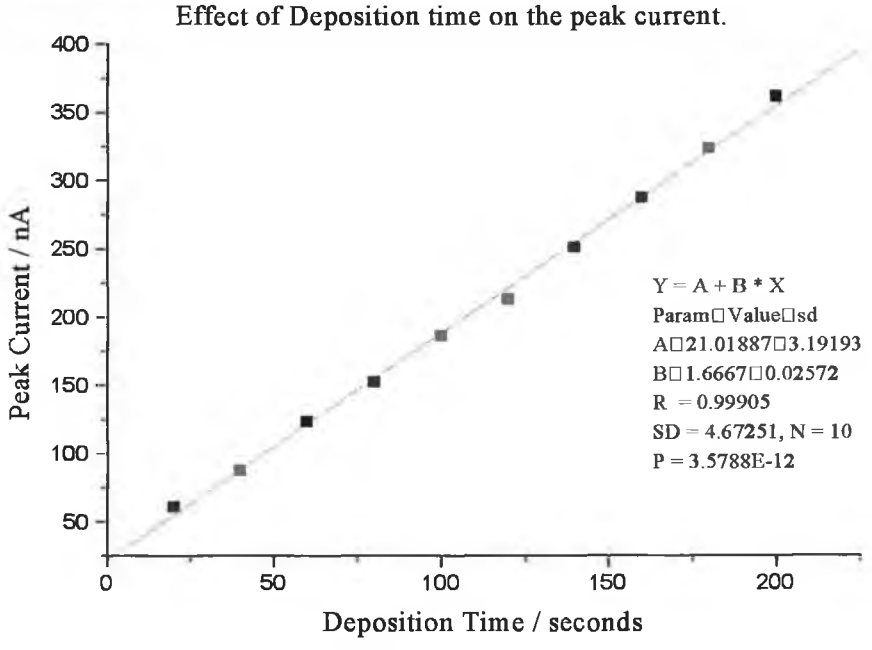

Fig 2.8

In the work reported here a deposition time of 120 s was normally used.

2.5.4 Reproducibility of a measurement.

The purpose of this experiment was to measure the reproducibility of the measured current. $10cm^3$ of the 1M HCl electrolyte was placed into the cell to which 60μL of 10ppm Se (as selenite made up in 0.1M HCl) was added. Nine successive polarographic runs were carried out without changing the solution. The resulting peaks were measured and recorded. Parameters are as in **Table 2.4** and results are given in **Table 2.7**.

The equations for calculating the mean, standard deviation, coefficient of variance and the 95% confidence limits are described in *Appendix Table 2.2*. The following statistical results were obtained using these equations.

$Mean(\bar{x}) = 191$

Standard deviation (s) = ± 7.549

Coefficient of variance (r) = 3.952

95% Confidence Limits = 191 ± 8.44

Table 2.7

Number of Sample	Current / nA
1	168
2	175
3	164
4	172
5	176
6	165
7	172
8	175
9	168
10	167

Diagram **Fig 2.9** illustrates the reproducibility of the measurements in the form of a control chart showing the mean and the upper and lower 95% confidence limits.

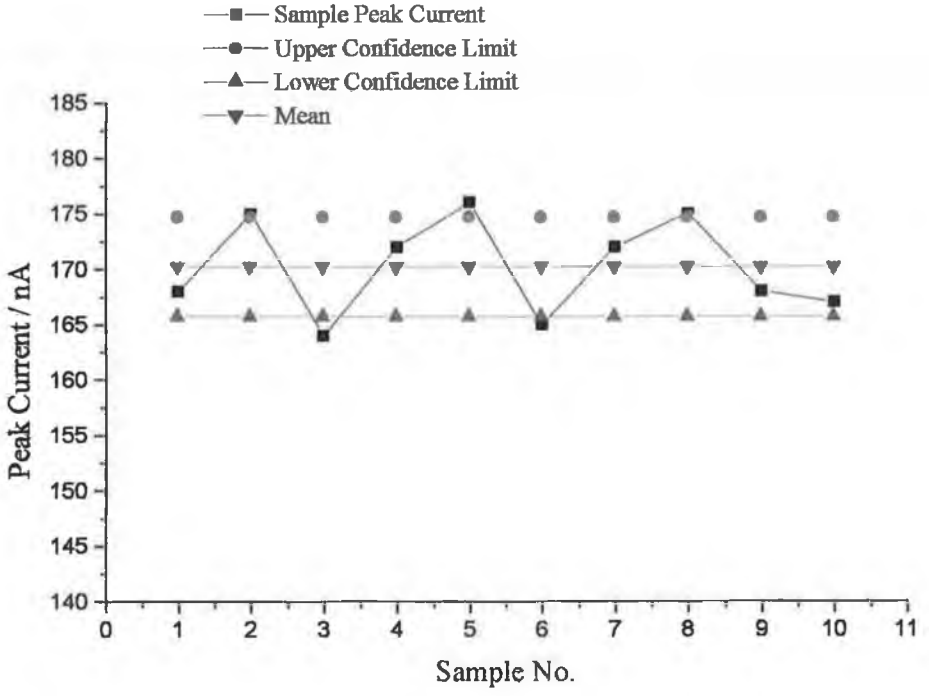

Fig 2.9

In a second experiment, the same concentration of Se was used but the cell solution was changed prior to each polarographic run. Parameters and as **Table 2.4** and the results are shown on **Table 2.8** and the control chart is shown on **Fig 2.10**.

Mean (x) = 170.2

Standard Deviation (s) = 4.366

Coefficient of Variance (r) = 2.565

95% Confidence Limits = 170.2 ± 3.5

Table 2.8

Sample Number	Current / nA
1	189
2	178
3	188
4	191
5	199
6	188
7	204
8	187
9	195

Diagram **Fig 2.10** illustrates the reproducibility of the measurements in the form of a control chart showing the mean and the upper and lower 95% confidence limits.

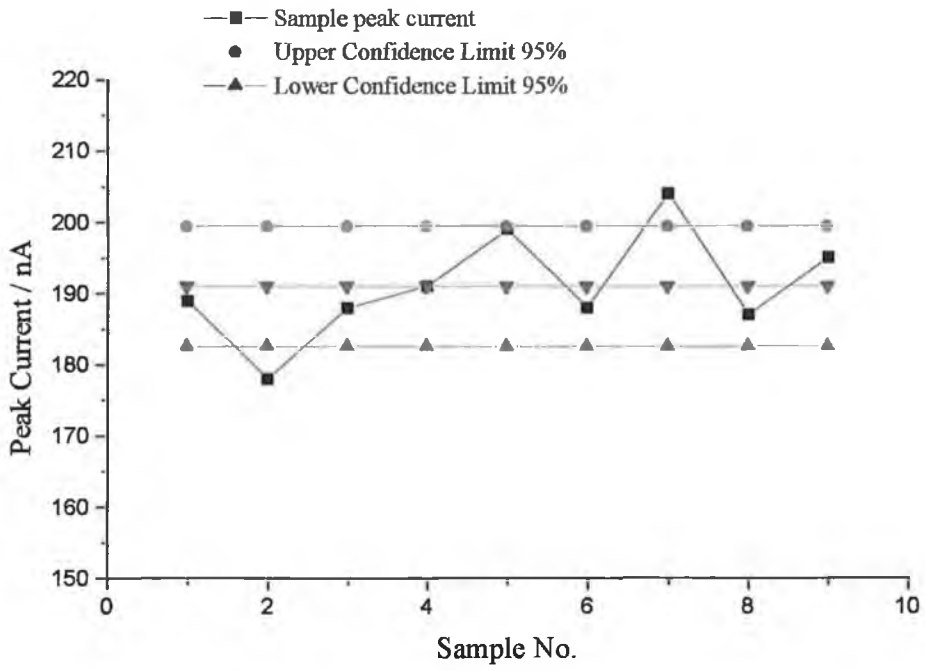

Fig 2.10

The latter experiment indicates clearly the reproducibility (r =2.565) of the selenium peak current. The average peak current however is significantly lower than that obtained in the first experiment. Using the data analysis tool in Excel a t-test for Two-sample means (assuming unequal variances) gave a calculated t-value of 7.25 and a critical t-value of 2.16. Since the calculated value exceeds the critical value the null hypothesis is rejected and there is a significant difference between the means. This test is discussed in detail in **Section 3.4.10**. This indicates a large variation from day to day in selenium peak current and rules out direct determination using a calibration curve as an analytical method. For this reason a standard additions procedure will be described later for analytical purposes.

2.5.5 Determination of the linear calibration range

In this experiment the Se concentration in the polarographic cell was varied over the range 0.0019 ppm to 0.45 ppm. The experiment was divided into two sections, (a) a lower concentration range (0.0019 to 0.025ppm) in which the electrolysis time had to be increased to 300 s to get a significant peak current. The second part of the experiment was (b) a higher concentration range (0.039 to 0.45 ppm) where the electrolysis time was reduced to 120 seconds. The remaining parameters were as shown in **Table 2.4**. The results are given in *Appendix Table 2.3* (lower concentration range) and *Appendix Table 2.4* (higher concentration range). Plots of peak current against Se concentration in ppm are given in **Fig 2.11** (lower concentration range) and **Fig 2.12** (higher concentration range).

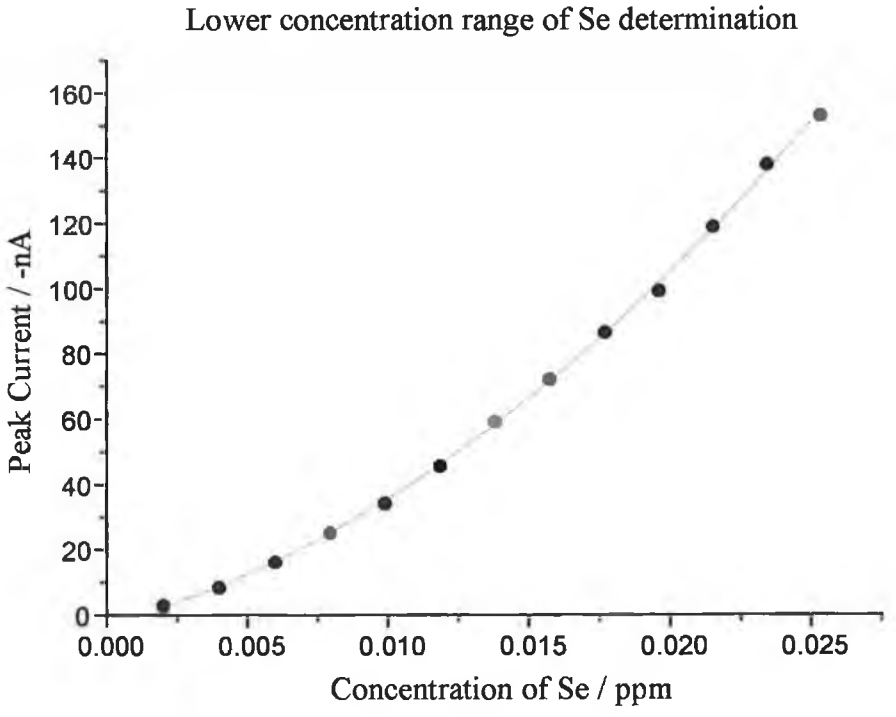

Fig 2.11

At lower concentrations, the calibration curve is not linear as can clearly be seen from **Fig 2.11**, while at higher concentrations, the curve becomes linear as shown in **Fig 2.12**.

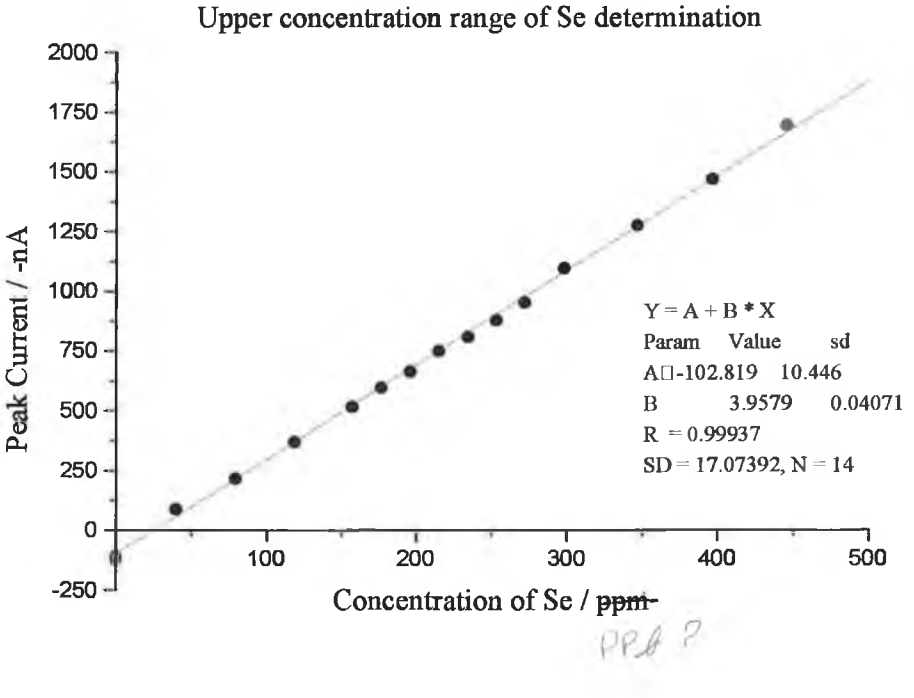

Fig 2.12

It is apparent that the linear range falls between 0.04 ppm and 0.4 ppm. Accordingly, it will be appreciated that if the linear range were extrapolated to the current axis a negative intercept would be obtained. The intercept of the graph is –82.47 nA. The conclusion that can be drawn is based on **Fig 2.11** that at very low concentrations the plot curves towards zero while at higher concentrations the line is linear. The result is in the linear region the intercept will always be negative.

2.5.6 Working Calibration Curve

Once the linear range had been established, 0.04ppm to 0.4ppm from **Section 2.5.5**, a working calibration curve was determined. A 10 cm^3 aliquot of 1M HCl was placed in the polarographic cell and aliquots of Se (10 ppm as selenite) were added. The peak current was obtained after each addition, using the operating conditions shown in **Table 2.4**. The experiment was repeated twice. The results are given in *Appendix Table 2.5*. The current readings were corrected for dilution and the calibration curve for each experiment was plotted separately. The statistical results for each curve are given in **Table 2.9** and their implications will be looked at in detail later.

Table 2.9

Parameter	First Exp.	Second Exp.	Third Exp.
Intercept (A)	-145.09 ± 3.446	-146.15 ± 3.597	-143.84 ± 5.875
Slope (B)	5.100 ± 0.036	5.094 ± 0.037	4.914 ± 0.061
R	0.9999	0.99989	0.99969
SD	2.596	3.127	5.106

A representative calibration curve using the data from the first experiment is given below (**Fig 2.13**).

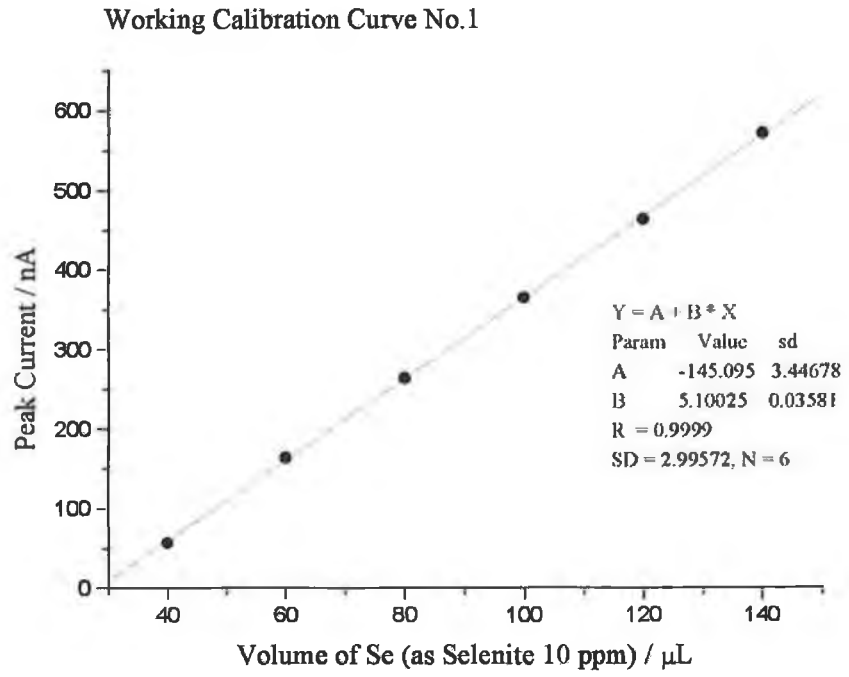

Fig 2.13

2.5.7 Effect of the supporting electrolyte

The effect of the supporting electrolyte has been investigated by many previous workers, using three supporting electrolytes namely HCl, H_2SO_4, and $HClO_4$. The number of peaks observed depended on the electrolyte used and on the deposition potential as shown in the **Table 2.10** below.

Table 2.10

Reference	Electrolyte	Deposition Potential	No. of Peaks	Peak Position
Potin-Gautier (1995)	0.1MH_2SO_4	-200 mV	1	-450 mV
Elleouet (1996)	0.1MHCl	-200mV	1	-610 mV
Mattsson (1994)	0.1M$HClO_4$	-350 mV	2	-600 mV and –850 mV
Mattsson (1994)	0.1MHCl	+50 mV	2	-50mV and –590 mV
Séby (1995)	0.1MH_2SO_4	-200 mV	1	-450 mV
Séby (1995)	0.1M HCl	-200 mV	1	-410 mV
Séby (1995)	0.1M $HClO_4$	-200 mV	1	-380 mV
Séby (1995)	H_2SO_4 + HCl	-200 mV	1	-440 mV

Typical polarographic scans of Selenium as sodium selenite in the various electrolytes are shown. Using HCl as the electrolyte the typical polarographic scan of Selenium as sodium selenite is given in **Fig 2.4**. The parameters that were used for the generation of this scan are given on **Table 2.4**. This shows two peaks, one at –80mV and the other at –480mV. This is similar to the scan of selenite in 0.1M $HClO_4$ **Fig 2.15**.

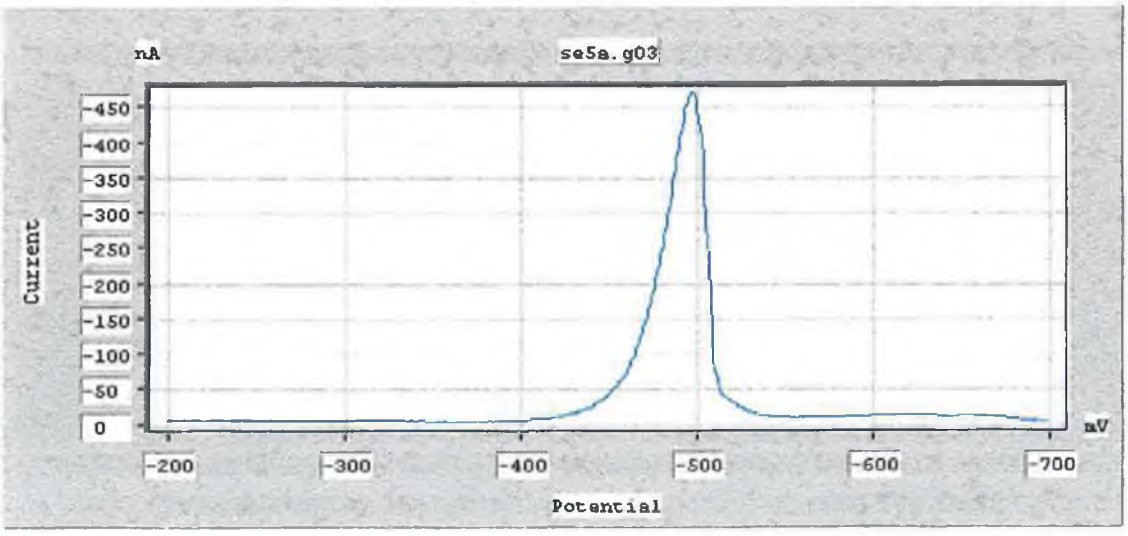

Fig 2.14 0.1M H_2SO_4

The second electrolyte that was investigated was H_2SO_4. Using 0.1M and the parameters as laid out in **Table 2.11** the polarographic scan of selenite in 0.1M H_2SO_4 was recorded **Fig 2.14**. No peak occurred for this electrolyte using the deposition potentials of the other two electrolytes. Therefore a deposition potential of –200 mV was used (Potin-Gautier 1995)

Table 2.11 Parameters for Fig 2.14 are as Table 2.4 except for the following:

Waiting time	20s
Initial Potential	-200mV
Pulse amplitude	-50mV
Pulse duration	0.2s
Step amplitude	1mV
Electrolyte	0.1M H_2SO_4
Standard	10ppm Se (as selenite) in 0.1M H_2SO_4

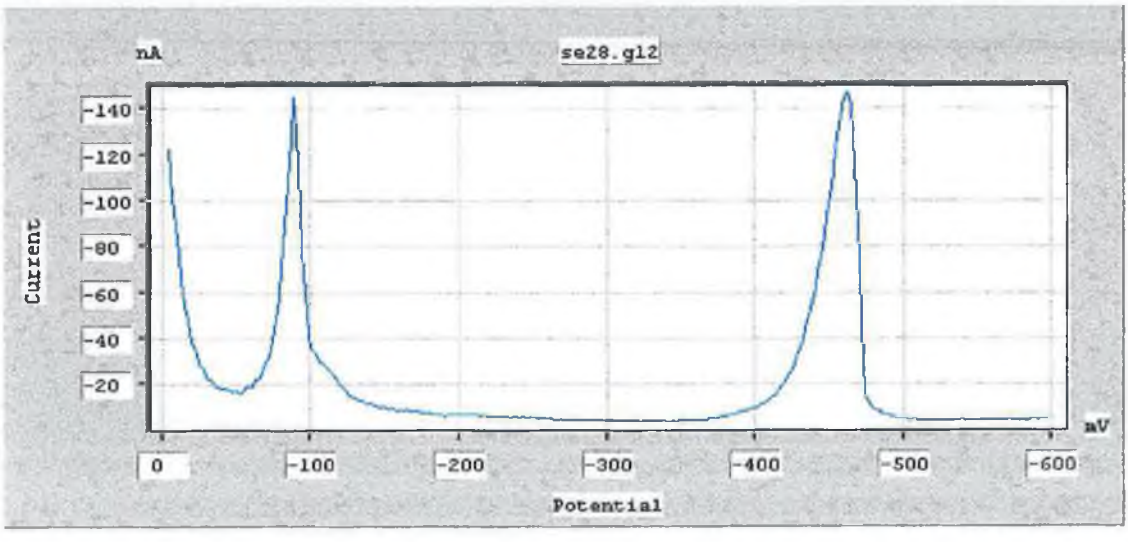

Fig 2.15 0.1M $HClO_4$

The third electrolyte under investigation was 0.1M $HClO_4$. Using the parameters laid out in **Table 2.12** a polarographic scan of selenium as sodium selenite was recorded and measured **Fig 2.15**. This scan has two peaks, as does the HCl scan. The first is at –95mV as opposed to –80mV for the HCl and the HgSe peak has shifted to –465mV as opposed to –480mV for HCl.

Table 2.12 Parameters for Fig 2.15 are as Table 2.4 except for the following:

Electrolysis	100s
Initial Potential	-5mV
Final Potential	-900mV
Scan rate	$12.5mVs^{-1}$
Step amplitude	5mV
Electrolyte	0.1M $HClO_4$
Standard	10ppm Se (as selenite) in 0.1M $HClO_4$

The 1M HCl was used in the analytical procedures for the following reasons.

- The reduction of selenate to selenite prior to analysis is carried out in 6M HCl so the electrolyte will contain HCl once the sample is added.
- The HCl electrolyte gives a smoother background scan than the other electrolytes.
- The HCl electrolyte gives the best-shaped Se peak with a good peak height.

2.5.8 Effect of increasing acid concentration on linearity.

The form in which selenium is adsorbed onto a mercury drop electrode is dependent upon the composition of the chosen supporting electrolyte. Acidic electrolytes such as hydrochloric, hydrobromic, sulphuric, and nitric acids show much greater sensitivity for selenium than either neutral or basic electrolytes (Adeloju *et al.*, 1983). Hydrochloric acid was chosen as the appropriate electrolyte for this work for a number of reasons.

(i) HCl gave the best sensitivity for selenium,

(ii) HCl enabled good resolution of the selenium peak

(iii) HCl is often used to reduce selenium to its electroactive Se (IV) state after decomposition of the sample material.

In the analytical procedures described below the sample solution contains 6M HCl. Addition of an aliquot of this solution to the supporting electrolyte could conceivably alter the HCl concentration in the supporting electrolyte and thus affect the resulting Se peak height.

In this experiment a calibration curve was prepared in the same way as described in **Section 2.4.2** except that one aliquot of standard Se solution contained 6M HCl instead of 0.1M HCl as was the case for the other standards. Two experiments were carried out. In the first experiment, the supporting electrolyte was 0.1M HCl and the resulting calibration curve is given in **Fig 2.16**. The results for the 0.1M HCl electrolyte are given in *Appendix Table 2.7*.

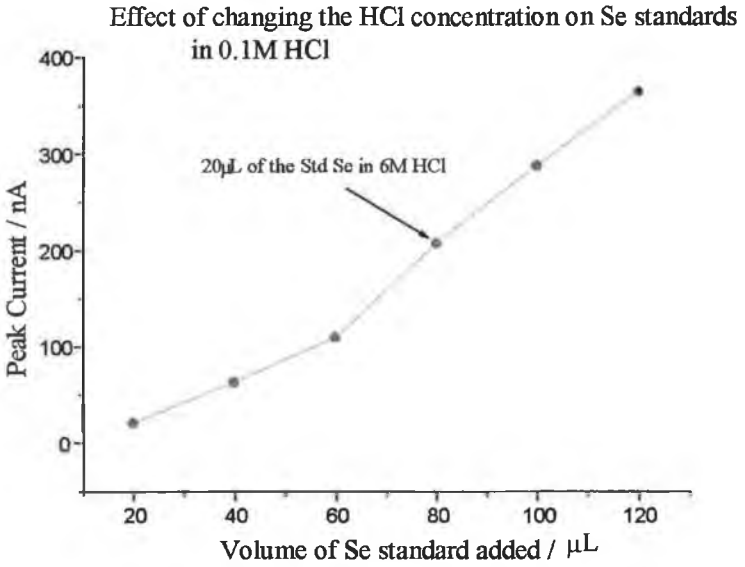

Fig 2.16

In the second experiment, the supporting electrolyte was 1M HCl and the resulting calibration curve is given in **Fig 2.17**. The results for the 1M HCl electrolyte are given in *Appendix Table 2.8* and *2.8a* and a plot of the calibration curve is given in **Fig 2.17**.

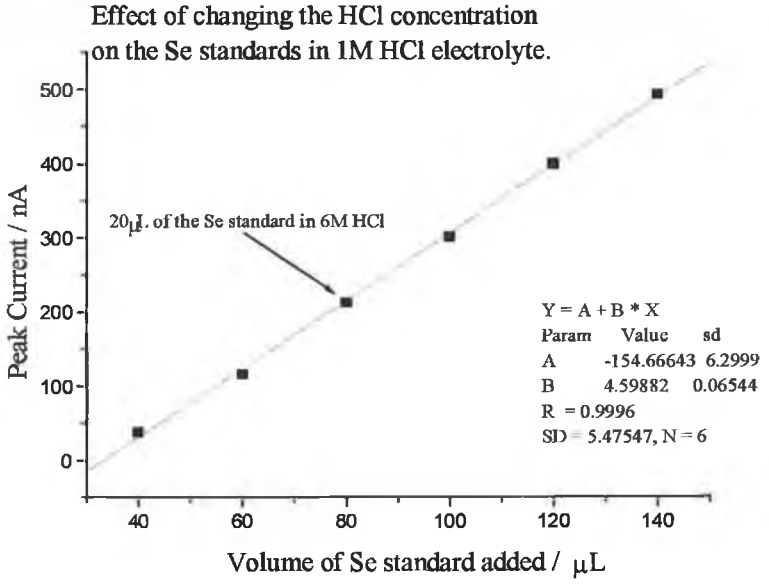

Fig 2.17

Therefore, 1M HCl was used as the supporting electrolyte for all subsequent analytical determinations.

2.5.9 Effect of Cl^- on the selenite peak.

By changing the electrolyte to 0.1M perchloric acid, all free chloride ions are removed from the solution, thereby allowing a study of the effect of chloride ions on the selenite peaks to be carried out. The electrolyte is still sufficiently acidic to keep the selenium in the electrochemically active form i.e. the selenite form. 100μL of the standard Se (as Selenite 10ppm) solution made up in 0.1M $HClO_4$ was added to the $10cm^3$ and scanned. This gave two peaks at –545 mV (-0.318 μA) and at –76 mV (-18.610 nA). 50μL aliquots of 1M HCl were then added and the results were scanned in each case. The concentration of the Se did not change over the course of the experiment because the amount of Se reduced was negligible. The parameters for this experiment are given in **Table 2.12** above. The results are given in *Appendix Table 2.6*.

Plots of peak height versus volume of 1M HCl added are given in **Fig 2.18** (-545 mV) and **Fig 2.19** (-76 mV).

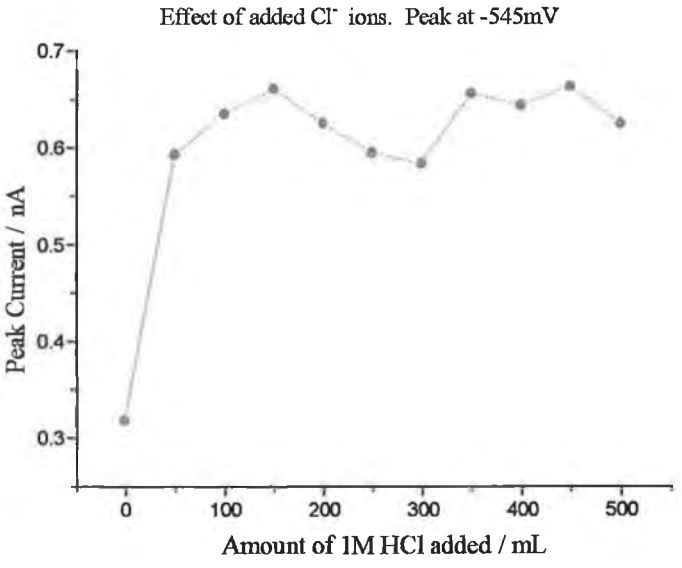

Fig 2.18

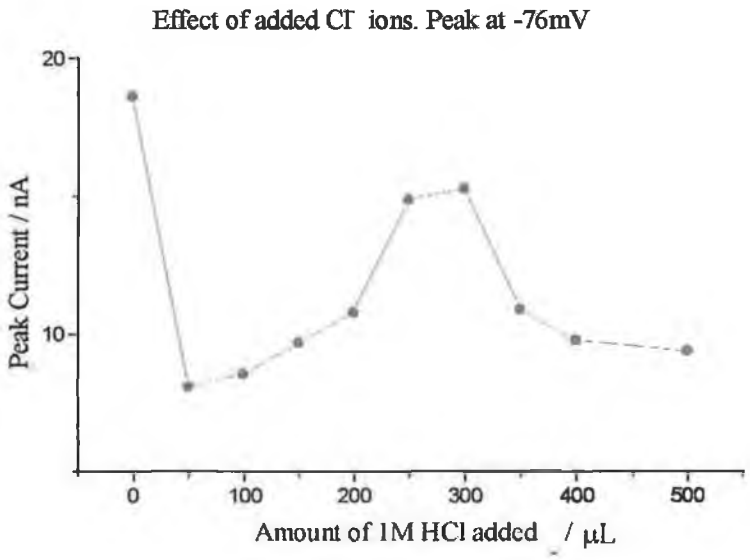

Fig 2.19

The results show that addition of a trace amount of chloride increases the selenium peak signal at –545mV. The effect quickly reaches a limiting value. The opposite effect is observed at the –76mV peak.

2.5.10 Reduction of selenate solution.

HCl reduces selenate to selenite as in the following reaction:

$$SeO_4^{2-} + 2H^+ + 2Cl^- \longrightarrow SeO_3^{2-} + H_2O + Cl_2 \qquad \textbf{Eqn 2.13}$$

The reaction rate is temperature dependent. An attempt to measure the rate of reduction of selenate to selenite at different temperatures was undertaken. The

parameters are as in **Table 2.4** except for the following alterations described in **Table 2.13**.

Table 2.13

Electrolysis	90s
Initial Potential	-50 mV
Final Potential	-600 mV
Standard	35ppm Se as selenite in 1M HCl

The selenite standard was only used in the room temperature experiment.

The next experiment was designed to find if the selenate could be reduced quantitatively to selenite, which is electrochemically active, and if so what temperature is the optimum for this reduction based on time, reproducibility and total reduction.

1. **Room temperature experiment**: a standard sodium selenate solution was made up in 6M HCl in a 100 cm^3 volumetric flask. The flask was mixed thoroughly to ensure a homogenous solution. Over a period of time aliquots of the reducing sample were extracted using a micro-pipette and added to the 1M HCl electrolyte and analysed. Initially 20mL of the standard Se (as selenite) was added to the electrolyte to give a selenium peak. Further increases in the peak height, with additions of the reducing solution, were analysed and the results plotted on **Fig 2.20**.

Room Temperature. The data for this experiment can be found in ***Appendix Table 2.9***.

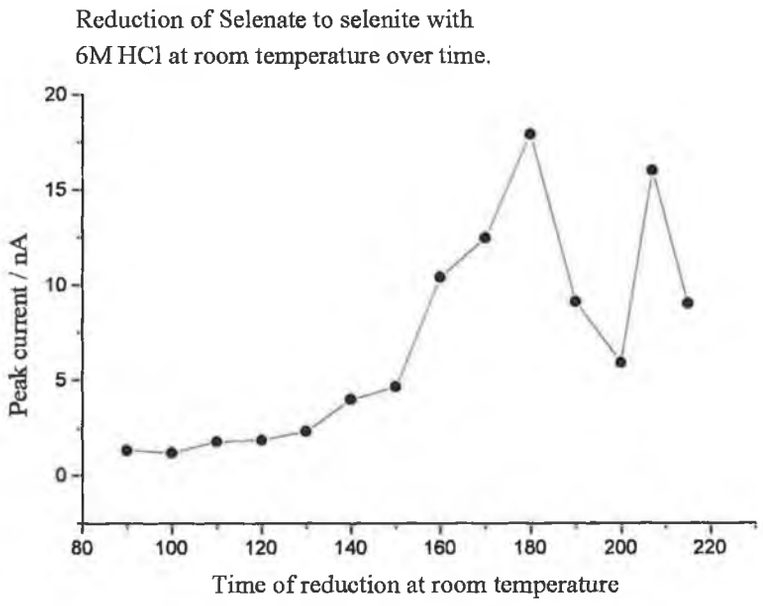

Fig 2.20

It is clear that at room temperature there is no significant reduction for 150minutes. The concentration of selenite increases with time up to 180 minutes but a plateaux is not observed.

2. Specific Temperatures [Other than Room Temperature]

When dealing with a specific temperature a water bath was employed. The water bath was set to the desired temperature and allowed to equilibrate. 6M HCl in a thin walled glass flask (thin walled to allow rapid heating) was placed in the water bath and weighed with a lead "O" ring to stop the flask from floating in the water bath. A 100cm^3 volumetric flask was also heated in the water bath. A certain volume of the standard sodium selenate solution made up in 0.1M HCl was added to the warm volumetric flask and was made up to the mark with the pre-heated 6M HCl. The flask was shaken to ensure a homogenous solution and then

replaced in the water bath. Over time aliquots of this reducing solution was added to the 1M HCl electrolyte, using the micro-pipette, and analysed. The results are plotted in **Fig 2.21** to **Fig 2.24**.

40^{0}C Temperature for reduction. The data for this experiment can be found in ***Appendix Table 2.10***.

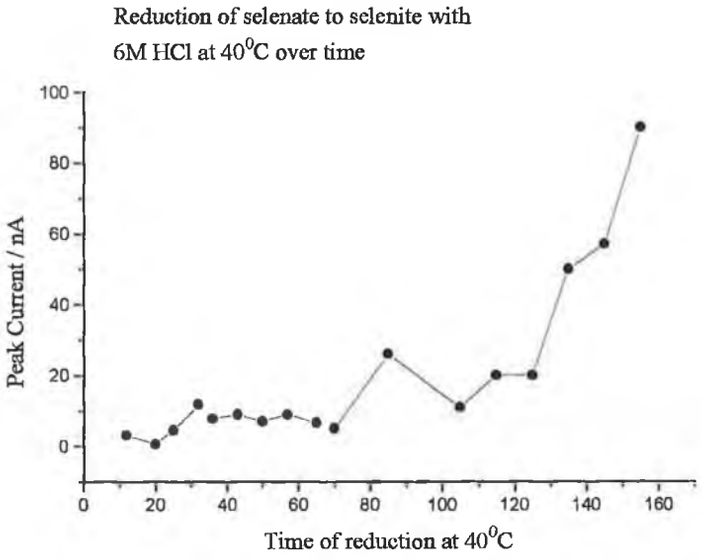

Fig 2.21

50^{0}C Temperature for reduction: The data for this experiment can be found in ***Appendix Table 2.11***.

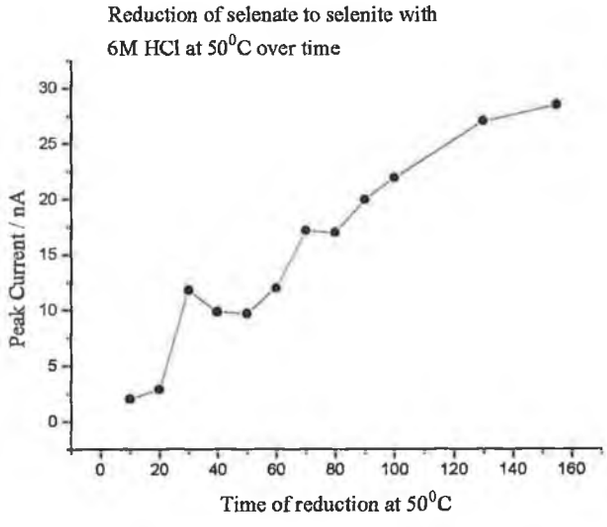

Fig 2.22

70^{0}C Temperature reduction. The data for this experiment can be found in ***Appendix Table 2.12***.

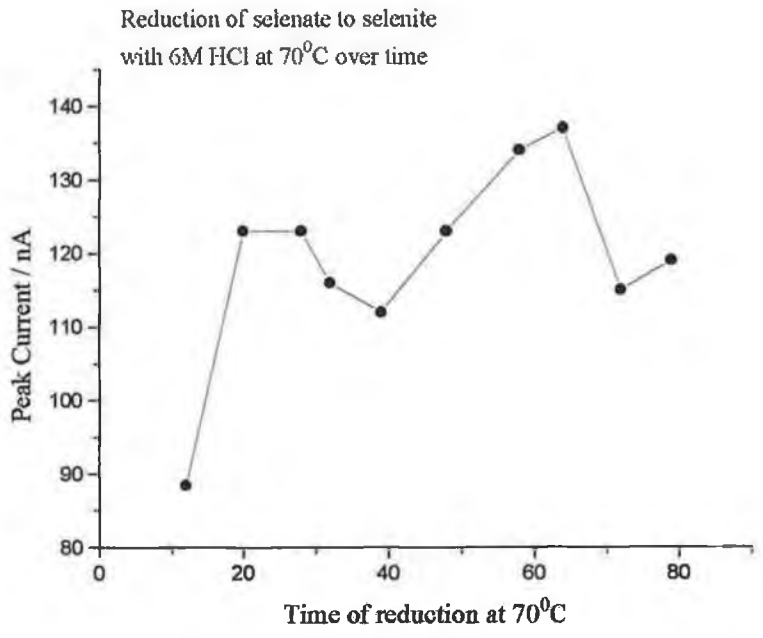

Fig 2.23

90^{0}C Reduction of Selenate Standard: The data for this experiment can be found in ***Appendix Table 2.13***.

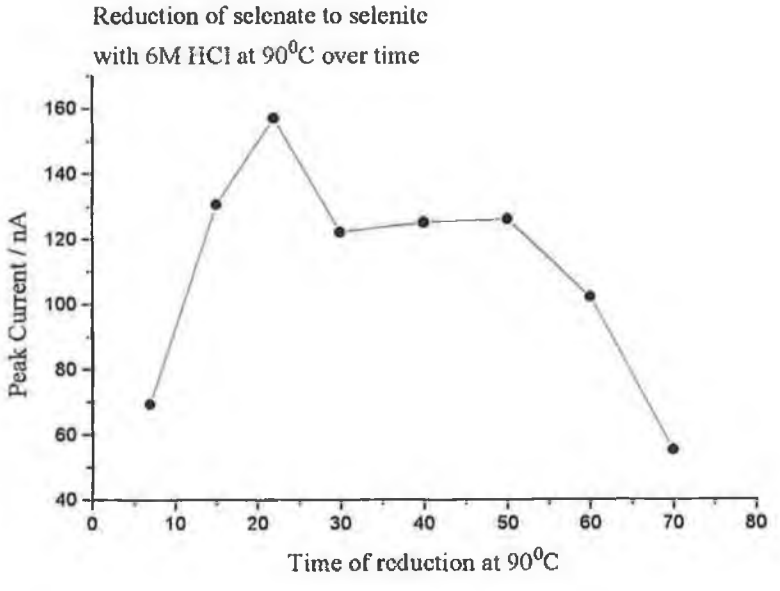

Fig 2.24

The rate of reduction at 40^0C is also very slow. No significant current is observed for 130 minutes. There is then an increase in Se current with time but no plateau is reached. At 50^0C selenium peak current is observed quite quickly (30 minutes) and appears to reach a limiting value after 140 minutes. At 70^0C reduction is rapid. There is large Se peak current after 20 minutes. However, no plateau is reached and behaviour is subsequently erratic. At 90^0C initial reduction is rapid. There appears to be a plateau from 30 to 50 minutes. Subsequently, the signal decreases indicating possible reduction of selenite to selenium. This is supported by the red solid that formed on the bottom of the vessel after time.

2.5.11 Effect of stoppering the reduction flask.

Boiling the solution at 98^0C should have no effect on the amount of selenium being reduced to H_2Se because it is supposed to be as stable as selenite. Two experiments were under taken: **(1)** to measure the amount of selenite present after 30 minutes reduction in 2M HCl at 98^0C **(2)** to measure the amount of selenite after 30 minutes reduction in 2M HCl at 98^0C with a cork stopper.

The procedure for both experiments was similar. A solution of 1000ppm SeO_3^{2-} was prepared [see description of preparation in **Section 2.2**]. This was digested as a yeast sample at 110^0C for 40 minutes with H_2SO_4 (conc.) and H_2O_2 (35%). All the Se present should then be in the form of SeO_4^{2-}. Therefore, it had to be reduced back to the selenite state before being analysed by the polarographic method. The digested sample was then made up to $50cm^3$ with 6M HCl, pre-heated to 50^0C, and analysed after 15 minutes. The standard was 10ppm Se (as selenite).

The parameters are the same as **Table 2.4** except that the electrolysis was reduced to 90 seconds and the step amplitude was increased to 5 mV thus increasing the scan rate to 20 mVs^{-1}. The results for the reduction of selenate to selenite in the open system are given in **Table 2.14** below and the results are plotted on **Fig 2.25** along with the data from the **Table 2.15** which is the stoppered flask (closed system).

Unstoppered Flask

Table 2.14

Volume of sample added / cm^3	Standard Se 10ppm (as selenite) added cm^3	Peak Current / nA
0.5	0	-232
0.0	0.1	-439
0.0	0.2	-638
0.0	0.3	-869

Stoppered Flask

Table 2.15

Volume of sample added / cm^3	Standard Se 10ppm (as selenite) added cm^3	Peak Current / nA
0.5	0	-85
0.0	0.1	-217
0.0	0.2	-395
0.0	0.3	-594

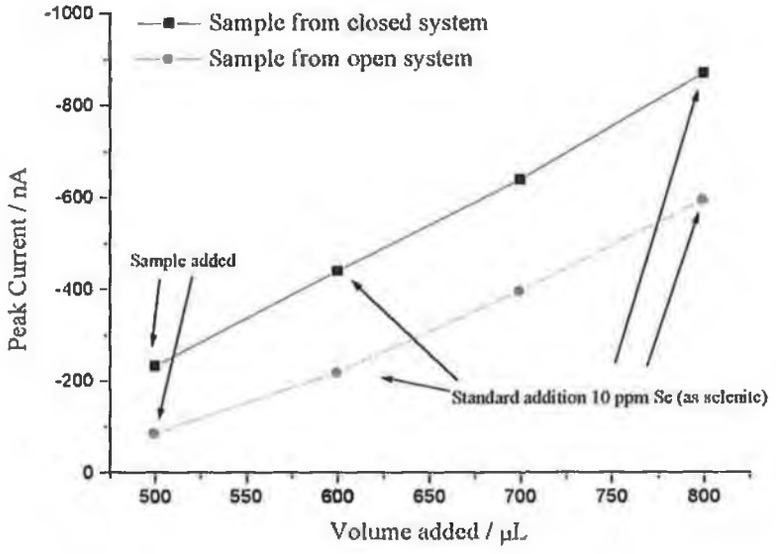

Fig 2.25

The graph clearly indicates that the stoppered sample had a higher content of Se than the unstoppered method, indicating that Se is being lost due to volatilisation.

2.5.12 Effect of the organic matrix on Se signal

The effect of the organic material must be accounted for in the digestion and reduction steps. The organic material is the yeast that both the non-enriched yeast and selenium enriched yeast was grown on. It was necessary to find out if the soluble products of the digestion process caused any interference in the determination of SeO_3^{2-} using this method. In order to investigate this, a yeast sample containing no selenium was digested. The effect of adding this extract to a standard solution of SeO_3^{2-} was investigated.

In the first experiment, $10cm^3$ of the 1M HCl, containing 50μL of 10ppm Se (as selenite), was placed in the polarographic cell and the polarogram recorded. The usual parameters [see **Table 2.4**] were applied with one exception, aliquots of organic blank (500mg of non-enriched yeast digested as in **Section 2.4.1**) were added and the polarogram recorded. A plot of peak current versus volume of blank added is given in **Fig 2.26**. The non-enriched yeast 500mg was digested and reduced with 6M HCl at 50^0C for 30 minutes as described above in **Section 2.2** and **2.4.2**. This solution is referred to as the "organic blank".

Table 2.16

Amount added μL	Material used	Peak current / nA
50	10ppm Se as selenite	34.46
25	non enriched yeast digested	10.661
50	non enriched yeast digested	128
75	non enriched yeast digested	112
100	non enriched yeast digested	125
125	non enriched yeast digested	124

150	non enriched yeast digested	120
175	non enriched yeast digested	115
200	non enriched yeast digested	125
225	non enriched yeast digested	123

After an initial decrease in the Se signal the peak current increased significantly and remained constant. Once 50μL of the blank was added the signal was not affected by the concentration of the blank but gave a better response than with just the electrolyte.

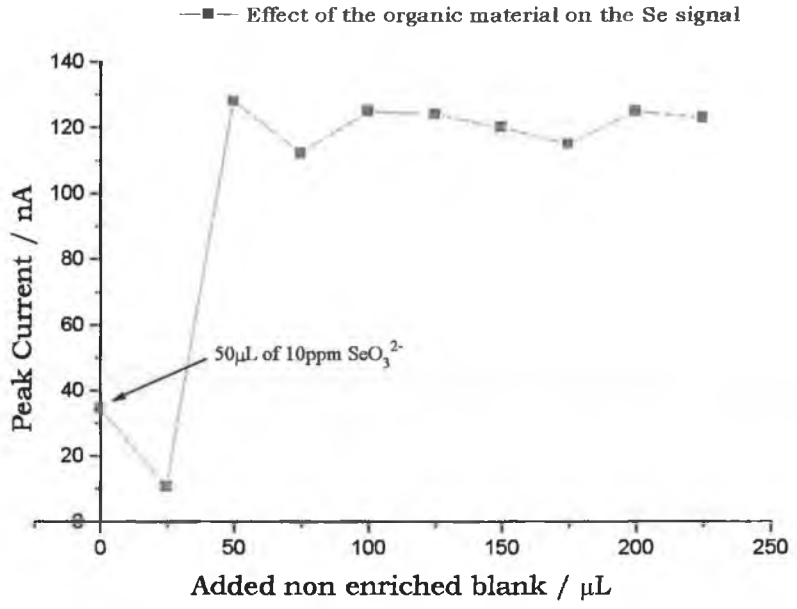

Fig 2.26

In the second experiment, the effect of the organic blank on linearity was investigated. $10cm^3$ of 1M HCl containing 500μL of "organic blank" was placed in the cell and increasing quantities of Se (10ppm as selenite) added, and the peak heights measured. A plot of the calibration curve is given below. 500mg of the Selenium enriched yeast was digested and reduced with 6M HCl at 50^0C for 30 minutes as described above in

Section 2.2 and **2.4.2**. This was added to the standard to also check if the Se yeast matrix is consistent with the non-enriched yeast matrix.

Table 2.17

Amount added µL	Material used	Peak Current / nA
500	digested organic "blank"	0
40	Standard 10ppm Se	93
60	Standard 10ppm Se	201
80	Standard 10ppm Se	312
100	Standard 10ppm Se	432
120	Standard 10ppm Se	562
20	sample of enriched yeast	678
140	Standard 10ppm Se	797
160	Standard 10ppm Se	913
180	Standard 10ppm Se	1024
200	Standard 10ppm Se	1165
220	Standard 10ppm Se	1292

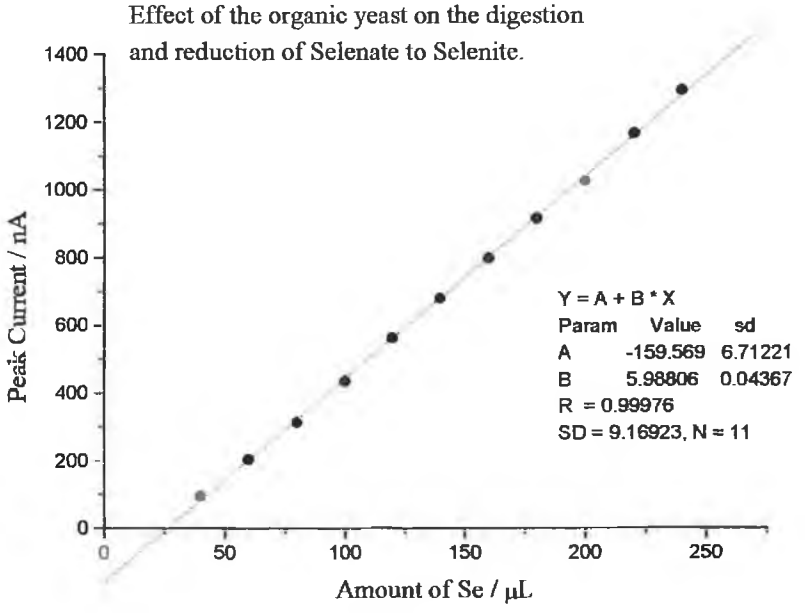

Fig 2.27

If the curve remains the same i.e. no change in slope before or after the addition of the organic matrix, then it is safe to say that the organic matrix or the digested organic matrix has no effect on the standard curve.

2.5.13 Analysis of the Se enriched yeast

In the analysis of an unknown yeast, the method of standard additions was used. A $10cm^3$ aliquot of 1M HCl was placed into the clean dry cell. The procedure described in **Section 2.4** was employed with the parameters given in **Table 2.4**. A large aliquot (120μL of 10ppm Se as SeO_3^{2-}) was added to bring the experiment into the linear range of the calibration curve. A further series of 20μL aliquots of 10ppm Se as SeO_3^{2-}, were added to check the linearity. The current reading at this point was estimated by regression from the calibration curve below [**Fig 2.28**] and used as a blank. A 20mL aliquot of the unknown was added followed by further 20mL aliquots of 10ppm Se as SeO_3^{2-}. The blank was subtracted from the current reading for the unknown and from each subsequent addition of standard. The concentration of Se was estimated by manual graphical standard additions initially to give a guideline for the future calculations.

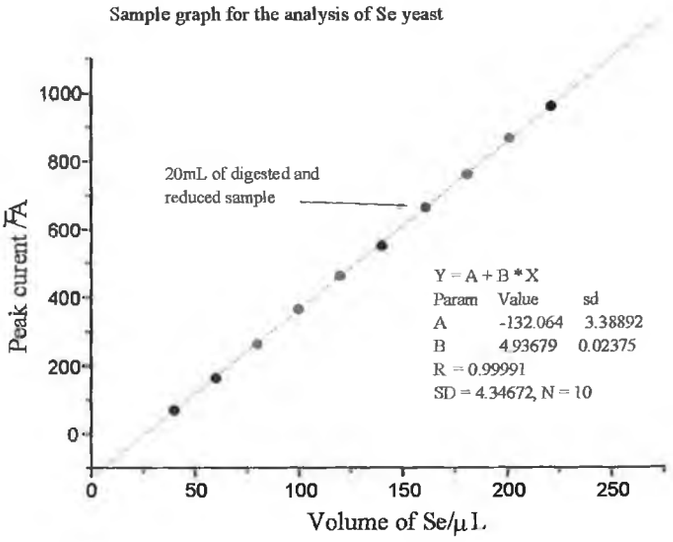

Fig 2.28

Using this method nine samples were measured and the results were compared with each other using statistical methods.

Table 2.18

Sample No.	Calculated volume of 10 ppm as selenite / μL	Concentration of Se in sample / ppm
1	23.7787	2377
2	23.3468	2335
3	24.1999	2420
4	25.5614	2556
5	22.844	2284
6	27.6087	2761
7	21.5184	2152
8	29.4996	2950
9	21.008	2101

The mean value for the volume of selenite used is 24.373μL which correlates to 2437ppm. The calculations were achieved using the Excel computer package and all calculations are shown in *Appendix 2.14* to *Appendix 2.15*.

3.1 X-Ray Fluorescence Spectroscopy (XRFS)

For trace element analysis X-Ray Fluorescence has the potential to be a very accurate and ideal instrument to use as it is non-destructive and requires little preparation. The theory behind XRF is a simple and well established one.

In an X-ray fluorescence spectrometer x-rays from the primary source (the x-ray tube) are used to excite the elements in a sample which then emit secondary x-rays which are characteristic of these elements. These emitted X-rays can be identified and quantified.

Excitation Sources.

In the photon excitation mode of XRFS X-ray tubes are still the most important sources of primary radiation. Typically a high voltage (60kV) is applied across a hot metal cathode and the electrons produced are accelerated by a tube current (80mA) towards a metal anode where the primary x-rays are produced. Various anodes are now available Cr, W, Sc, Rh. To provide good sensitivity for both light and heavy element determinations, dual -anode X-ray tubes have been developed. This works by having a thin layer of a light element (Cr,Sc) on a heavy element anode (Ag, Mo, Au, W). For light element excitation, the dual anode is operated at a low voltage so that almost all the electron energy is deposited in a top layer, while for heavy element excitation, the tube is operated at higher voltage, so that most of the electrons penetrate into the back of the anode.

A typical spectrum of the radiation [**Fig 3.5**] is given below and consists of a series of sharp peaks on a continuous background. The continuous part is due to the electrons radiating excess energy as they are decelerated in the target. The line frequencies are

characteristic of the target element. X-rays often accompany radioactive decay and isotopes such as ^{55}Fe, ^{109}Cd, and ^{238}Pu have been used as a source of x-radiation in portable instruments.

Origin of X-rays

X-ray photons are produced following the ejection of an inner orbital electron from an atom that has been irradiated and the subsequent transition of atomic orbital electrons from states of high to low energy, i.e. filling the vacant site that was left by the emission of the electron. This decrease of energy is followed by an emission of a photon of energy that falls in the x-ray region.

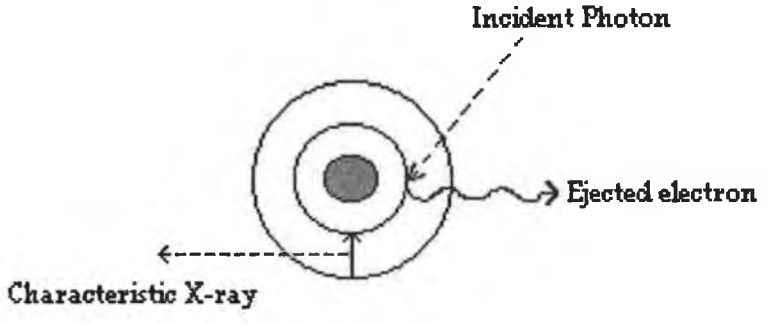

Fig 3.1

When a monochromatic beam of x-ray photon falls onto a specimen, three basic phenomena may result: scatter, absorption or fluorescence. The coherently scattered photons may undergo subsequent interference, leading in turn to the generation of diffraction maxima. The angles at which the diffraction maxima occur can be related to the spacing between planes of the atoms in the crystal lattice, and hence X-ray generated diffraction patterns can be used to study the structure of solid materials.

X-ray powder diffractometry involves characterisation of materials by use of data that is dependent on the atomic arrangement in the crystal lattice. An ordered arrangement of atoms contains planes of high atomic density. A monochromatic beam of X-ray photons will be scattered by these atomic electrons, and if the scattered photons interfere with each other, diffraction maxima may occur. In general, one diffraction line will occur for each unique set of planes in the lattice.

X-ray absorption effects

When a beam of x-ray photons falls onto a specimen an amount of the beam will be absorbed and an amount will pass through the specimen. The amount that passes through is given by the equation

$$I(\lambda) = I_0(\lambda_0)\mu\rho\chi \qquad \textbf{Beer's Law 3.1}$$

$I_0\lambda_0$ = Intensity of the x-ray photons(incident beam)

μ = mass absorption coefficient

ρ = density

χ = distance travelled through the material

As we see from the equation the amount of material used and the density of the material reduce the intensity of the transmitted beam. The denser the material the more shielding that is received from x-rays. This is why in hospitals' radiography nurses go into a lead lined room when taking x-rays and have lead lined aprons.

The primary beam may be scattered over an angle and can emerge as two types, **coherent** and **incoherently scattered wavelengths**. In the scattering process the x-rays interact with the electron cloud in the sample giving scattered x-rays of the same energy as the incident x-rays (elastic or Raleigh scattering), or giving x-rays of

slightly less energy (inelastic or Compton scattering). Both types of scattering result in the background radiation from the sample reaching the detector, a factor, which limits the sensitivity of the technique. *Compton scattering* results in broad peaks to the low energy side of the characteristic tube lines. Secondary fluorescence radiation may also arise from the sample. The depth *(d)* of the specimen contributing to the fluorescence intensity is related to the absorption coefficient (μ) of the sample for the fluorescence wavelength and the angle of emergence (the angle at which the beam exits the specimen) at which the fluorescence beam is observed.

The photoelectric effect is the ejection of electrons by photon impact. This results in the emission of x-rays of energy slightly lower than the energy of the incident photon. It is always accompanied by IR, UV, and Auger electron emission.

Photoelectric absorption occurs at each of the energy levels of the atom, thus the total photoelectric absorption is determined by the sum of each individual absorption within a specific shell. Where the specimen is made from a variety of elements, which is normally the case, the total absorption is made up of the sum of the products of the individual elemental mass absorption coefficients and the weight fractions of the respective elements.

The photoelectric absorption is made up of each absorption in the various atomic levels, and is dependent on the atomic number. A plot of the mass absorption coefficient as a function of wavelength contains a number of discontinuities called absorption edges, at wavelengths corresponding to the binding energies of the electrons in the various subshells [**Fig 3.2**].

Since each atom has a unique set of excitation potentials for the various subshells, these excitation potentials are labelled the K, L and M edges. The actual position of

the K, L, M, etc edges vary with atomic number and the single K edge, the three L edges and the five M edges correspond respectively to the one, three and five allowable J values described later. As the K, L and M edges vary this leads to each atom exhibiting a characteristic absorption curve, thus giving each element a characteristic "finger print" which can then be used for determination in the future.

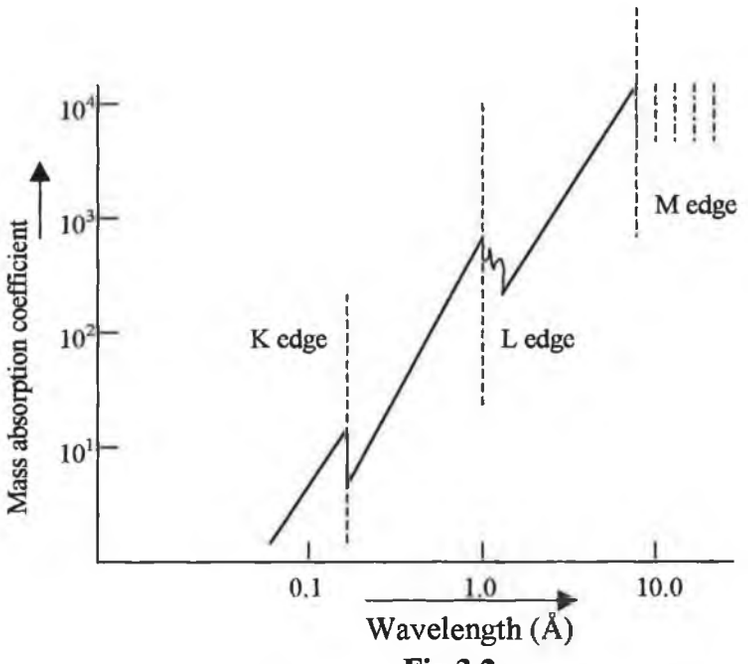

Fig 3.2

(Diagram from Lab-X 3000 Operator's Manual)

The magnitude of the signal i.e. the fraction of incident X-ray photons lost in passing through the absorber, increases significantly with the average atomic number of the absorbing material, (as the cube of the atomic No) $\Rightarrow$ Pb $\rightarrow$ Fe $\rightarrow$ Al.

Secondary radiation produced from the specimen is characteristic of the elements making up the spectrum. The technique used to isolate and measure individual characteristic wavelength is called X-ray spectrometry. Because the relationship between emission wavelength and atomic number is known, isolation of individual characteristic lines allows the unique identification of the element to be made, and elemental concentrations can be estimated from the characteristic line intensities.

When a high energy electron beam is incident upon a specimen, one of the products of the interaction is an emission of a broad wavelength band of radiation called "the continuum". Continuous radiation occurs following deceleration of the excited electrons, due to interaction of impinging electrons with those of the target. The **continuum** i.e. the number of photons as a function of their respective energy, is characterised by a short wavelength limit λ_{min}, corresponding to the maximum energy of the exciting electrons and by a peak maximum approximating to $2\lambda_{min}$. Short wavelength limit is inversely proportional to the applied potential (V_0). (Duane and Hunt, 1915 from Jenkins and DeVries 1970)

$$\lambda_{min} = \frac{hc}{V_0}$$

Eqn 3.2

h = plank's constant

c= velocity of light

hc = 12.4

V_0 = Voltage in kilovolts

The intensity of the overall intensity of the continuum increases with applied current (I) and potential (V) and also with the atomic number (Z) of the target material.

Characteristic Radiation

If a high energy electron (particle) strikes a bound atomic electron and the energy E of the particle is greater then the energy needed to bind the atomic electron to the atom it is probable that the atomic electron will be ejected out of the atomic orbital, departing

the atom with a kinetic energy, E - ϕ, where ϕ is the amount of energy holding the atomic electron in the orbital. The ejected electron is called a photoelectron and the interaction is referred to as the *photoelectric effect*. Now there is a hole or vacancy in the orbital, so the atom is in an unstable state, while its preferred state is stable. There are two processes by which it can revert to its original stable state.

If an electron is first ejected from the K shell, the resulting hole is filled by an L electron. The energy associated with this transference will be equivalent to $E_K - E_L$, this is termed the K_α line. The hole in the L shell may then be filled by an M electron, with the emission of an L line of energy ($E_L - E_M$). This process will continue until the energy of the atom is lowered to a value approximating to that associated with normal electron vibration in the outer orbitals – in general a few electron volts. There are rules that can be expressed in terms of quantum numbers which govern the number of lines and their energies. The energy of an electron is determined by its configuration, which in turn is dependent only upon **n** and **l**. The influence of the spin quantum number "**s**" however is sufficiently large to confer significant changes in **l** and it is necessary to consider the vector sum of **l** and **s**. This vector sum is called "**j**" and is the projection on the direction of the magnetic field, i.e.

$$j = l + s \qquad \textbf{Eqn 3.3}$$

The selection rules which determine the allowable transactions are that $\Delta l = \pm 1$ and $\Delta j = 0$ or ± 1.

Thus for the K series only p→s transitions are allowed, yielding two lines for each principal level change. The L series allows p → s, s → p, and d → p transitions. In general, transitions to the K shell give between two and six K lines and transitions to the L shell gives about 12 strong to moderately strong L lines.

The lines are named according to the transitions as shown in the following diagram [**Fig 3.3**]. The K_α line is the most intense.

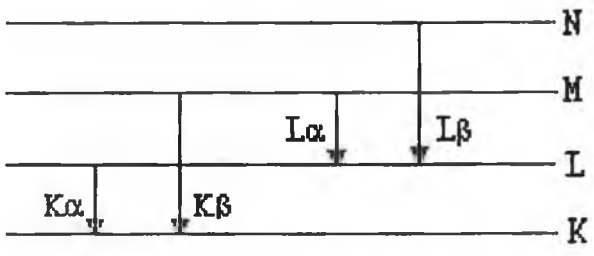

Fig 3.3

Since the wavelength of the radiation is inversely proportional to the difference in energy between the initial and final states of the transferred electron, it necessarily follows that wavelengths of lines within a series will decrease as the energy gap increases. Therefore, lines involving $\Delta n = 2$ will be harder (i.e. of shorter wavelength) than those arising from $\Delta n = 1$. Thus the K_β line is harder then the K_α line and so on. It will also be apparent that the wavelengths of different series will increase from K to L to M etc. A general expression relating the wavelengths (λ) of a characteristic line with the atomic number (Z) of the corresponding element is given in Mosely's Law (Smeaton, 1965).

$$\frac{1}{\lambda} = K(Z - \delta)^2$$

Mosely's Law Eqn 3.4

λ = Wavelength

Z = atomic number

K = constant for each spectral series

σ = shielding constant

Thus, although the intensity ratios of the various characteristic lines is constant for a given atom, they will gradually change with the atomic number [Z]. For instance, the intensity ratio K_α:K_β is about 5:1 for Cu but for smaller for the heavier elements (3:1 for Sn) and much higher for the lighter elements (25:1 for Al).

A second process by which the unstable atom reverts to its stable state involves a rearrangement of electrons which does not result in an emission of an X-ray photon, but in the emission of the other photoelectrons from the atom. This is known at the *Auger effect.*

Instead of giving off an X-ray, this energy may be used to reorganise the electron distribution within the atom itself, leading to the ejection of one or more electrons from the outer shell (Auger, 1926). The probability of this type of ionisation will increase with a decrease in the difference of the corresponding energy states. For example, when ($E_K - E_L$) is only slightly larger than E_L, this ionisation probability is large which in turn means that only in a small number of the total original K ionisation energy is emitted as K radiation (Burhop, 1952)

Fluorescent yield.

Since there are two processes competing to return the exciting atom to a stable state, the intensity of an emitted X-ray beam will be dependent on the effectiveness of the two processes. The actual number of useful X-ray photons produced from an atom is less than would be expected. The ratio of the useful X-ray photons arising from a certain shell to the total number of primary photons absorbed in the same shell is called the *fluorescent yield* (w). The value of w decreases markedly with atomic number, since the probability of producing an Auger electron increases (Jenkins and DeVries, 1970).

X-ray tubes.

The primary X-rays are produced in the X-ray tube and this can vary. The tube constituents are relevant in the choice of excitation energy and element under investigation. A tungsten filament is heated by means of a current producing a high electron cloud. This electron cloud is accelerated along the anode focusing tube by means of a large potential difference (the tube high voltage) applied between the anode and the filament. Electrons striking the anode produce X-radiation, a significant proportion of which passes through the window. Only about 1% of the total applied power emerges as useful radiation. The majority of the energy appears as heat, dissipated by cooling the anode. It is vital that the anode is a good heat conductor or is welded to a water-cooled copper block. This is necessary because scattered electrons can also raise the temperature of the X-ray tube window to several hundred degrees centigrade. The thickness of the window is dependent almost exclusively on its ability to dissipate heat.

X-ray dispersion methods

There are two types of instruments used in X-ray dispersion:

(A) energy dispersive systems [EDXRF]

(B) wavelength dispersive systems [WDXRF].

(A)

In the EDXRF, the voltage pulse from the detector is fed to a pulse processor where the amplitude of the pulse is measured. The amplitude is proportional to the energy of the x-ray photon, which caused the voltage pulse. Each measured pulse is registered in the appropriate channel of a multi-channel analyser, which has sufficient channels to cover the expected energy range. The energy dispersive spectrum consists of a plot of the number of counts per second (cps) against the channel number (or Energy). This is the basis of the instrument on which this experiment was based.

Each peak can be identified from its position. The primary disadvantage of this method is that there are several possibilities for each line. Adjacent elements in the periodic table give overlapping peaks in a low resolution system.

(B)

This dispersive system gives a better resolution than that of EDXRF. The secondary beam is directed on to a Li crystal of fixed 2d which produces a diffraction pattern in accordance with Bragg's Law :

$$n\lambda = 2d \sin \theta \qquad \textbf{Eqn 3.5}$$

Each wavelength will be diffracted at a unique diffraction (Bragg) angle. Thus by measuring the diffraction angle θ, knowledge of the d-spacing of the analysing crystal

allows the determination of the wavelength. Since there is a simple relationship between wavelength and atomic number (as given by Moseley's Law (**Eqn 3.4**)) one can establish the atomic number(s) of the element(s) from which the wavelengths were emitted. The main disadvantage of this method is that it is slower than the ED system.

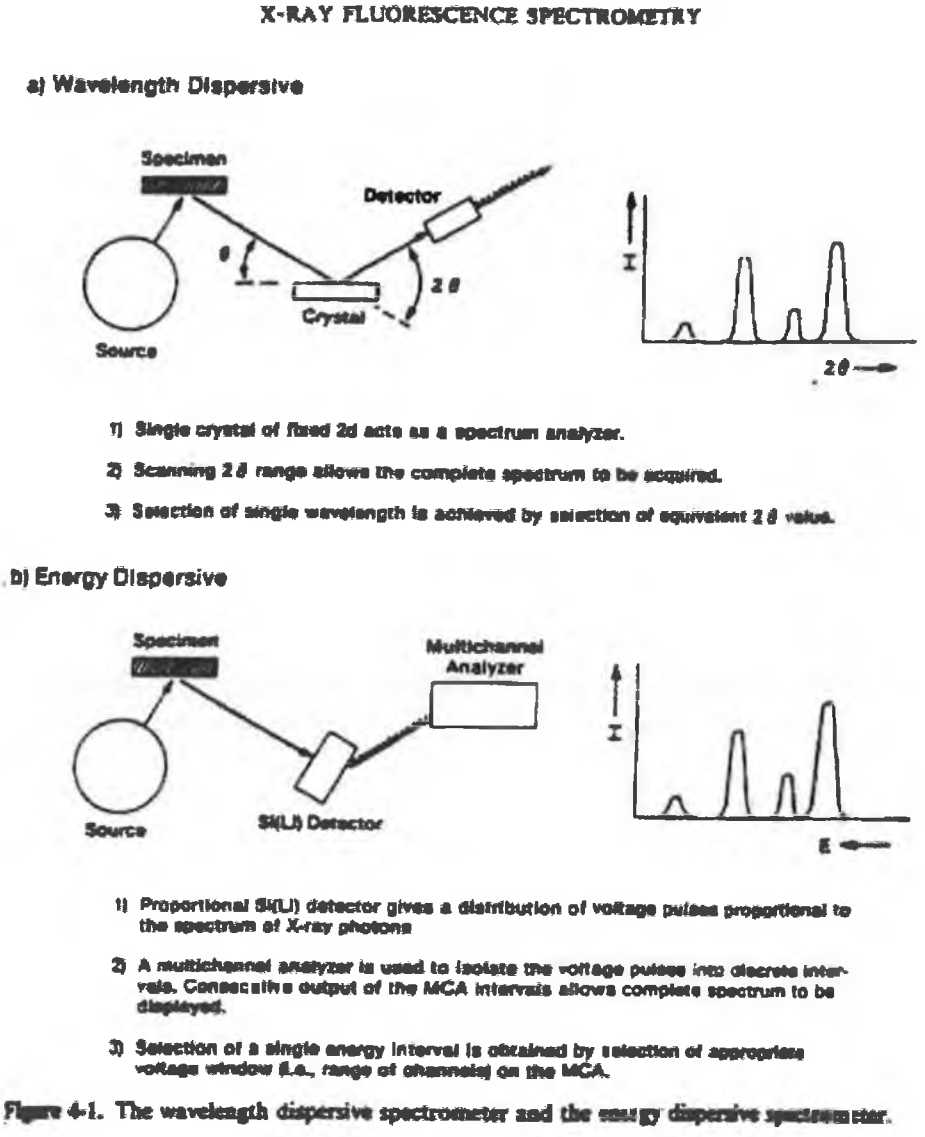

Figure 4-1. The wavelength dispersive spectrometer and the energy dispersive spectrometer.

Fig 3.4

Diagram taken for X-ray Fluorescence Spectrometry: by Ron Jenkins. (1988) Wiley & Sons, New York.

Escape peak.

An escape peak is an additional pulse which rises whenever the incident radiation can excite characteristic radiation from the inert gas. All atoms have a very low absorption for their own characteristic radiation. Consequently, when such radiation is produced it escapes from the counter and an extra pulse is produced having an amplitude corresponding to the difference in energy between the incident radiation and the energy of the characteristic radiation of the inert gas (Jenkins and DeVries, 1970).

3.2. Instrumentation

Oxford Lab-X 3000 (Oxford Instruments, 19-20 Nuffield Way, Abingdon, Oxon. England)

Dell Optiplex 466/Le with Pentium processor

Spex Certiprep ∞ 8000 Mixer/Mill (Glen Creston Ltd. England)

Spex 31mm stainless steel die with stainless steel pellets 31mm (3880 Park Ave, Edison, New Jersey U.S.A.)

15,000 pound press

Aluminium caps

Polystyrene vial with polyethelyene slip on cap

Methacrylate balls

3.3 Experimental Procedures

3.3.1 Setting up the computer.

1. On an operating computer, double click the LX3000 icon and open the LX-SERVER application. Click **Comms:Disconnect** to disconnect the server. Click **Comms:Setup** to open the communications window. Make the following settings:

Table 3.1

COM PORT	1
BAUD RATE	9600
DATA BITS	8
STOP BITS	1
PARITY	none
FLOW	Hardware
Output	CTS inactive : DSR active
Input	DTR inactive : RTS inactive

2. Click **OK** to close the communications setup window and click **COMMS:CONNECT**. Minimise the LX-SERVER window.

3. Open the Analyser application and Click the **Tools** menu and ensure the **LABX Disconnect** is displayed. If not click the **LABX Connect**. Minimise the **Program manager** window. The only window open at this point should be the Analyser window.

3.3.2 Setting up the LABX-3000

Having ensured that the instrument has power, carry out the following procedures.

A. From the main menu choose option **2 = Other Functions**. Press enter (without entering a password).

B. Choose option **3 = utilities** for the utilities menu. Option **2 = set time and date** allows you to set these values. When you have completed this, choose option **4 = Turn Page** until option **3 = Print Configuration** is displayed. Obtain the printout and press **4 = Turn Page** and option **2 = Quit** to return to the **Other Functions** menu.

3.3.3 Detector Resolution Test

From the **Other Functions** menu proceed to the Utilities menu. Choose option 1 = **Detector** test. The turntable rotates and measures the response of an in-built reference standard. After about 30 seconds, the results are printed. The DAC value should be about 3000 and the % Resolution should be about 21%. The detector should be replaced when this reaches 27%. Return to the **Other Functions** menu.

3.3.4 Setting up RS232 Parameters

From the **Other Functions** menu go to the **Utilities** menu and press 4 = **Turn page** until 1 = **Setting RS232** is displayed. Complete this setting using the same parameters as used for the computer in **Table 3.1**. Return to the **Other Functions** menu.

3.3.5 Recording a spectrum

From the **Other Functions** menu select option 1 = **Spectrum scan**. Enter the following settings, which have been optimised for Se analysis, pressing enter after each entry. [Note: You may correct an entry before pressing enter by using the delete key.]

Table 3.2

Energy range	High Energy
Tube voltage/ kV	20
Tube current / mA	35
Primary Filter	A9
Secondary Filter	V1
Helium Path	NO
Scan Time /s	50
Sample Label	SUMI65B

Press enter twice and wait until spectrum has been recorded. Choose option 1 = **Print Scan** and wait until the spectrum has been printed.

3.3.6 Peak Identification

Having printed the spectrum, press 1 = **Identify Peaks** and enter the channel number (based on the position of element of interest on the scan) of the first peak when requested. A printout of all peaks occurring within ±10% of this channel number is obtained. The K_α line of one of the expected elements should be among the possibilities. Label the peaks with the chemical symbol of this element. Repeat for the remaining peaks and finally press 4 = **Turn page**.

3.3.7 Transmitting a spectrum to the computer

When you have printed a spectrum turn the page and press option 3 = **Send scan by RS232**. When you see the message "Please connect the computer", press enter to transmit the spectrum. When this is complete, press enter again to return to the menu and **Quit** the spectrum scan.

3.3.8 Peak Identification on the computer

1. Using the mouse, select **Tools: Smooth** if desired to smooth spectrum. If Smooth is not required do not select Tools. Change the number of channels to 5 and smooth as often as necessary.
2. Click **Tools: Identify Peaks** and drag the peaks window down out of the way of the analyser screen so that you can see the spectrum.
3. Click on the main peak using the right-hand mouse button to identify the possibilities (Si, Ca, Fe, and As).

   (a) If the list includes the K_α line of the one of the expected elements, click on that line in the list of possibilities. Then label the peak and proceed to the next one.

   (b) If the list does not include the K_α line for the element of interest, scroll through the elements box in order of atomic number until the element is listed and select on the element of interest. Then click on K_α line and label the peak.
4. When peak labelling is complete cancel the peak identification window and select **File : Save Spectrum**. Save the spectrum as a A:/ file.
5. Select **View: Erase** spectrum to remove the spectrum from memory.

3.3.9 Sample Preparation

Processing a sample always contaminates it. Successful analysis depends on recognising the sources of contamination and controlling or minimising them. Care is especially needed in the analysis of trace elements to minimise sources of contamination. The grinding process poses a significant problem of contamination. An automated process was not available and therefore a mortar and pestle was used in this work. Both were made from ceramic and were cleaned several times with HNO_3 before use. The non-enriched yeast sample was particularly tough and force was needed to crush the yeast. This lead to some loss of yeast over the edge of the pestle. This was deemed contaminated and discarded. Once the yeast was ground into a fine powder it was transferred to a sterile plastic container and stored until used.

The same procedure was followed for the grinding of the Se 2000-yeast prill. Less force was needed to grind this and as a result, there was less wastage. The sodium selenate and the sodium selenite were bought as a fine powder also and stored in their containers until use.

3.3.10 Blending/Mixing

In order to get a representative sample spectrum the sample must be homogenous. The blank (2g non-enriched yeast finely ground) was placed in the polystyrene vial and one methacrylate ball was included with it. The container was sealed with the polyethylene cap. The vial was then clamped in a mixer/mill and the timer set for 20 minutes after securing the lid. Mixing was continued for 20 minutes after switching on the machine.

This procedure was repeated for the selenate and selenite standards and for all mixtures containing yeast samples. Using the Spex I.R. press the mixture was poured into the die, the top pellet was placed on top of the mixture and 15,000 pounds of pressure added. The resulting disk was labelled and kept in a desiccator. All dicks will absorb water, the desiccator is used to minimise the amount of water absorbed by the same over time. This procedure was repeated for all other samples.

3.3.11 Preparation of selenium standards in non-enriched yeast.

15g of the non-enriched yeast was weighed out accurately using a 4 place decimal analytical balance. Using a mortar and pestle, this was ground into a fine powder as **Section 3.3.9** prior to weighing of the standards. Standards were prepared using the quantities of sodium selenate given in **Table 3.3** below. The sodium selenate was weighed exactly as the non-enriched yeast above. Each sample was weighed directly into a polystyrene sample tube with a polystyrene sphere and cap and mixed in a mixer mill for 30 minutes, to ensure a homogenous mixture was obtained as described in **Section 3.3.10**. The mixture was then pressed into a disk using an I.R. dye of 33mm diameter under a pressure of 15 tonnes for 4 minutes. No aluminium cap was used in the preparation of these disks. The aluminium cap appeared to give a larger total background count, giving the selenium peak less of a peak height and peak area. It was for this reason that the aluminium cap was disposed of.

Table 3.3

Amount of Na_2SeO_4 / g	Amount of non-enriched yeast / g	Selenium /g	ppm
0.0000g	2g	0.0	0.0
0.0018g	2g	7.594×10^{-4}	759.4
0.0035g	2g	1.4866×10^{-3}	1486.6
0.0056g	2g	2.3636×10^{-3}	2363.6
0.0075g	2g	3.123×10^{-3}	3123.0
0.0089g	2g	3.7219×10^{-3}	3721.9

3.3.12 Preparation of a Standard Curve.

A typical XRF spectrum of Selenium enriched yeast is given in **Fig 3.5**.

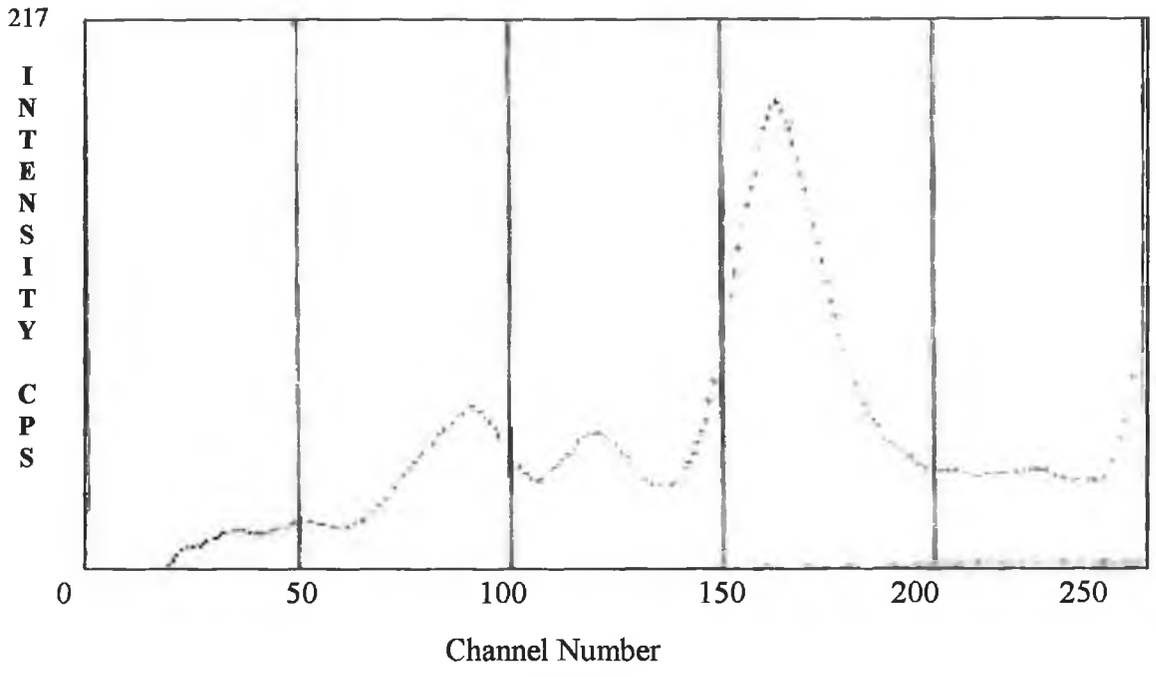

Fig 3.5

Three peaks are evident, Selenium K_α (Channel No. 140-205), Selenium escape peak (Channel No. 106-139) and Fe tube peak (Channel No. 60-105). All three are superimposed on a background which is assumed to be the same in the standards, which are prepared in a non-enriched matrix, and in the selenium enriched yeast sample for analysis. The total counts per second in each of these segments and in a segment of the background (Channel No.206-235) were measured using the following procedure.

1. From the main menu choose **Other Functions** and press **Enter**. Choose **Calibration**, **New Calibration** and **Create Calibration** in that order.

2. Enter Se Standard Curve as the title of the calibration and choose 1 = **Conditions**. Enter YES to enter conditions for the first metal, which is Iron. Enter the following conditions:

Table 3.4

Sample label	Voltage/ kV	Current/mA	Filters	CT RT	HE
Se yeast	20	35	A9 V1	50 100	No

Check that the printed conditions are correct and press YES or NO as appropriate. When asked if you want to set conditions for a second metal answer NO.

3. Choose 2 = Segments to establish the upper and lower channel numbers used in calculating the total X-Ray count for each analyte. Enter the data in the first row of **Table 3.5** for segment 1. Check that the printed conditions are correct and press YES or NO as appropriate. When asked if you want to set conditions for a second segment answer YES. Continue the procedure until the data for all four segments has been entered. When asked for data for fifth segment answer NO.

Table 3.5

Name	Lower Channel	Upper Channel	Conc. units	Decimal Places	Tolerances
Escape peak	106	139	ppm	3	None
Selenium	140	205	ppm	3	None
Backgrd	206	235	ppm	3	None
Fe	60	105	ppm	3	None

4. Press 1 = **Continue** to go to the calibration procedure. Choose 1 = **Standards**. For each of the six standards follow the same procedure. Enter the label (A,B,C, ...or 1,2,3....) and the concentrations (as ppm) as appropriate. Press 2 to continue and select **Measure** to measure the standard. Enter YES to confirm that the measurement is okay. When asked for standard number 7 answer NO.

5. If re-calibration is required enter 1 = **Low and High Susses**. If no SUS's are available then continue to step 6 after saving the method. The term SUS means setting up standard. The susses are two stable standards which can be used to recalibrate the instrument in the future without going through the above process. Enter the low SUS label and place the Low Sus in position 0. Enter 1 = **Measure** and follow the instructions on the LCD. Continue the procedure for the High Sus. Press **Continue** twice and Save the calibration and list it.

6. For the analysis of an unknown sample recall the method and Press 6 = **Measure** and 1 = **Analyte.** Data in each of the four segments is printed. And may be used to calculate the concentration. Press 3 = **End**.

3.4 Results and discussion

3.4.1 Optimisation of conditions for X-ray analysis of selenium

Voltage

At 15 kV the energy of excitation for the K shell had not been reached for Se. By controlling the tube voltage, some degree of selectivity can be gained over the excitation of the elements. The general rule is that the operating voltage (kV) should exceed the K edge value for an element, if the element is to be excited. As the kV was increased in 1000V steps the Se peak finally became separate from the background (the K edge value had been exceeded). As the voltage was being increased beyond the 20kV, the signal to noise ratio decreased and the Se peak to the Fe peak ratio decreased. The 20kV was adopted because it gave the best-shaped peak with the minimum interference from the background and other peaks. A list of the K edge energies for the elements are given in *Appendix Table 3.1*.

Filters

There are two filter positions in the LabX-3000, a primary filter (between the tube and the sample) and a secondary filter (between the sample and the detector). In the LabX there are only two primary filters A5 and A9, both are aluminium filters. The excitation voltage used for a particular range of elements is only that which effectively excites the highest energy line and no more. This avoids producing large amounts of continuum background above the highest element to be analysed under these conditions [**Fig 3.6**].

The purpose of placing the primary filter between the X-ray tube and the sample is to modify the position of the peak energy available for excitation. In this way, the X-ray beam reaching the sample has a spectral distribution, which favours good excitation and low backgrounds for a particular region of the spectrum, usually containing a maximum of 5 to 10 elements. The choice of filter is matched with an appropriate combination of tube voltage and beam current. Such analytical procedures may be stored for automatic repeat use, where the stored sets (methods) of analytical conditions are re-used.

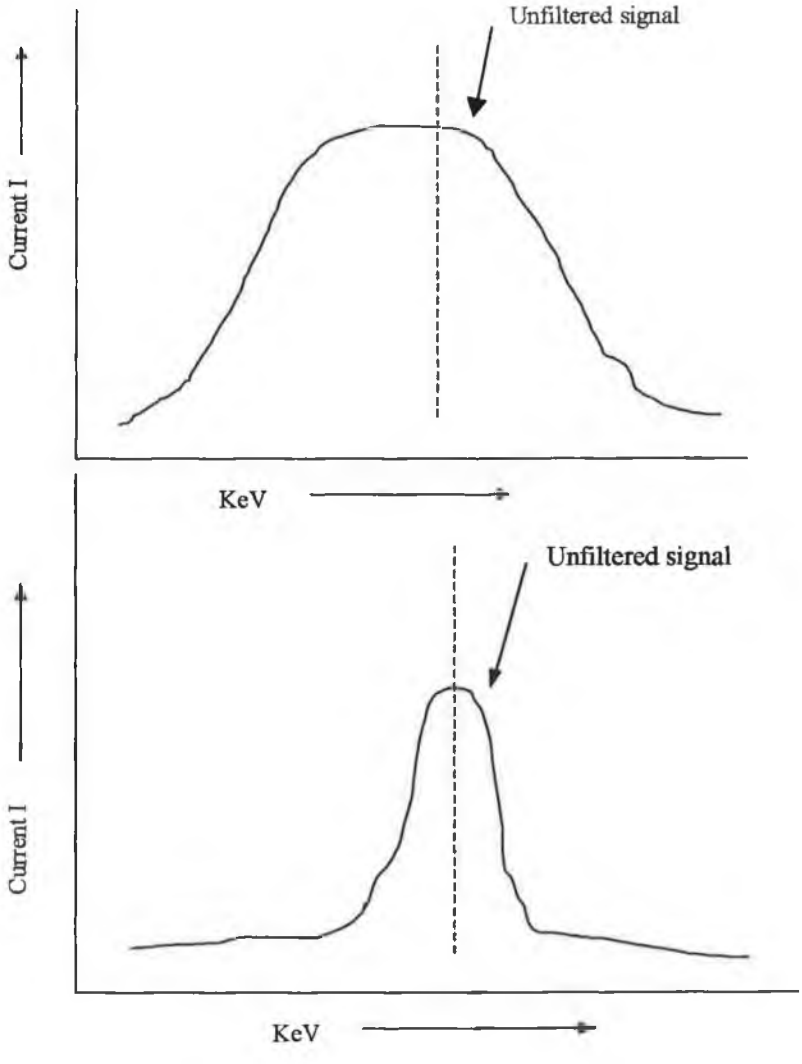

Fig 3.6

The use of a single filter mounted in front of the detector, known as the secondary filter, plays a very important role. The secondary filter is used to selectively absorb the

X-rays from one element while transmitting those of an adjacent element. The secondary filter should be chosen according to its absorption edge. A filter transmits lines of lower energy than its absorption edge and blocks lines above its absorption edge [**Fig 3.7**]. These secondary filters work particularly well in the region from Al to Ti, where it is now possible to separate Al from Si, P from S, S from Cl and so on.

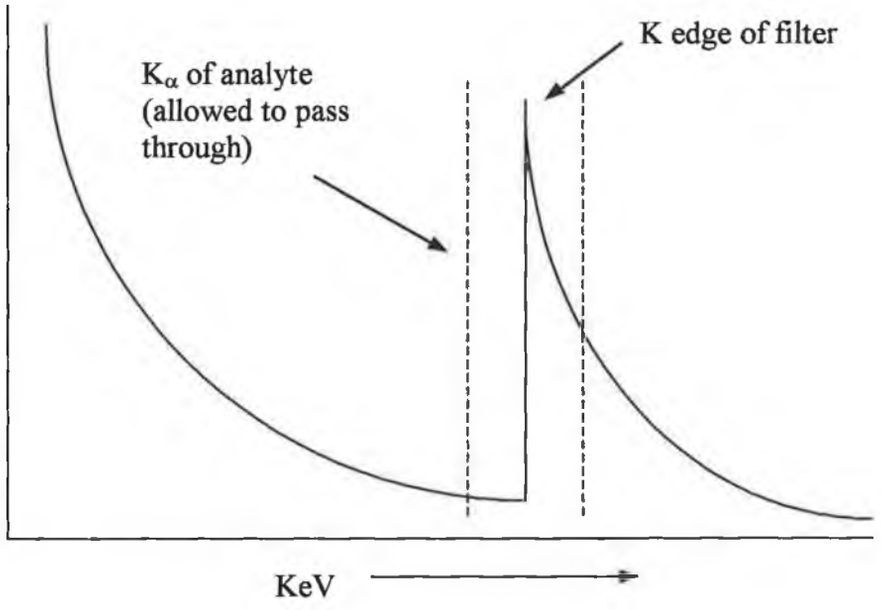

Fig 3.7

In this experiment, the best results came from using the primary filter A9. There are three secondary filters Manganese M1, Aluminium A1 and Vanadium V1. These were each examined in conjunction with the A9 filter and also the A5 filter. The best results were found to be the A9 primary filter in conjunction with the V1 secondary filter. It can give a suitably shaped Se peak and a good signal to noise ratio.

Current

The current applied to the x-ray tube allows the operator to control the electron flux inside the tube. If this flux is increased, then the number of photon emissions per second from the tube anode materials will increase, with the consequence that the

count rate from the sample will increase. Under normal operation, the current is adjusted to give an increased intensity subject to a maximum total count of 30,000. The current was started at 15μA with 20kV and the A9 and V1 filters on. As the current increased so did the Se peak increase in its intensity. The shape of the Se peak stayed constant once the current got past the 25μA level. The 35μA level was chosen because it gave reasonable intensity with a well shaped Se peak. Any further increase in current caused distortion of the Se peak.

3.4.2 X-ray spectra of enriched and non-enriched yeast

A 2g sample of selenium yeast was prepared and pressed into a disk (as described in **Section 3.3.9)**. An X-R.F. spectrum was recorded (as described in **Section 3.3.5)**. The resulting spectrum is given in **Fig 3.8a**. The spectrum of non-enriched selenium yeast is given in **Fig 3.8b**.

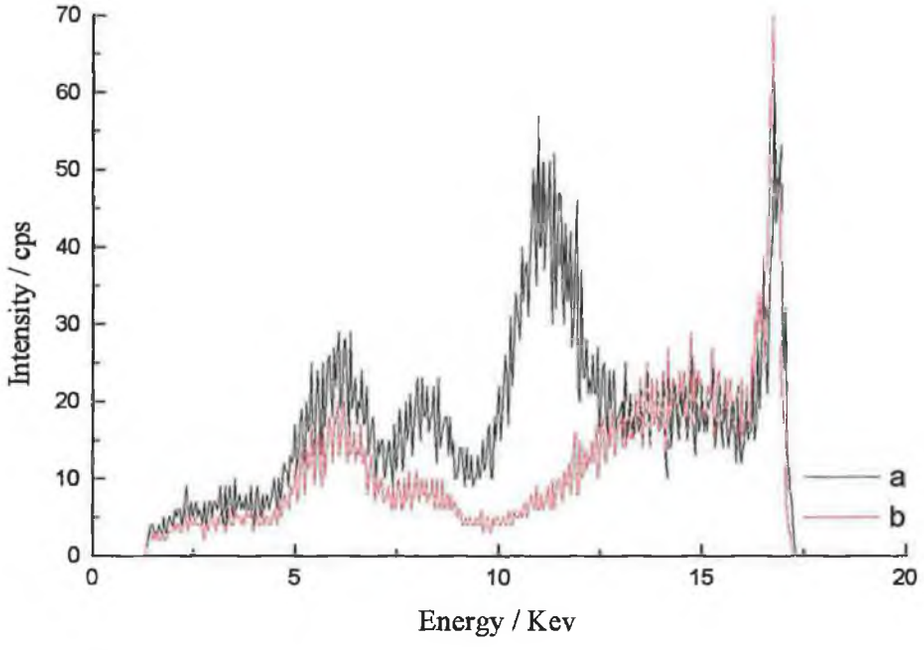

Fig 3.8

There are four distinct regions of interest, which are listed in the table below [**Table 3.6**].

Table 3.6

Name	Lower Channel	Upper Channel
Fe tube peak	60	105
Se Escape peak	106	139
Selenium Kα peak	140	205
Background region	206	235

The iron peak is present in both spectra and is an artefact of the instrumentation. The selenium K_α is present only in the selenium yeast and consequently the selenium escape peak is present here also. A small peak occurs in the non-enriched yeast in the region of the selenium escape peak. This has not been assigned and as it is not in the region of quantification it does not hinder the experiment.

It was decided that the non-enriched yeast might be used as a matrix for the preparation of standards for the analysis of selenium enriched yeast. The resulting calibration curve would be valid only if the background in the samples and standards was identical. To confirm this, a synthetic selenium enriched yeast specimen was prepared containing approximately 2000ppm Se by mixing Na_2SeO_4 (9.57mg) with 2g of non-enriched yeast and pressed into a disk as in **section 3.3.9**.

Adding the selenium to the non-enriched yeast results in the appearance of the Se K_α and Se escape peaks. The iron tube peak is also enhanced by addition of the Se while the background region is largely unchanged.

The spectra of the selenium yeast sample (**Fig 3.8a**) and the synthetic yeast sample were compared quantitatively as follows. Five 2g samples of the 2000ppm Se enriched

yeast and four 2g samples of the non-enriched yeast were analysed (as described in **Section 3.3.5)** [*Appendix Table 3.12*] and the count rate in each segment was recorded. The data for each segment was quantified using the Se standard curve [**Fig 3.11**] and is shown below in **Fig 3.7**.

Table 3.7

Segment	Se yeast	Synthetic yeast
Fe tube peak (40-105)	1492.8±17.11	1483.5±23.78
Se Escape peak (106-139)	1041±14.92	1014.5±15.72
Selenium K a peak (140-205)	3532±44.54	3476±53.61
Background region (206-240)	1133.4±11.97	1127±5.29

The corresponding peaks were compared statistically using a t-test (a t-test is used to compare an experimental mean with a known or standard value). The equations used for the t-test are only valid if the mean values are of equal variance. Therefore, an F-test (an F-test considers the ratio of the two sample variances) was carried out on the corresponding variances (s^2) to test whether or not the variances are equal. If not true more complex equations are used in the t-test. The F value is given by

$$F = \frac{s_1^2}{s_2^2}$$

Eqn 3.6

If the calculated F value is less than the critical $F\nu_1\nu_2$ (ν_1 and ν_2 = No. of degrees of freedom) as obtained from a two tailed F test table then there is no significant difference in the variances. The results of the calculations are given in **Table 3.8**. A sample calculation is given in *Appendix Table 3.14*. In each case, F_{calc} is less than F_{crit}

implying no significant differences in the variances. Therefore, the t-test was carried out as described below.

The calculated value of t is given by the equation.

$$t = \frac{(x_1 - x_2)}{s\sqrt{(\frac{1}{n_1} - \frac{1}{n_2})}}$$

Eqn 3.7

where x_1 and x_2 are the values to be compared; n_1 and n_2 are the numbers of replicates of each sample and s is the pooled standard deviation. The pooled standard deviation is calculated from the pooled variance (s^2) which is given by

$$s^2 = \frac{\{(n_1 - 1)\, s_1^2 + (n_2 - 1)\, s_2^2\}}{(n_1 + n_2 - 1)}$$

Eqn 3.8

The calculated t value is then compared with the critical t value obtained from a t-table assuming no. of degrees of freedom = $n_1 + n_2 - 1$. The results of the calculations are given below [**Table 3.8**]. A sample calculation is given in *Appendix Table 3.13 to 3.16.*.

Table 3.8

Segment	F_{calc}	F_{crit}	t_{calc}	t_{crit}
Fe tube peak	1.93	9.12	0.68	2.36
Se escape peak	1.11	9.12	2.59	2.36
Se K_α peak	1.45	9.12	1.72	2.36
Background region	5.12	9.12	0.98	2.36

In each case, the calculated value of t (P = 0.05) is less than the critical value. This indicates that there is no significant difference between the synthetic and the original yeast, except in the case of the Se escape peak. There is only a very slight increase of the t_{calc} over the t_{crit}. This could be due to a slight difference in that region between the sample yeast and the non-enriched yeast. The fact that the other three regions are not significantly different, implies that the background is identical in both. The Selenium escape peak is not used in the analysis itself so this is not important in the final analysis of the sample. The non-enriched yeast therefore was used in the preparation of Se standards.

3.4.3 Effect of Specimen thickness

The size and thickness of the specimen has a bearing on the legitimacy of the results. In order to investigate the effect of thickness on the Se peak count rate a series of pressed disks containing selenium yeast in increasing amounts from 0.5g up to 5g were prepared. The Se count rate was measured under the conditions described for the Se standard curve (**Section 3.3.12**) in the Se segment (Channel 140-205) and plotted against mass of selenium yeast (**Fig 3.9**). The data is given in *Appendix Table 3.4*.

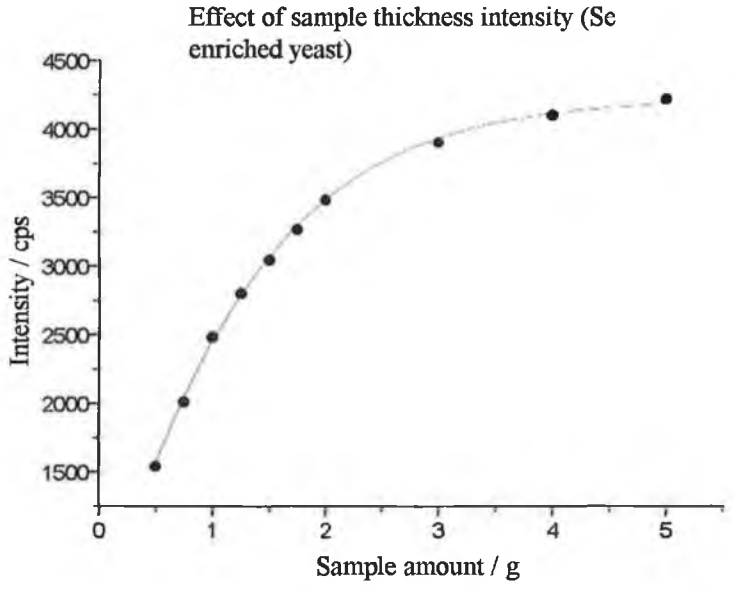

Fig 3.9

From the curve it is clear that as the quantity of sample is increased, the Se signal increases rapidly initially, before reaching a plateau in the 4g to 5g region. Further increase in thickness will not give an increased signal. The experiment was repeated under the same conditions with the non-enriched yeast. The plot is given in **Fig 3.10**. The data is in *Appendix Table 3.5*.

Effect of sample thickness on intensity (non-enriched yeast)

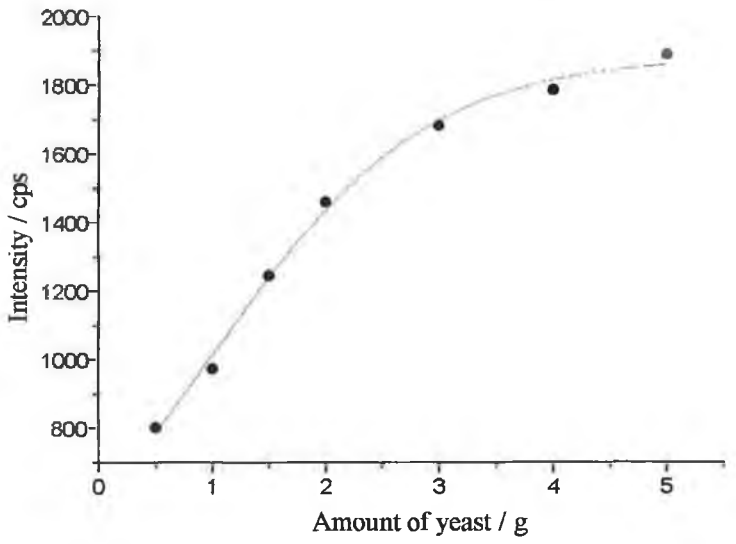

Fig 3.10

The effect of thickness in the case of non-enriched yeast mirrors the behaviour of the Se enriched yeast.

3.4.4 Selenium calibration curves

A number of calibration curves were obtained, using the procedures described in **Section 3.3.12**. A calibration curve using 2g disks given in **Fig 3.11** is a plot of the count rate in the Se K_α segment against ppm Se. The data is given in *Appendix Table 3.2*.

A second calibration curve was obtained from the same standards, except that data from two narrower segments (Channel No. 150-175 and Channel No. 220-230) were measured. The results are given in *Appendix Table 3.3* and the calibration curve is given in **Fig 3.12**.

3.4.5 Matrix effects in selenium analysis

It is possible that the measurement taken only once at approximately 2000 ppm is valid, while measurements taken above and below this value are invalid. Therefore, a calibration curve was prepared using 2000ppm selenium enriched yeast as a standard **(Section 3.3.12)** The percentage selenium enriched yeast increased from 0-100% while the percentage non-enriched yeast decreased in proportion. The slope (B) and intercept (A) of the graph **(Fig 3.14)** were measured and compared to the same parameters for the calibration curve, prepared using sodium selenate and the non-enriched yeast **(Fig 3.17)** and the following results were obtained.

Table 3.9

	A	B
Fig 3.13	1411±14.9	1.033±0.0123*
Fig 3.18	1437±31.5	1.030±0.0136

[*Slope corrected for the fact that 100% Se enriched yeast is equivalent to 2000ppm Se.]

Using a t-test, it is possible to see if the difference in the slopes are statistically significant. An F-test was first performed to determine whether or not the variances are equivalent, as described in **Section 3.4.2**. This was followed by a t-test to determine if there were any significant differences in A and B. The results of the calculations are given below in **Table 3.10**.

Table 3.10

Parameters	F_{calc}	F_{crit}	t_{calc}	t_{crit}
A	2.15	5.05	-9.3	2.22
B	1.10	5.05	-0.05	2.22

In performing the test, the number of measurements of the intercepts (A) in each case was assumed to be equal to the no. of points in the corresponding calibration curve. A similar criterion was applied to the comparison of the slopes (B). It is clear that in each case, F_{calc} is less than F_{crit}, implying equal variance. Also t_{calc} is less than t_{crit}, implying no significant difference in the slope and the intercept of the curves as a result of changing the matrix from non enriched yeast to a matrix containing increasing proportions of Se enriched yeast. A significant difference in the slope might be expected if the two matrices had different absorption properties.

3.4.6 Validation of linearity

Following the procedure described in **Section 3.3.9** five 2g standards as pressed disks were made at five concentration levels, from 50% to 150% of the target analyte concentration. The count rates for the Se segment (Channel 140-205) and for the Fe segment (Channel 60-105) were measured using the same conditions as described in **Section 3.3.12**. The standards were analysed in triplicate. The composition of the standards and the results for the two segments are given in *Appendix Table 3.11*. A plot of Se concentration versus the intensity in counts per second for the Se segment (Channel 140-205) can be seen below (**Fig 3.15**). The correlation coefficient of the calibration curve was 0.99965. A correlation coefficient >0.999 is generally considered to satisfy the criterion for linearity (Anal. Chem. 1996).

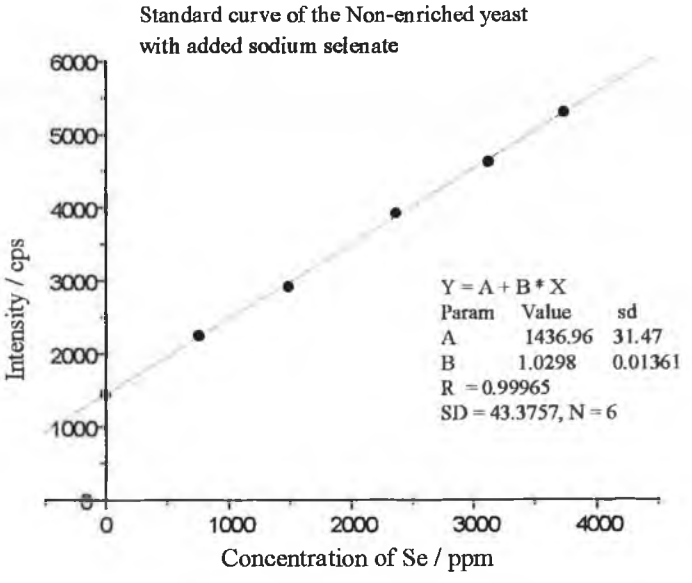

Fig 3.15

3.4.7 The Limit of detection (L.O.D.)

The limit of detection is commonly taken to be three standard deviations above the background reading.

$$L.O.D. = Y_{bkg} + 3(SD) \qquad \textbf{Eqn 3.9}$$

Using the data from the calibration curve (**Fig 3.15**) the

$$L.O.D. = 1436.96 + 3(43.38) \text{ c.p.s.}$$

$$= 1567.1 \text{c.p.s.}$$

This corresponds to a Selenium concentration of 126.36ppm. There are three factors that affect the detection limit:

- sensitivity of the instrument in terms of the counting rate per unit concentration of the analyte.
- the background counting rate
- the available time for counting peak and background photons.

3.4.8 Reproducibility of selenium analysis

20g of Se enriched yeast was ground into a fine powder with a mortar and pestle. Ten 2g samples were taken and pressed into disks. These were scanned using the same conditions employed in obtaining the standard curve in **Section 3.3.12** and **Fig 3.15**. Each sample was measured in triplicate. The results are given in **Table 3.11** as p.p.m. Selenium in yeast.

Table 3.11

Sample	Replicate 1	Replicate 2	Replicate 3	Average [Se] / ppm
A	2042.5	2034.5	2033.6	2036.9
B	2027.6	2036.7	2031.5	2031.9
C	2127.1	2007.8	1993.7	2042.9
D	2033.3	2037.5	2039.4	2036.7
E	2066.1	2018.3	2036.4	2040.3
F	2014.9	2017.4	2017.8	2016.7
G	2068.2	2004.0	2017.9	2030.0
H	2048.2	2009.2	2009.0	2020.1
I	2065.3	2058.2	2041.2	2054.9
J	2046.6	2007.8	2016.1	2023.5

The results of the ten determination gave a selenium concentration of 2033 ± 11.49ppm. The coefficient if variation is therefore 0.57% which is within the acceptable value of 2% (J.M. Green 1996).

3.4.9 Analysis of Se using standard addition

The sample has an unknown concentration of analyte c_x, which gives a measured intensity of I_x. On deliberate addition of a standard amount 's' of the analyte, the new intensity will equal I_{x+s}. Thus the new concentrations $c_x + c_s$, substituting both of these into the equation it now takes on the form.

$$\frac{c_x}{c_x+c_s} = \frac{I_x}{I_{x+s}} \qquad \textbf{Eqn 3.10}$$

Since I_x and I_{x+s} are both measured, and c_s is known, a value for c_x can easily be obtained. The technique of standard addition is especially useful for the determination of analyte concentration below about 5%. A linear relationship between concentration and intensity, is assumed and if this is not the case, errors will occur.

It is also necessary to subtract the background intensity from both the unknown (x) signal and the combined unknown with added standard (x+s) signal.

A 2g sample was prepared with 1.5g of the finely ground Se enriched yeast and 0.5g of the finely ground non-enriched yeast. The counts per second in the selenium segment (Channel 150-175) were measured using the same conditions employed for obtaining the standard curve in **Section 3.3.12** except for the smaller channel size for the Se segment. A second disk was prepared which contained the same amounts of enriched and non-enriched yeast and 500 ppm Se added as sodium selenate. The selenium count rate was measured in the same segment. The background intensity was obtained from a 2g disk of non-enriched yeast in the same Se segment.

The results are set out in **Table 3.12**.

Table 3.12

Sample No	Se Yeast/g	Non-Enriched yeast/g	Na_2SeO_4/g	Se cps	Background/ cps
1A	1.5	0.5	0	1006.0	277.3
1B	1.5	0.5	0.0025	1288.5	277.3
2A	1.5	0.5	0	1101.0	277.3
2B	1.5	0.5	0.0028	1385.0	277.3

The equation for standard addition may be manipulated to give the formula for the calculation of c_x.

$$c_x = \frac{c_s I_x}{(I_{s+x} - I_x)}$$

Eqn 3.11

The parameters necessary for the calculation of c_x and the resulting concentrations are given in the table below. (**Table 3.13**)

Table 3.13

Sample	c_s/ppm	I_x	I_{x+s}	c_x/ppm
1A	0	728.7	-	1392.9
1B	540	-	1011.2	
2A	0	823.7	-	1696.7
2B	585	-	1107.7	

The expected concentration was 1525 ppm based on the direct determination. The percentage deviation in sample 1 was 8.8% while in sample 2 the deviation was 11.2%. These are relatively large deviations and this method of standard additions was not further investigated.

3.4.10 Analysis of Variance

The purpose of this analysis was to determine if the sample was homogenous. In **Section 3.4.8** the results of analysing ten 2g samples from the bulk yeast sample are presented. Each sample was analysed in triplicate. The analysis of the data was carried out using the ANOVA capability of the Microsoft Excel spreadsheet.

Two estimates of the population variance are obtained, the between-sample estimate and the within-sample estimate. The F-test may be used to decide if the between-sample variance differs significantly from the within sample variance.

$$F = s^2 \text{ (between-samples)}/s^2\text{(within-sample)}$$

If the calculated F value is greater than the critical value $F_{v1,\ v2}$ then the sample means differ significantly from place to place.

Calculation of within-sample variance

The variance in any series of measurements is defined by the formula:

$$s^2 = \sum \frac{(x_i - \bar{x})^2}{(n-1)}$$

Eqn 3.12

where n is the number of results in the series, and (n -1) is the number of degrees of freedom.

The within-sample variance is the average of the variance of each replicate series of measurements. The variance of each replicate series is calculated and the average of these values, referred to as the mean square variance, is then calculated.

Calculation of s^2(between-sample)

The variance of the ten mean values is also calculated using the equation

$$\text{variance} = \sum \frac{(x_i - \bar{x})^2}{(n-1)}$$

Eqn 3.13

The variance of the mean is more reliable than the variance of the population and one must multiply the variance of the mean by the number of measurements used in calculating the mean, in order to get an estimate of the population variance.

$$s^2 \text{ (between-sample)} = 3 \text{ x variance}$$

The results are given in the table below.

Table3.14

Analysis of variance - XRF

	Replicate		
Sample	**1**	**2**	**3**
A	2042.5	2034.5	2033.6
B	2027.6	2036.7	2031.5
C	2127.1	2007.8	1993.7
D	2033.3	2037.5	2039.4
E	2066.1	2018.3	2036.4
F	2014.9	2017.4	2017.8
G	2068.2	2004	2017.9
H	2042.2	2009.2	2009
I	2065.3	2058.2	2041.2
J	2046.6	2007.8	2016.1

Anova: Single Factor

SUMMARY

Groups	*Count*	*Sum*	*Average*	*Variance*
Row 1	3	6110.6	2036.867	24.00333
Row 2	3	6095.8	2031.933	20.84333
Row 3	3	6128.6	2042.867	5371.143
Row 4	3	6110.2	2036.733	9.743333
Row 5	3	6120.8	2040.267	582.4233
Row 6	3	6050.1	2016.7	2.47
Row 7	3	6090.1	2030.033	1140.823
Row 8	3	6060.4	2020.133	365.2133
Row 9	3	6164.7	2054.9	153.37
Row 10	3	6070.5	2023.5	417.43

ANOVA

Source of Variation	*SS*	*df*	*MS*	F_{calc}	*P-value*	F_{crit}
Between Groups	3565.612	9	396.1791	0.489868	0.864291	2.392817
Within Groups	16174.92667	20	808.7463			
Total	19740.53867	29				

The calculated value of $F_{calc} = 0.4898$ is less than the critical value of $F_{crit} = 2.3928$ indicating that the bulk sample does not differ significantly from place to place.

Chapter 4: Determination of Selenium by Hydride Generation Atomic Absorption Spectroscopy

4.1 A brief history.

By the start of the 18th Century the phenomenon of light absorption had already been investigated by many great minds. In 1666 Sir Isaac Newton had discovered the solar spectrum. Lambert et al, (1760) found using Bouguer's (1729) work that the amount of light passing through a layer of uniform thickness of a homogenous medium is dependent/proportional to the thickness d of the layer and that the ratio of the intensity of the transmitted light I_{tr} to the intensity of the incident light I_0 is independent of the radiant intensity. Lambert's law underwent a thorough examination by Beer (1852) and became the form that is seen today.

$$\log I/I_o = -e\,[j]\,l \qquad \text{Beer-Lambert Law} \qquad \textbf{Eqn 4.1}$$

$\mathbf{I_o}$ = is the incident intensity (at a particular wavenumber).

I = is the intensity after passage through sample of length l.

[j] = is the molar concentration of absorbing species j.

ε = is the molar absorption coefficient (extinction coefficient).

$$\mathbf{A} = \varepsilon[J]l = \text{absorbance} \qquad \textbf{Eqn 4.2}$$

$$\mathbf{T} = I/I_o = \log T = -A = \text{Transmittance} \qquad \textbf{Eqn 4.3}$$

It states that the absorbance A (the logarithm of the reciprocal transmission) is proportional to the concentration of the absorbing substance and to the thickness of the absorbing layer. Wollaston recreated Newton's work and in 1802 discovered that

the spectrum obtained from the sun had a number of dark lines. Fraunhofer investigated further into these lines "Fraunhofer lines" in 1814 and by 1823 was able to measure their wavelength. In 1820 Brewster expressed his view that these lines originated in absorption in the sun's atmosphere. But it took Kirchhoff and Bunsen until 1859 to present the exact explanation by their systematic examination of the line reversal in the spectra of alkali and alkaline earth metals (Welz 1985). Kirchhoff showed that the lines were due to elements not compounds. They demonstrated that the typical yellow line emitted by sodium salts in a flame is identical to the dark lines from the sun's spectrum. These D lines were attributed to sodium atoms present in the sun's atmosphere. It is by this technique the composition of the atmosphere of distant planets and stars are being investigated by astronomers today. According to Kirchhoff's law, all matter absorbs light at the same wavelength at which it emits and that the same quantity of radiation is involved. This phenomenon is therefore termed "resonance fluorescence". Based on this and many other experiments Bohr (1913) proposed his atomic model, which was that atoms do not exist in random energy states, but only in certain fixed states which differ from each other by exact measurable units or integral quantum numbers (Welz 1985). Atomic absorption spectrometry is the term used when the radiation absorbed by atoms is measured.

The energy of the radiation absorbed is quantised according to Planck's Equation. The use of the AAS technique as a common tool available to the chemist was somewhat delayed due to the assumption that very high resolution, to make quantitative measurements, was needed. It took until 1953, when Walsh (1953) overcame the problem by, instead of using a continuous source, he used a line source. This idea was pursued independently by Alkemade (1955) with the same results.

Basic Instrumentation.

In atomic absorption spectroscopy the source is viewed directly and the attenuation of radiation measured.

Radiation Sources.

Very many of the advantages of atomic absorption spectrometry can be directly or indirectly traced to the narrow half-intensity width of the resonance lines, i.e. the absorption of an element takes place within a limited spectral range. This advantage becomes very noticeable if the radiation sources used for excitation emit the spectrum of the analyte element in spectral lines that are narrower than the absorption lines. Atomic absorption corresponds to transitions from low to higher energy states. Therefore, the degree of absorption depends on the population of the lower level.

When thermodynamic equilibrium prevails, the population of a given level is determined by Boltzman's law:

$$\frac{N_i}{N_j} = e^{-E_i - E_j / kT}$$

Eqn 4.4

N = number of particles

Ei = states with energies.

k = Boltzmann's constant = 1.38×10^{-23} J K^{-1}

T is the temperature.

This formula is used for the calculation of the population of states of various energies and was derived by Ludwig Boltzmann towards the end of the 19th Century. It gives the ratio of the numbers of particles in states with energies E_i and E_j.

As the population of the excited levels is generally very small compared with that of the ground state, absorption is greatest in lines resulting from transitions from the ground state; these lines are called resonance lines.

Monochromators capable of isolating spectral regions narrower than 0.1nm are excessively expensive, yet typical atomic absorption lines may often be narrower than 0.02nm. The amount of radiation isolated by the conventional monochromator, and thus viewed by the detector, is not significantly reduced by the very narrow atomic absorption signal, even with high concentration of analyte. Thus, the amount of atomic absorption seen using a continuum source, such as is used in molecular absorption spectroscopy, is negligible.

Walsh's contribution was to replace the continuum source with an atomic spectral source e.g. if you are interested in the element mercury, you would choose a mercury spectral source. The monochromator only has to isolate the line of interest from other lines in the lamps (mainly filter gas lines). The atomic absorption signal exactly overlaps the atomic emission signal from the source due to the both having the same wavelength and very large reductions in radiation are observed. The very narrowness of atomic lines now becomes an advantage. The lines being so narrow, the chances of an accidental overlap of an atomic emission line of one element with an atomic emission line of another is almost negligible. This high selectivity is known as Walsh's "lock and key" effect. The best sensitivity is obtained when the source line is narrower than the absorption profile of the atoms in the flame.

Hollow Cathode Lamp.

The central feature is a hollow cylindrical cathode, lined or filled with the analyte metal of interest. The cathode is contained within a glass cylinder filled with an inert gas usually neon or argon, at a pressure of several hundred pascal (a few Torr). The anode is usually in the form of a thick tungsten or nickel wire. If a voltage of several hundred volts is applied across the electrodes, at the pressures used, a glow discharge takes place. It occurs almost completely within the cathode. Currents of 2-30 mA are normally used. There are two processes that take place, firstly the inert gas becomes charged at the anode when the voltage is applied. The positive ions that are produced are attracted to the cathode at the same time they are being accelerated by the field generated. These ions bombard the surface of the cathode material. Secondly, these atoms pass into the region of the intense discharge where further collisions, with the concentrated stream of the excited gas, excite the metal atoms. Hence, an intense characteristic spectrum of the metal is produced. The resultant beam is relatively well concentrated as they all originate from the small area within the cathode.

Human et al., (1969) found that for hollow cathode lamps whose gas pressure was approaching zero, temperature had a negligible effect on the line width. So the spectral lines emitted from the hollow cathode lamp will have an appreciably smaller half intensity width than the absorption lines in the flame whose lines are strongly broadened at atmospheric pressure and higher temperatures. Therefore, hollow cathode lamps represent the ideal radiation source for atomic absorption spectrometry.

The Hydride Technique.

Many elements are now routinely analysed by generating their covalent gaseous hydrides and atomising these in a flame. The advantage of volatilisation as a gaseous

hydride is in the separation, enrichment of the analyte element and preconcentration, and thus resulting in a reduction or complete elimination of interference.

Initially there were numerous techniques to form hydrides. Arsenic and selenium caused a problem for AAS because of their low-wavelength, primary-resonance lines. Their hydrides were generated with zinc – hydrochloric acid reduction and the gaseous products were conducted into solutions containing ammonium molybdate or hydrazine sulphate, which trapped the hydrides and which form characteristic coloured complexes with hydrides.

Holak (1969) studied the hydride generation of arsenic and atomic absorption spectrum. Using the zinc-HCl solution the hydride was trapped in a liquid nitrogen trap. Once enough of the hydride had been collected the trap was warmed and conducted the arsine with a stream of N_2 into an argon/hydrogen diffusion flame to measure the atomic absorption. This was also done by Manning (1971).

However, Landsford et al (1974) found that by using the zinc – HCl technique to determine selenium considerable interference was caused. They therefore proposed the use of tin (II) chloride, which they added to the sample solution acidified with 6M HCl. Metal/acid reactions still had too many disadvantages to allow them to become more widely acceptable. It wasn't until the introduction of sodium borohydride that there was a marked interest in the hydride technique.

Using this method people like Schmidt and Royer (1973), Pollack and West (1973) determined antimony, bismuth, selenium, and germanium. The $NaBH_4$ was used in pellet form in 6M HCl solution but only about 10% of the hydride was released (McDaniel et al 1976). But once $NaBH_4$ solutions stabilised in NaOH solution were used the technique had found the necessary reproducibility and control of reaction.

The replacement of inefficient nebulisation by gaseous sample transport improved the detection limit.

Initially the hydride generated was trapped and stored before being measured in the flame, this was done by cooling the gas in a liquid nitrogen trap or by collecting the hydride generated in a balloon. But the disadvantage of this was that the hydrides could not be stored too long because they decomposed very easily. Dalton and Malanoski (1971) proposed conducting the hydride directly into the flame. With a slow inert gas stream through the sample solution the yield of hydride could be improved markedly (McDaniel et al. 1976). The trapping method brings the highest yield and the best absolute sensitivity, but the direct system gave sufficient sensitivity and the higher speed is often decisive in choice of methods.

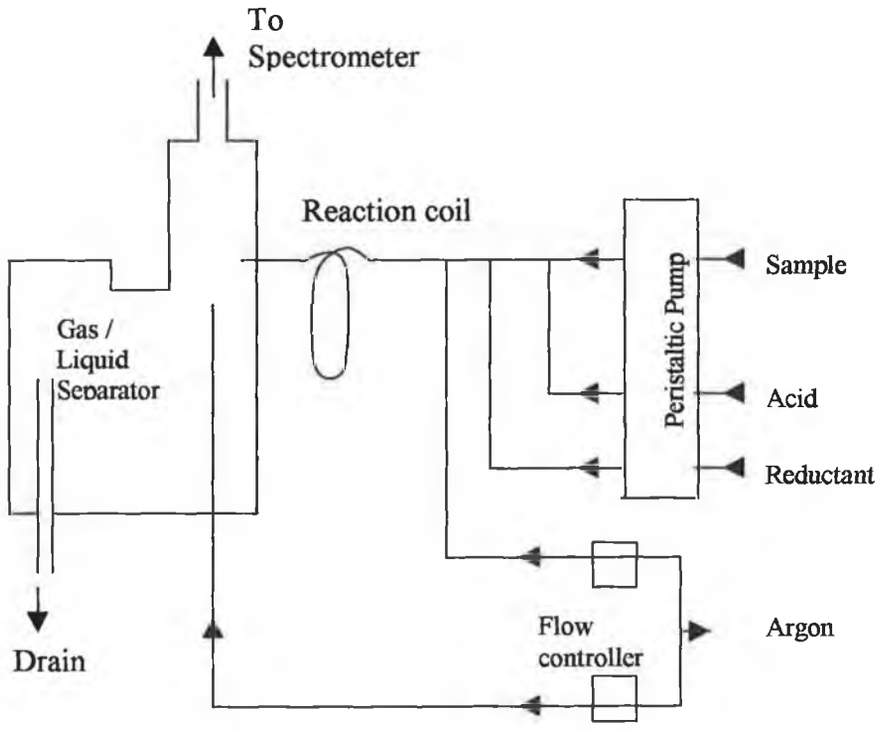

Fig 4.1

Atomisation of the Hydride.

The temperature of the flame is fully sufficient to atomise the hydrides and it has adequate transparency in the far U.V. range to permit the determination of arsenic and

selenium with a favourable signal to noise ratio. The development of a quartz tube heated in the flame for atomisation of the hydride was proposed. Compared to a flame, a quartz tube offers the advantage of higher sensitivity and, especially for arsenic and selenium, negligible spectral background and thus gives an improved signal to noise ratio (Thompson and Thomerson 1974). Dedina and Rubeska (1980) found that in a cool, fuel gas rich oxygen/hydrogen flame, a very high degree of atomisation (possibly 100%) for selenium was attained. They further showed that the atomisation of selenium was not based on the thermal dissociation of the hydride, but was brought about by free radicals (H•, •OH) produced in the flame **Eqn 4.5**. A variety of circumstances led to the assumption that atomisation is a simple thermal dissociation; the analyte element reaches the atomiser as the gaseous hydride and then decomposes with the release of free atoms.

Dedina and Rubeska (1980) investigated the atomisation of selenium in a cool oxygen /hydrogen flame burning in an unheated quartz tube. They found for all hydrogen flow rates that with increasing oxygen flow rates there was an initial steep rise in the sensitivity followed by a slow decrease. The maximum was only dependent on the diameter of the quartz cell. The slow decrease in sensitivity corresponds to the increase in temperature and to the expansion of the gas streaming through the tube. Demonstrating that an increase in the oxygen flow rate above the sensitivity maximum does not enhance the efficiency of atomisation. Thus the atomisation cannot be the result of thermal dissociation. Dedina and Rubeska (1980) stated that atomisation is brought about by free radicals that are produced in the primary reaction zone of the diffusion flame according to the following equations:

$$H\bullet + O_2 \rightleftharpoons OH + O\bullet$$

$$O\bullet + H_2 \rightleftharpoons \bullet OH + H\bullet$$

$$\bullet OH + H_2 \rightleftharpoons H_2O + H\bullet \qquad \textbf{Eqn 4.5}$$

In the presence of the excess hydrogen it can be assumed that only OH and H radicals are formed and in quantities corresponding to the total amount of oxygen. The concentration of H radicals is several orders of magnitude larger than that of the OH radicals. Atomisation is via a two step mechanism with the predominating H radicals. Corresponding reactions with •OH radicals, because of their low concentration are considered negligible. The recombination reaction must also be taken into account.

The probability for the forming of free selenium atoms from H_2Se is thus proportional to the number of collisions with free radicals and the efficiency of atomisation should increase with increasing number of radicals. Some people attributed sensitivity losses to devitrification of the quartz through sodium hydroxide traces in the carrier gas and, especially, burnt in metal traces (Meyer et al 1979). This effect can be eliminated by bathing new quartz tubes in hydrofluoric acid for a few minutes; they then exhibit maximum sensitivity from the first determination (Welz 1985)

4.2 Materials, Instrumentation and Solutions

Glassware

All volumetric glassware was Grade A. Glassware was washed with 10% nitric acid prior to use and rinsed with distilled water.

Materials and Solutions

Chemicals

Na_2SeO_4 : Mr = 188.94 g / mol (Fluka Chemika #71948)

Na_2SeO_3 : Mr = 172.94 g / mol (Aldrich # 21,448.5)

H_2SO_4: Extra pure 96-97% (Riedel-de-Haën Sulphuric acid)

H_2O_2 35 % = 34.01 g / mol (Riedel-de Haën # 18304)

HCl 37 % = 36.46 g / mol (Reidel–de Haën # 07102)

NaOH pellets

$NaBH_4$ pellets Mr = 37.83 g / mol 96% minimum assay (BDH Chemicals: Lennox England)

Preparation of 1000 ppm Se as Sodium selenate

This solution was prepared as described in **section 2.2**. The solution was made up freshly every two weeks. Dilutions were made up in different media using this stock for the relevant experiments.

Preparation of 1000 ppm Se as Sodium Selenite

This solution was prepared as described in **section 2.2**. The solution was made up freshly every two weeks. Dilutions were made up in different media using this stock for the relevant experiments.

HCl dilutions:

Concentrated HCl is 37% and contains 36.46 g mol^{-1}. Dilutions were carried out using distilled water in clean dry volumetric flasks. 10M HCl was prepared by diluting 850 cm^3 of the concentrated acid to 1000cm^3 with distilled water. 6M HCl was prepared by diluting 510 cm^3 of the concentrated acid to 1000cm^3 with distilled water. 1M HCl was prepared by diluting 85 cm^3 of the concentrated acid to 1000cm^3 with distilled water. For any concentration of hydrochloric acid below 1 M HCl this solution was diluted further. This was made up using Analytical Grade Hydrochloric acid and distilled water using clean volumetric flasks. This is made up as needed. As 10M HCl is stable, it can be stored in a heavy-duty plastic container to save any leaching of trace metals from glassware. It has been reported that the increased acid concentration (up to 6 M HCl) in the reduction step effectively reduces or even eliminates interferences in the hydride technique [Kos et al (1998)].

Dilution of selenate and selenite solutions

10ppm Se (as sodium selenate or as sodium selenite) were prepared as previously described in **Section 2.2**.

0.6% $NaBH_4$ in 0.5% NaOH

A 250 cm^3 aliquot of 0.5 % NaOH was prepared by dissolving 1.25 g of NaOH pellets (accurately weighed) and diluting to 250 cm^3 with distilled water. When the pellets had dissolved 1.5 g of $NaBH_4$ was added to the 0.5 % NaOH. This solution was now 0.6 % $NaBH_4$ in 0.5 % NaOH which was used as the reductant. The solution was freshly prepared each day as the solution deteriorates over night.

Instrumentation

SpectrAA 50 Atomic Adsorption Spectrometer (Varian Australia)

SpectrAA Worksheet Oriented AA 50 Version 2.00 (Varian Australia)

VGA 77 Vapour Generation Accessory (Varian Australia)

Dell Personnel Computer with Intel pentium processor.

Nitrogen N_2 (Oxygen free) (BOC Gases Bluebell, Dublin 12)

Acetylene gas. (BOC Gases Bluebell, Dublin 12)

Air Compressor (GAST) Model : DAA – 808 - EG

Analytical balance Explorer (4 decimal) (OHAUS).

4.3 Experimental Procedure

4.3.1 Hydride Generation Procedure.

Vapour Generating Accessory (VGA77)

Make sure that this accessory is correctly installed in the Spectra AA 50 instrument. Then make sure that freshly prepared 0.6% $NaBH_4$ in 0.5% NaOH and 10M HCl are placed in the correct containers. Check that all plastic tubing is in good condition and correctly connected.

Ensure that the quartz "T" cell is connected to the vapour outlet and is installed in the burner head.

Switch on the nitrogen gas (or Argon if possible) cylinder and bring up the head pressure until the "low pressure" light on the VGA goes off.

Method Setup From Worksheet

1. Double click on the **SpectrAA** icon.
2. Click on the **work sheet** window.
3. Click on "**New Worksheet**".
4. Name the New Worksheet "Selenium determination in yeast"; Name the analyst and any other comments that are relevant to the analysis. Reduce the number of samples to 10. Then click **OK**.
5. Click on "**Add Methods**".
6. Make sure **Load from "Cookbook"** is highlighted as this selects pre-set conditions for the computer / instrument maximum parameters.

7. Type "Se" in **search: element** window and "water" in **matrix** window.
8. Highlight "Flame" in **Method type** box.
9. Click on "Se" from **Element Matrix** box. Then click **OK**.

On the following "tabs" set these parameters

10. Click **Edit Methods**. A Type/Mode page opens. Make the following settings.

Element: Se

Matrix: Water

Units: mg/L

Sampling Mode: highlight Manual.

Instrument Mode: highlight Absorbance.

Flame type & Gas Flow (L / min): Air / Acetylene.

Air flow 3.50

Acetylene flow 1.50

Use **SIPS** "off".

11. Click **Next**. A measurement Page opens. Make the following settings

Measurement Mode: Integration

Calibration Mode: Concentration

Minimum readings: 0.000 **Replicates**: Standards 3, Sample 3

Smoothing: 5 point **Time**: Measurement 5.0s **Read Delay** 50s

12. Click **NEXT**. An Optical Page opens. make the following settings

HC lamp Lamp position 1 Lamp current 10.0mA

Monochromator Wavelength (nm) 196.0

Slit width (nm) 1.0

Background correction (off)

13 . Click **NEXT**. A SIPS page opens. This page remains unchanged.

14. Click **Next**. A standards page opens. Enter the concentrations for the standards as necessary. A sample set of data is given below.

Table 4.1

Standard No.	1	2	3	4	5
Conc/ppb	5.00	10.0	15.0	20.0	25.0

Other parameters are unchanged except for **Calibration Algorithm** for which Linear Origin is selected..

15 Click **NEXT.** A QC test page opens. This remains unchanged.

16. Click **Next**. A Sampler page opens. This remains unchanged.

17. Click **Next**. A notes page opens. This remains unchanged.

18. Click **Next**. A Cookbook Page opens. This remains the unchanged.

19. Click **OK**.

Instrument Set-up From Worksheet.

Click **Select** button. Use highlighter pen to select the number of samples to be analysed. Click **Select** again to return to the instrument page.

Click **Optimise**. Click **OK** on new window. The **Flame optimisation** window appears. Ensure that air and acetylene are switched on and click OK in the checklist window.

Insert the Selenium lamp into position 1 in the SpectrAA 50. To optimise the lamp signal adjust the two screws at the bottom of the lamp holder whilst looking at the height of the bar on the computer. If the bar goes too high then click on **rescale**, adjust the two screws to give the maximum height on the bar.

To optimise the **flame signal** align the burner correctly using the target card. Then switch on air pump, switch on acetylene flow and ignite the flame. Using a standard selenite solution aspirate it with the VGA 77. Adjust the burner height both vertically and horizontally until the optimum height is achieved. These parameters can then be saved for future dates and experiments. If the burner is undisturbed this step may be skipped.

The instrument is now ready for use.

4.3.2 Procedure for the reduction of sodium selenate standard to sodium selenite at various temperatures.

1. The sodium selenite and selenate solution standards have been prepared in the same method as has been previously described in **Section 2.2**.
2. $100cm^3$ of 100ppm SeO_4^{2-} standard solution in distilled water was heated to the desired temperature i.e. 50^0C in a water bath.
3. $200cm^3$ of 6M HCl was also heated to 50^0C in the water bath.
4. Once the two solutions had reached the correct temperature then 1 cm^3 of the selenate solution was added to 99 cm^3 of the 6MHCl solution and mixed thoroughly. The stop clock was started at the time of mixing. The resulting concentration of Se in the solution was 1 ppm (1000ppb).
5. The volumetric flask was then returned to the water bath and maintained at the desired temperature.
6. At certain intervals $1cm^3$ aliquots of the partially reduced selenate was extracted using a micro-pipette and added to 1M HCl at room temperature and made up to $100cm^3$ using 1M HCl. The resulting concentration was then 10ppb.
7. The solution was then mixed thoroughly and analysed by the VGA 77 and the HGAAS as described in **Section 4.3.1**. The resulting rate curve at 50^0C is given **Fig 4.3**.
8. This procedure was followed exactly for all further temperature experiments.

4.3.3 Procedure for digestion of the Selenium yeast sample and reduction of selenate to selenite and the subsequent selenium analysis.

1. 500mg of the Se enriched yeast was accurately weighed out onto a glass boat.
2. This was transferred into a 250cm^3 conical flask.
3. 4cm^3 of concentrated Sulphuric Acid (H_2SO_4) was added.
4. The flask was placed on the heating mantle (Bibby: HB502) at 7 bar or 150^{0}C for 40 seconds until the solution had turned brown. The conical flask was then moved off the direct heat as the hydrogen peroxide was added.
5. 5cm^3 of 35% H_2O_2 was added drop-wise and the solution effervesced for a while before going clear. The hydrogen peroxide was added drop-wise to avoid splashing and to avoid too vigorous a reaction.
6. The conical flask was replaced onto the direct heat once all the peroxide had been added. As the water was driven off from the solution the sample turned a light brown colour again.
7. Another 5cm^3 of the 35% H_2O_2 was added and the steps 5 and 6 were repeated until 15cm^3 of the 35% H_2O_2 had been used.
8. The resulting solution was transferred to a 100cm^3 volumetric flask and the washings of the conical flask added to the volumetric flask by rinsing the flask with 6M HCl at 80^{0}C. The volumetric flask was made up to the mark with 6M HCl at 80^{0}C.
9. Once the volumetric flask had been made up to the mark the flask was then returned to the water bath at 80^{0}C for a further 10 minutes at 80^{0}C to allow the selenate to be reduced to selenite as in **Section 4.3.2**.

10. 150μL of this solution was taken using an analytical micro-pipette and added to 100cm^3 of 1M HCl at room temperature.

11. This was mixed thoroughly and analysed directly using the H.G.A.A.S. as described in **Section 4.3.1**.

4.3.4 Procedure for determination of a sample by standard addition.

1. Prepare up to six 100cm^3 volumetric flasks. In the first, place only 100cm^3 1M HCl.

2. In the subsequent volumetric flasks add increasing volumes of 1ppm Na_2SeO_3 (e.g. 2.5cm^3, 5cm^3, 7.5cm^3...) and make the solution up to the mark with 1M HCl. The concentration of the volumetric flasks are now 2.5 ppb, 5 ppb, 7.5 ppb ...etc.

3. Add an aliquot (100μL) of the digested sample to each of the six 100cm^3 volumetric flasks and shake until the solution is homogenous.

4. The solutions are then analysed as described in **Section 4.3.1**.

5. An example of the graph that results from a standard addition experiment, it can be seen in **Fig 4.14**. The intercept of the line with the X-axis is the concentration of the sample.

4.4 Results and Discussion

4.4.1 The effect of HCl concentration on the Se peak.

The purpose of this experiment was to determine which concentration of HCl, in the sample solutions, gave the maximum sensitivity. A standard solution of Se (10 ppb as selenite) in different concentrations of HCl were prepared as described below.

1cm^3 of a 100 ppm SeO_3^{2-} standard in water (as described in **Section 2.2**) was taken using a graduated pipette and added to a 100cm^3 volumetric flask. The flask was then made up to the mark with 6M HCl. 1cm^3 aliquots of this solution was added to 7 different 100cm^3 volumetric flasks. Aliquots of 6MHCl were added to give final HCl concentrations of zero, 1M, 2M, 3M, 4M, 5M and 6M HCl respectively after dilution to the mark with distilled water. The final concentration of the Se in the solution is 10ppb.

The above solutions were analysed by hydride generation AA. The results are as shown in ***Appendix Table 4.1***. These were plotted with Mean Absorbance versus Concentration of HCl and shown in **Fig 4.2**.

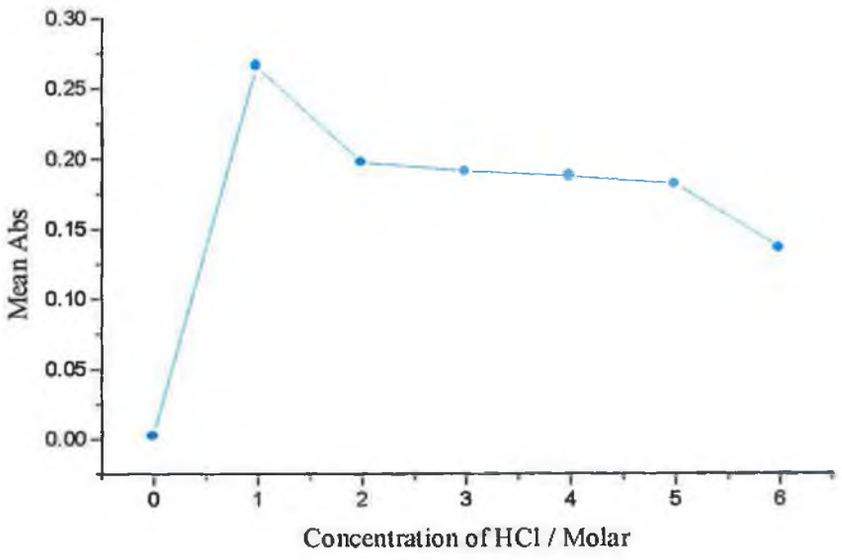

Fig 4.2

Based on these results a concentration of 1M HCl was used for the following calibration curve, as the signal gave a maximum reading at this concentration. The experiment shows that an adequate signal is obtained over the range 1-6M HCl by hydride generation A.A. This was thought not to be possible as the concentrations were deemed too dilute for an adequate signal.

4.4.2 Standard Curve for Sodium Selenite.

100ppm Se (as Sodium selenite) was prepared in distilled water as described in **Section 2.2**. 1cm^3 of 100ppm was made up to 100cm^3 with 1M HCl giving a 1000ppb Se concentration. Aliquots of this solution were diluted to 100 cm^3 with 1M HCl as shown in the following **Table 4.2**.

Table 4.2

Solution No.	Volume of 1000 ppb Se/ cm^3	Final [Se]/ppb
1	0.3	3
2	0.6	6
3	0.9	9
4	1.2	12
5	1.5	15

The standard solutions were analysed by the method described in **section 4.3.1**. The calibration curve is given below in **Fig 4.3**.

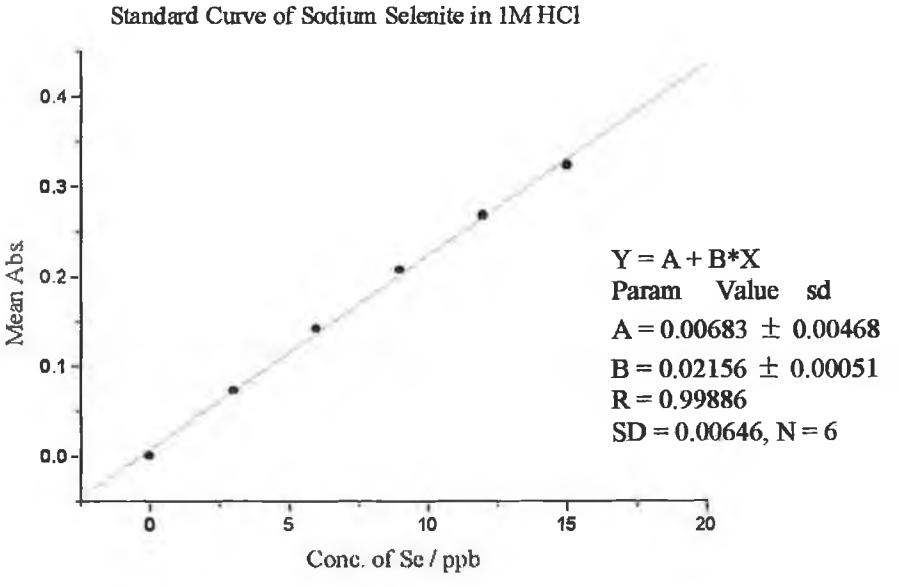

Fig 4.3

The results are given for this graph in the *Appendix Table 4.2*. This calibration curve shows good linearity with an intercept of zero and coefficient of 0.9986. This proves that for standard solutions made up using pure solutes the calibration is linear and either standard addition or direct measurement from the calibration curve is possible theoretically. This is shown not to be true for direct measurement in a later section.

4.4.3 Rate of reduction of SeO_4^{2-} in 6M HCl.

It is convenient to follow the rate of reduction of SeO_4^{2-} to SeO_3^{2-} using hydride generated AA as only the lower oxidation state is detectable using the technique. In the experiment the hydride generation AA technique allows very fast measurements to be taken, giving a detailed map of the rate of reduction of SeO_4^{2-} to SeO_3^{2-} by 6M HCl. The study was carried out at various temperatures. The rate constants and Arrhenius parameters were measured and calculated.

The temperature was increased in 10 degree intervals starting at 50^0C as it had a long reduction time but did not exceed a days working time, up to 90^0C where the selenate is reduced in a matter of minutes. Each experiment was carried out in triplicate at each temperature.

Sample Calculation of the rate constant for reduction of SeO_4^{2-} to SeO_3^{2-} at 50^0C in 6M HCl.

When calculating the rate constants for the reduction reaction the Origin computer program was used. Assuming that the reaction is first order then the concentration of the product should increase according to the equation.

$$c = c_{\infty}(1 - e^{kt})$$

Eqn 4.6

where c is the concentration of selenite after time t and c_∞ is the final concentration of the selenite. As absorbance is directly proportional to concentration, the equation may be rearranged to the form

$$A = A_\infty*(1-EXP(-k*t))$$

Eqn 4.7

where A is the absorbance after time t. The parameter A_∞ is the final absorbance and the parameter k is the rate constant. Using the Origin package the data was fitted to the above equation and the best fit values for A_∞ and k were determined using non-linear least squares. The only constraints used were $A_\infty > 0$ and $k > 0$. The Chi Squared value is a measure of the goodness of fit. The result of the fitting process is given below **(Fig 4.4)**

Reduction of SeO_4^{2-} to SeO_3^{2-} at 50^0C in 6M HCl.

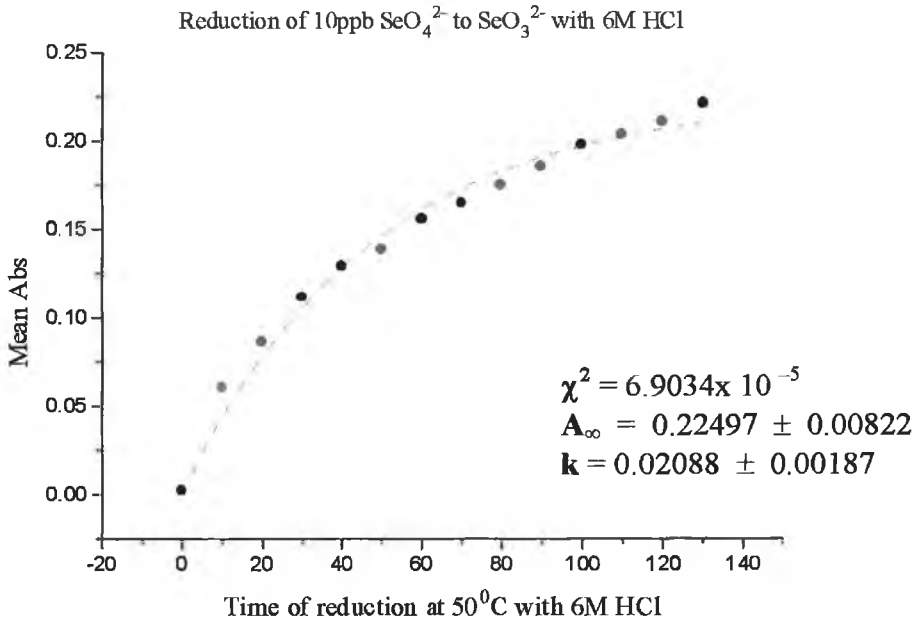

Fig 4.4

Results for experiments at 60^0, 70^0, 80^0 and 90^0 are given below (**Fig 4.5** to **4.9**). The best first order fit is plotted using the Origin computer package. This is shown as the red dashed arc. The points on the graph are in reasonable agreement with the first order rate curve. At 90^0 C the rate of reduction did not obey first order kinetics. In one experiment, a plateau was reached [**Fig 4.8**] while in three subsequent experiments a bell shaped curve was obtained [**Fig 4.9**]. In the latter case a red precipitate was observed indicating reduction of selenite to selenium. As a result it was decided to carry out reduction at 80^0C for 10 minutes in 6M HCl, in all analytical applications.

Reduction of SeO_4^{2-} to SeO_3^{2-} at 60^0C in 6M HCl.

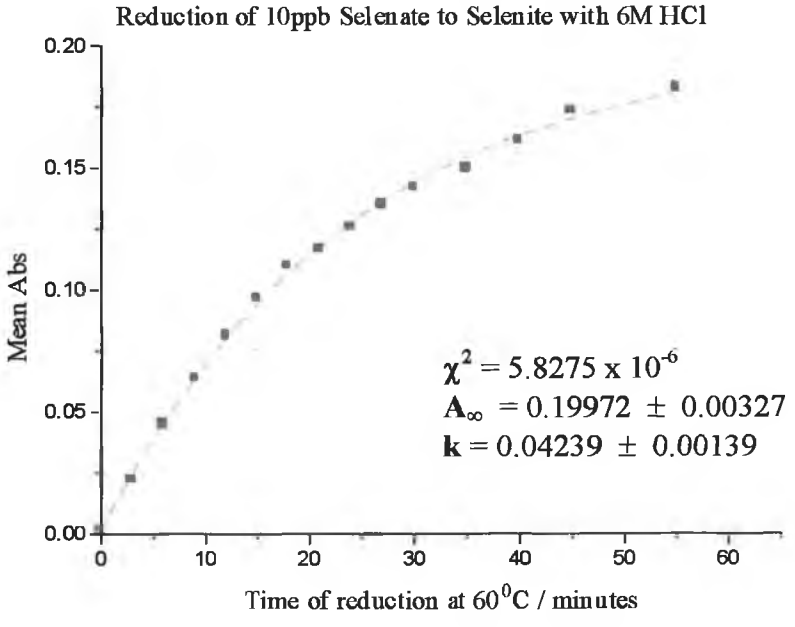

Fig 4.5

Reduction of SeO_4^{2-} to SeO_3^{2-} at 70^0C in 6M HCl.

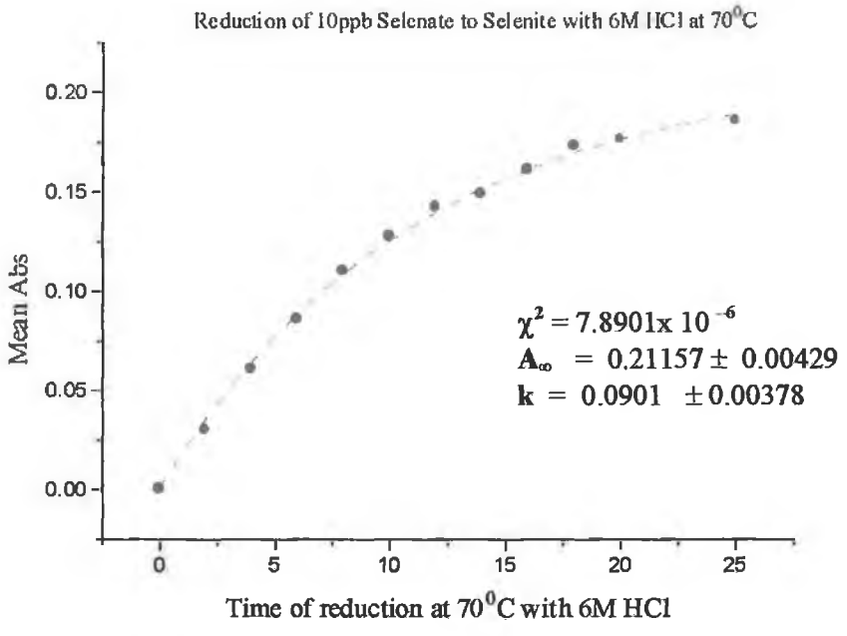

Fig 4.6

Reduction of SeO_4^{2-} to SeO_3^{2-} at 80^0C in 6M HCl.

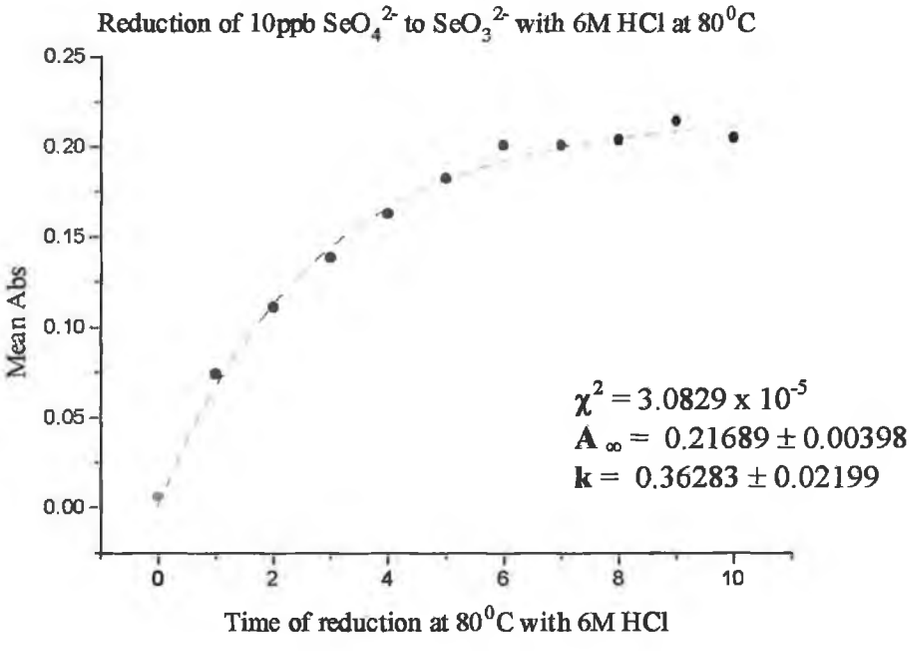

Fig 4.7

Reduction of SeO_4^{2-} to SeO_3^{2-} at 90^0C in 6M HCl.

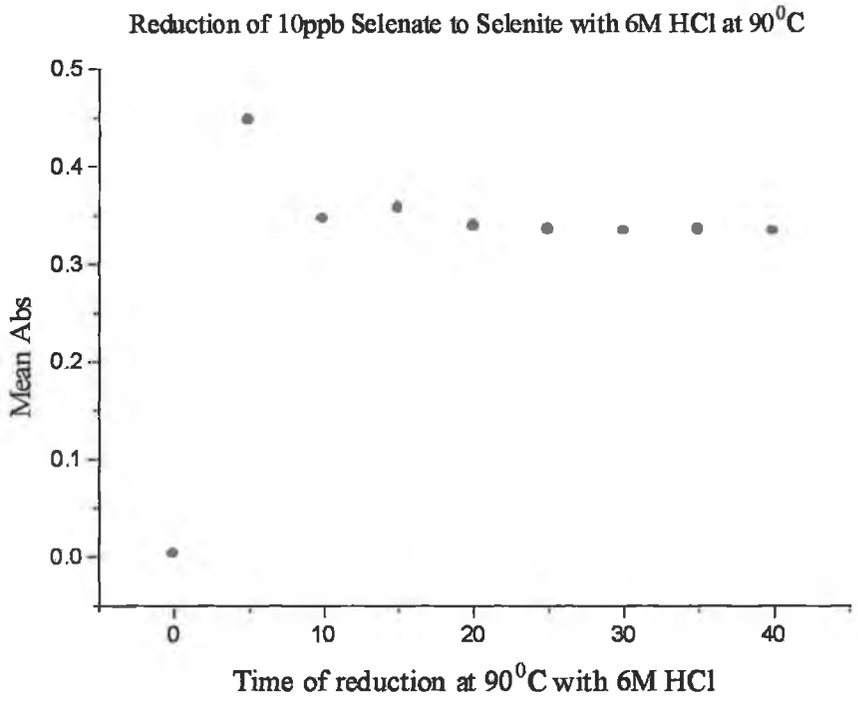

Fig 4.8

Reduction of SeO_4^{2-} to SeO_3^{2-} at 90^0C in 6M HCl.

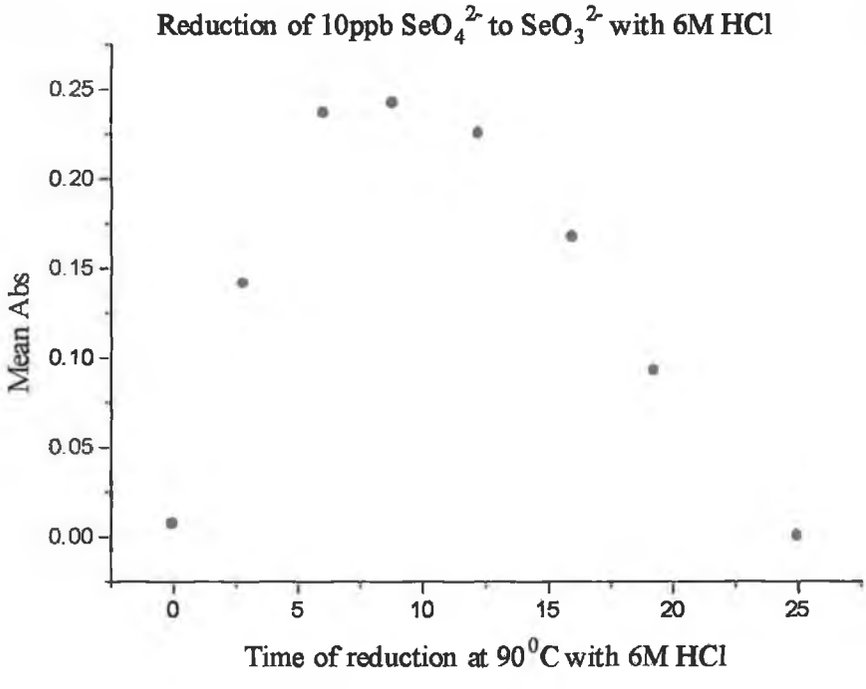

Fig 4.9

The rate constants for the various temperatures were calculated and are given below on **Table 4.3**.

Table 4.3

Temperatures / °C	Temperature / K	$\frac{1}{K}$	Rate Constant k / min^{-1}	ln k
50	348.15	2.87exp-3	0.0209	-3.869
60	358.15	2.79exp-3	0.0424	-3.161
70	368.15	2.72exp-3	0.0901	-2.407
80	378.15	2.64exp-3	0.3628	-1.014
90	388.15	2.57exp-3	none	none

The Arrhenius equation relates k to the absolute temperature.

$$\ln k = \ln A - E_a/RT \qquad \textbf{Eqn 4.8}$$

A = pre-exponential factor.

E_a = activation energy.

T = temperature in Kelvin.

R = Universal Gas Constant = 8.314 $JK^{-1}mol^{-1}$.

A plot of Ln k versus 1/T for the rate constants in **Table 4.3** is given in **Fig 4.10**.

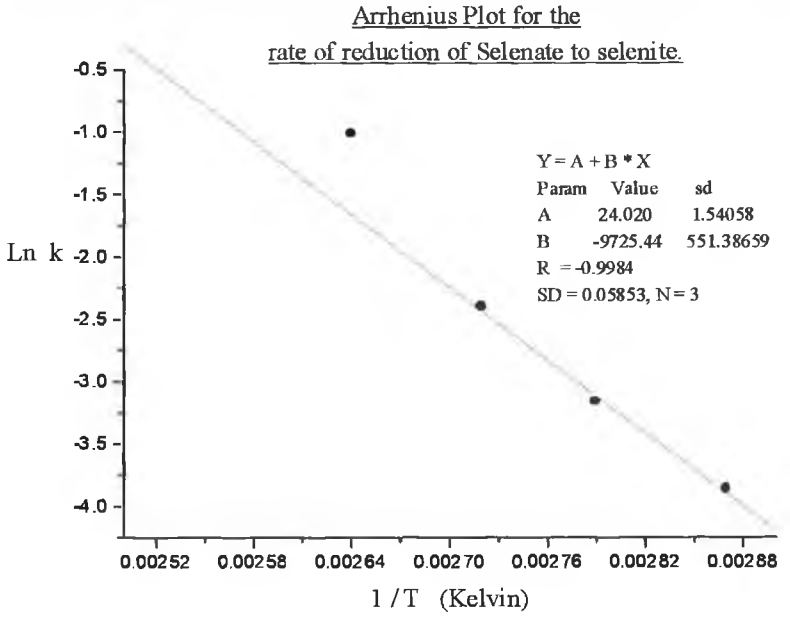

Fig 4.10

From the linear Arrhenius plot it is easy to see that at the lower temperatures the reaction obeys the Arrhenius equation. But at the 90^0 C temperature this changes. The In k value for the reaction at 90^0 C is not on the line with the other points and thus indicating that possibly a different order of kinetics is being obeyed here. The conclusions that can be drawn from this are as follows.

- the reaction occurred at too fast a rate which cannot be measured accurately by the method used, implying that the value is false and the correct value is on the line and that the reaction is first order all the way.
- secondly and more probably is that at higher temperatures the reaction alters from being first order to something else.

Due to time restrictions, this hypothesis was not possible to investigate further. Although studies into this are being carried out. The activation energy for the reaction may be calculated from the slope of the graph in **Fig 4.10**.

Slope = $-E_a/R = -97255.44$

$\Rightarrow E_a = 97255.44 \times 8.314$ J mol^{-1}

$\Rightarrow E_a = 808.58$ kJ mol^{-1}

This appears to be a remarkably high value for the activation energy and may indicate a more complex mechanism than simple first order. The pre exponential factor (A) from the Arrhenius equation is obtained from the intercept of the graph [**Fig 4.11**] and gives ln A = 24.02 $\Rightarrow$ A = 2.7×10^{10} min^{-1}.

4.4.4 Effect of Temperature on digestion step.

Initially following the method laid out by Metrohm, the initial temperature for digestion was set at 150^0C. This proved to be too high as the results showed a loss of Se due to charring of the sample releasing volatile Se. The following experiment was undertaken to achieve the correct temperature of digestion.

Calculation of amount of Selenium present:

A sample of Se yeast was digested, reduced at the desired temperature as described in **Section 4.3.3**. Analysis of Se was carried out by Standard Addition as described in **Section 4.3.4**. The concentration of Se in the final solution was compared with the expected concentration (assuming 2000ppm Se in the yeast sample). The expected concentration may be calculated as follows. Suppose 500mg of Se enriched yeast is digested. This contains 1 mg of Se approximately. Following digestion and reduction (at 80^0C for 10minutes in 6M HCl), the reduced solution has a volume of $100cm^3$, implying a selenium concentration of 10 ppm. A 150μL aliquot (V) of this solution diluted to $100cm^3$ in 1M HCl has an expected concentration of 15 ppb. Results for digestion at 150^0C and at 110^0C are given in **Table 4.4**.

Table 4.4

[V] / μL	Expected [Se] / ppb at 150^0C	[Se] determined / ppb from H.G.A.A.S.
50	5	4.006
100	10	15.73
150	15	11.76
200	20	21.95
	at 110^0C	
20	20	19.91

[V] = volume of digested sample used in standard additions. All data for this table can be seen in ***Appendix Tables 4.8*** to ***4.12*** inclusive.

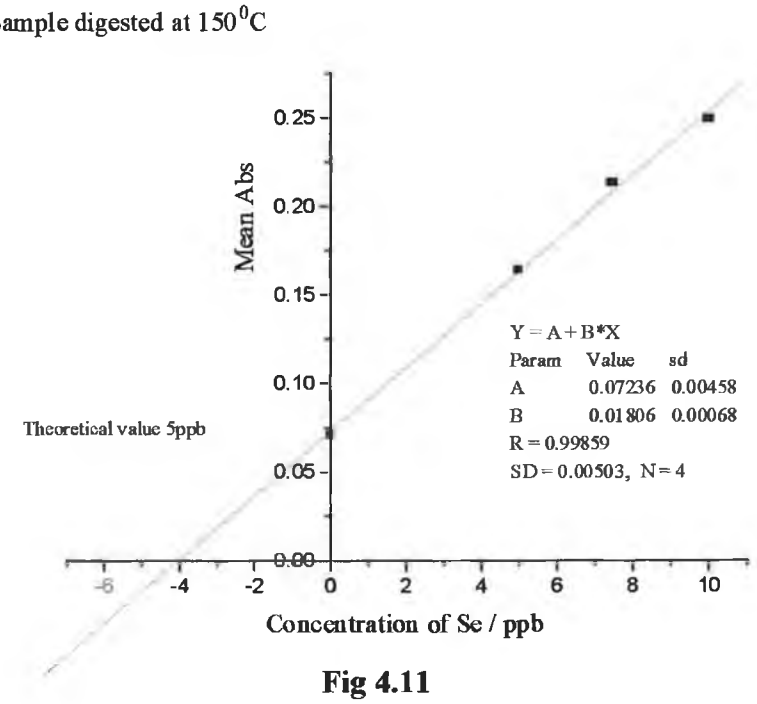

Fig 4.11

An example of the way that the value for standard addition is calculated in given in **Fig 4.11** above. The intercept of the X-axis is the concentration of the sample under investigation.

These results show that there is a loss of selenium with the use of higher temperatures for digestion. The lower temperature gave the correct result and was chosen as the ideal initial digestion temperature for further digestions unless specified. Due to time restrictions this ideal temperature of digestion was not used as the digestion temperature of the sample for the polarographic technique.

4.4.5 Analysis of selenium enriched yeast by Standard Addition.

If the analyte is present in low concentration and no suitable standards are available, and if only one element is to be assessed at a time, the standard addition technique can be applied. It involves the addition of known amounts of sample, intimate mixing and production of a set of targets under identical conditions. The added element portion will, in principle, undergo the same matrix effects as the originally present fraction, and from the intensity increase due to the addition of the standard spike, one can directly convert the characteristic absorbance signal of the analyte into concentration. (Hewett.)

In this experiment 500mg of Se enriched yeast was digested and reduced as described in **Section 4.3.3** and analysed by standard addition as described in **Section 4.3.4**. Full results are given in *Appendix Tables 4.13* to *4.19*. The compiled results are given in **Table 4.5** below.

Table 4.5

[V] / μL	[Se] / ppb found by H.G.A.A.S.	[Se] / ppm in yeast
150	15.51	2068
150	14.87	1982
150	15.61	2081
150	16.08	2144
200	19.97	1997
200	20.58	2058
200	20.12	2012

[V] = volume of digested sample used in standard addition.

The mean value is 2048.85 ± 58.35 ppm.

A control chart is plotted in **Fig 4.12**, using the data from column two of **Table 4.5**.

The confidence limits are calculated using the formula

$$\bar{x} = st / \sqrt{n}$$

Eqn 4.9

Mean = 15.368

S.D. = 0.4207

Upper Confidence Limit = 15.757

Lower Confidence Limit = 14.979

Analysis of Se yeast samples.

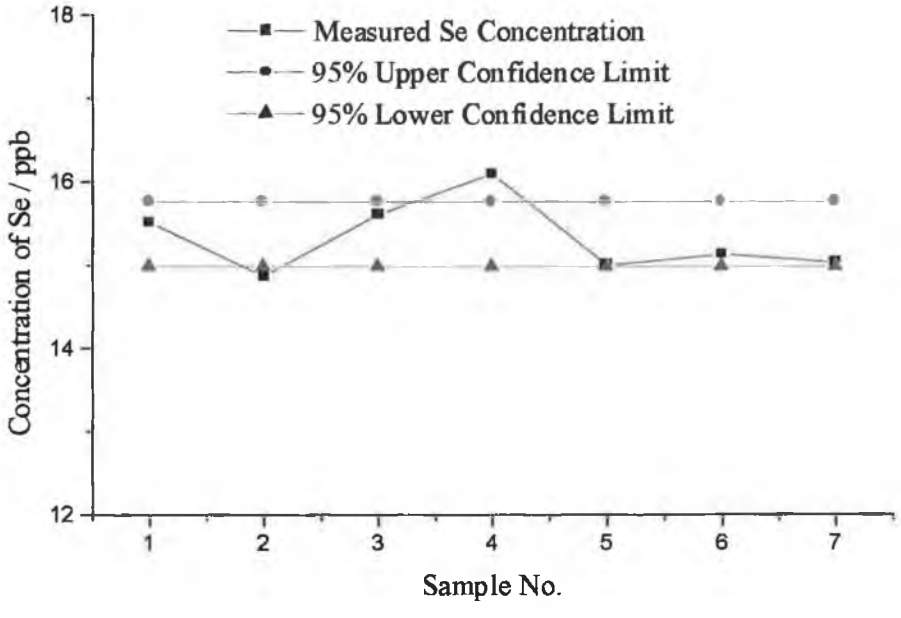

Fig 4.12

This experiment showed that the practice of standard addition on this Se enriched yeast sample is of sound reasoning and produces an accurate, reproducible result in a short space of time, which is ideal for routine analytical work where large volumes of samples would be analysed. With high precision.

4.4.6 Method Validation

The sample may be spiked before the digestion and reduction steps with a known quantity of selenate to determine percentage recovery of added Se.

A known amount of selenate in aqueous form was added to the 500mg of Se enriched yeast. The sample and selenate were digested and reduced together. The result should equal the sum of the predetermined Se and the added Se.

It was decided to use sufficient added selenate to give a final concentration of 15ppb in the solution for analysis.

Since 500mg of selenium enriched yeast contains 1 mg of Se and $0.5cm^3$ of 1000ppm Na_2SeO_4 contains 0.5 mg of Se, a mixture of these contains 1.5 mg of Se. The mixture was digested and reduced as described in **Section 4.3.3**. The reduced solution should contain 15 ppm Se. An aliquot of this solution was diluted to $100cm^3$ using 1M HCl and analysed as described in **Section 4.3.4**. This solution should contain 15 ppb Se. Six determinations were made and the results are given in **Table 4.6**.

Table 4.6

Expected Amount of Se / ppb	[Se] / ppb by H.G.A.A.S.
Sample A = 15	15.18
Sample B = 15	16.08
Sample C = 15	15.86
Sample D = 15	14.78
Sample E = 15	16.23
Sample F = 15	15.03

All data for this table can be seen in ***Appendix Tables 4.20*** to ***4.25*** inclusive.

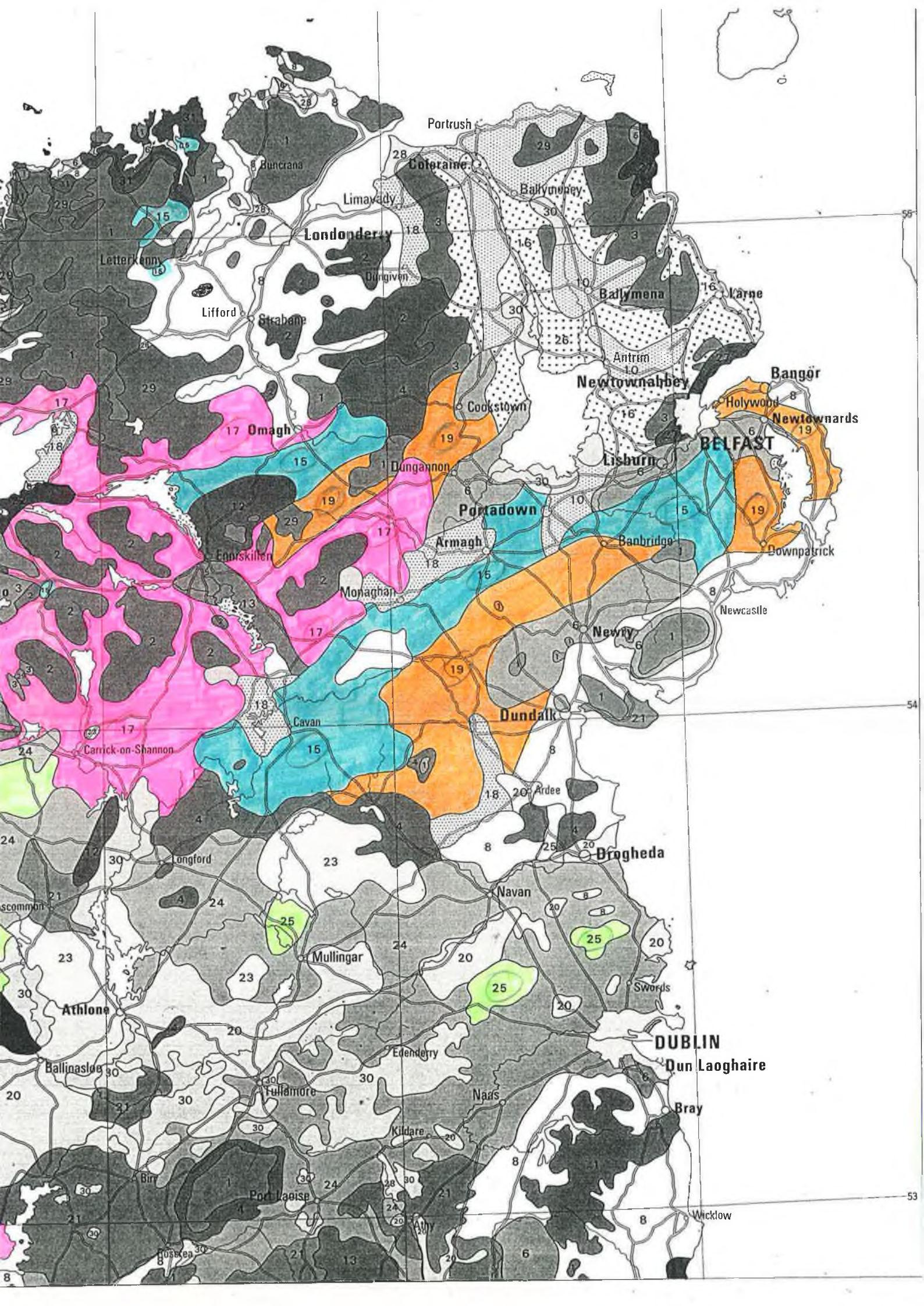
Portrush
Coleraine
Buncrana
Limavady
Ballymoney
Londonderry
Letterkenny
Dungiven
Ballymena
Larne
Lifford
Strabane
Antrim
Newtownabbey
Bangor
Holywood
Newtownards
Cookstown
Omagh
BELFAST
Lisburn
Dungannon
Portadown
Armagh
Banbridge
Downpatrick
Enniskillen
Monaghan
Newcastle
Newry
Dundalk
Cavan
Carrick-on-Shannon
Ardee
Drogheda
Longford
Navan
Mullingar
Swords
Athlone
DUBLIN
Dun Laoghaire
Edenderry
Ballinasloe
Tullamore
Naas
Bray
Kildare
Birr
Port Laoise
Wicklow
Athy
Tuosist
55
54
53

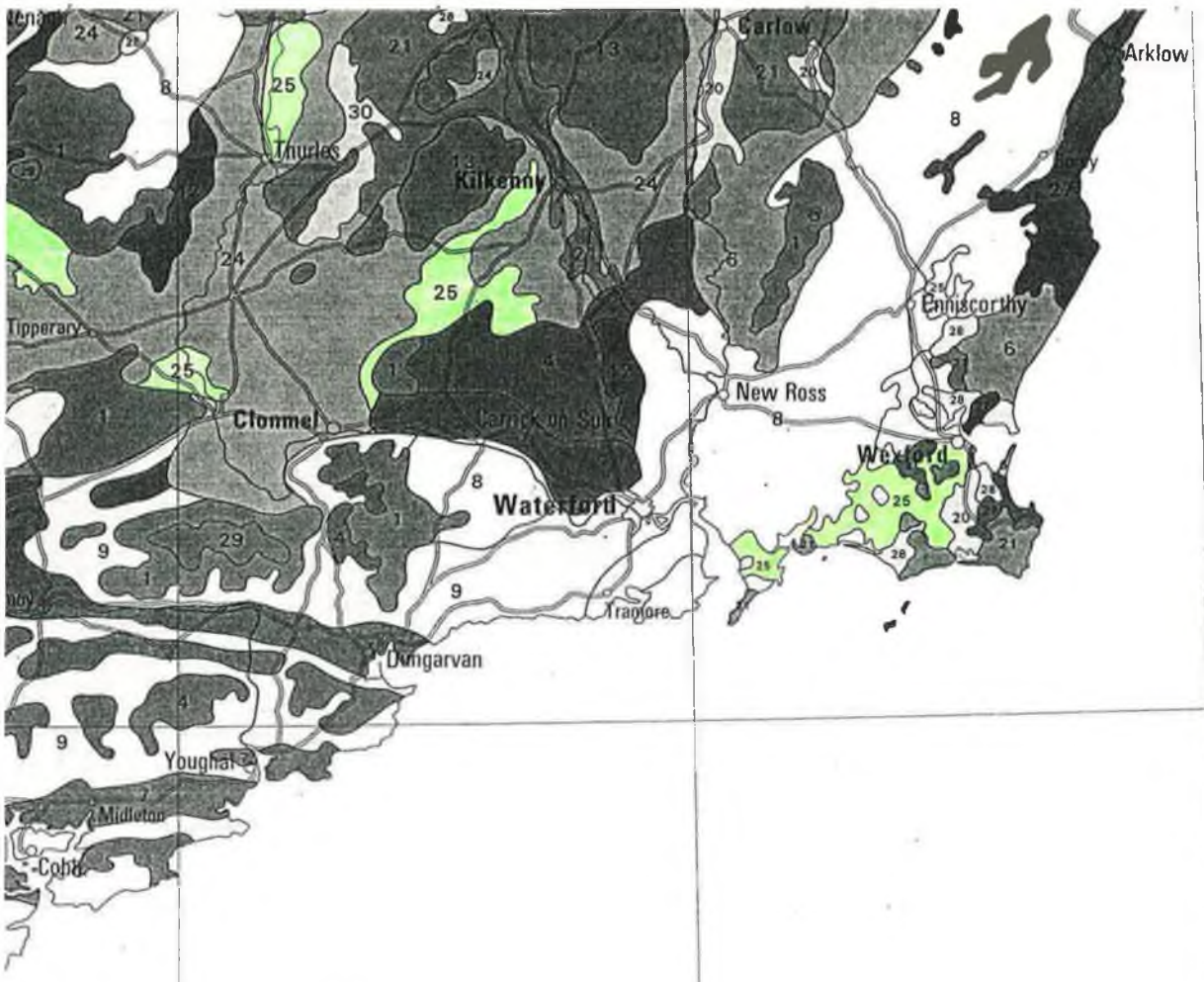

Appendix 1.1

ion with Soil Map f the World	Physiographic Division	No.	Soil Associations: Principal Soil	Soil Associations: Associated Soils	Parent Material	Correlation with Soil Map of the World
Podzols, Dystric ls, Lithosols	Drumlin (Wet Mineral and Organic Soils)	15	Gleys*	Acid Brown Earths	Shale–Old Red Sandstone Till	Dystric Gleysols, Dystric Cambisols
Gleysols, Histosols		16	Gleys*	Acid Brown Earths	Basalt Till	Dystric Gleysols, Dystric Cambisols
Histosols, Cambisols		17	Gleys*	Peaty Gleys* Interdrumlin Peat and Acid Brown Earths	Shale–Old Red Sandstone Till	Dystric and Humic Gleysols
Podzols, Gleysols	Drumlin (Drier Mineral and Organic Soils)	18	Grey Brown Podzolics	Gleys* Peaty Gleys* and Peat	Carboniferous Limestone–Old Red Sandstone Till	Orthic Luvisols, Eutric Gleysols
c Lithosols		19	Acid Brown Earths	Gleys* and Peaty Gleys	Shale–Old Red Sandstone Till	Dystric Cambisols, Dystric Gleysols
Cambisols, dystric, Cambisols	Flat to Undulating Lowland (Mostly Dry Mineral Soils)	20	Grey Brown Podzolics	Basin Peat and Regosols	Carboniferous Limestone–Gravels and Sands	Orthic Luvisols, Eutric Histosols
Cambisols, Luvisols		21	Grey Brown Podzolics	Gleys**	Carboniferous Limestone Gravelly Drift	Orthic Luvisols, Eutric Cambisols
Cambisols, dystric Cambisols		22	Degraded Grey Brown Podzolics	Gleys** and Basin Peat	Carboniferous Limestone Drift	Orthic Luvisols, Eutric Gleysols and Podzoluvisols
dystric Cambisols, Cambisols,		23	Shallow Brown Earths	Rendzinas	Carboniferous Limestone Rock and Drift	Calcaro-eutric Cambisols, Rendzinas
Cambisols, Gleysol		24	Grey Brown Podzolics	Gleys**	Carboniferous Limestone Till	Orthic Luvisols, Eutric Gleysols
Podzols, Gleysols	Flat to Undulating Lowland (Mostly Wet Mineral Soils)	25	Gleys*	Grey Brown Podzolics	Limestone–Sandstone–Shale Till	Dystric Gleysols, Gleyic Luvisols
and Humic Gleysols		26	Gleys*	Peaty Gleys* and Acid Brown Earths	Basalt Till	Dystric and Humic Gleysols
Gleysols and Cambisols		27	Gleys*	Grey Brown Podzolics	Glacial Muds of Marine Origin	Eutric Gleysols, Gleyic Luvisols
Podzols, ystric Histosols		28	Regosols	Gleys**	Alluvium	Eutric Fluvisols, Eutric Gleysols
	Organic Soils	29	Climatic Peat	Organo-Mineral Soils	—	Dystric Histosols, Placi-dystric Histosols
		30	Basin Peat	Organo-Mineral Soils	—	Eutric Histosols, Dystric Histosols
			Reclaimed Podzols and			Dystric Histosols

The mean, standard deviation and 95% confidence limits [**Eqn 4.9**] were calculated as before. A control chart is given in **Fig 4.13**.

Mean = 15.527

Standard Deviation = 0.606

Upper Confidence Limit = 16.162

Lower Confidence Limit = 14.890

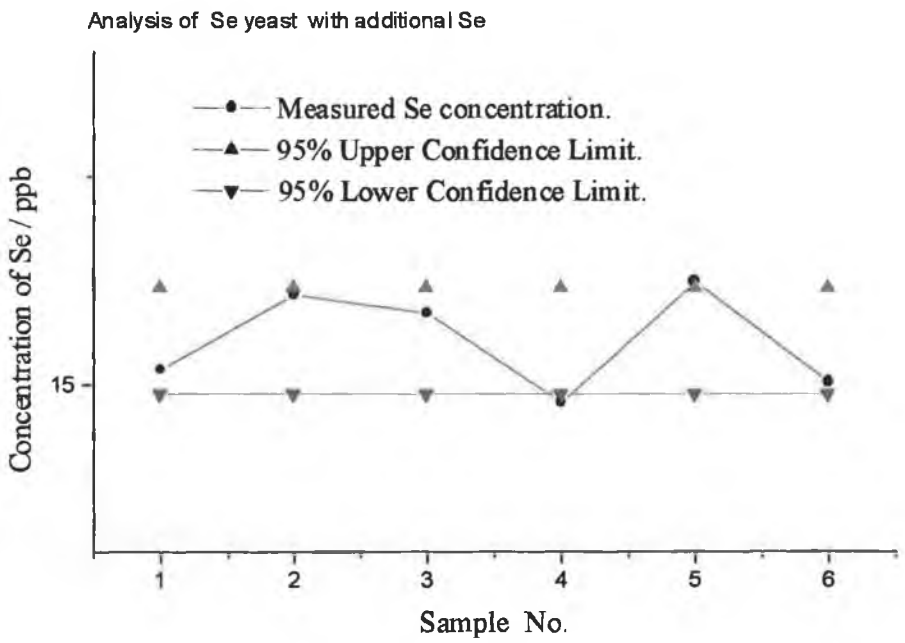

Fig 4.13

Calculation of % recovery of Se (as selenate)

The % recovery of Se as selenate may be calculated by subtracting the previously measured Se concentration in the yeast from the total Se concentration. Since 500mg of yeast would contribute (15.368*100)/150 ppb = 10.245 ppb (**Section 4.4.5**) the concentration of Se recovered is (15.527 – 10.245) = 5.28 ppb. The percentage recovery was therefore 105.6%.

Chapter 5: Conclusion

Polarography.

Initially the various physical conditions were analysed and the optimum settings were chosen, based on the best peak current for standard sodium selenite. The deposition potential was chosen at –50mV even though it is on a sharp decline as indicated in **Fig 2.6**. The combination of sensitivity, peak symmetry and peak current gave the best results over other conditions. The other physical settings were chosen under the same criteria which lead to a pressure of 1.2 bar being chosen as the pressure on the mercury drop. The relationship between the pressure on the mercury drop and the peak signal was found to be linear [**Fig 2.7**]. The greater the pressure, the greater the amount of mercury forced out, the greater the surface volume for reacting, the greater the peak current upon reduction. 120 seconds was chosen as the electrolysis time, as another linear relationship was discovered between the electrolysis time and the peak current [**Fig 2.8**], so a balance was struck between peak current and sample run time.

The reproducibility of the technique was investigated [**Section 2.5.4**]. Two sets of measurements were recorded. One was the within-sample variance [a repeated number of measurements on the same sample without altering any conditions] and the other was the between-sample variance [number of measurements based on the same conditions as the within-sample variance but changing the cell contents each time while keeping the concentrations the same each time]. The within-sample variance is 3.952 and the between sample variance is 2.565, both variances were compared to each other and the result showed that direct determination using a calibration curve was not a viable possibility because between runs and changing the electrolyte, significant differences can occur.

At low concentrations it was found that the concentration curve had a definite curve [**Fig 2.11**] so a linear range was needed to be established [**Fig 2.12**] within which all analytical work was to be completed. This range was determined as lying between the concentration range of 0.04 ppm and 4ppm in the cell [**Section 2.5.5**].

The working electrolyte was studied and compared with various other workers [**Table 2.8**]. The electrolyte chosen was 1M HCl. The HCl gave the best peak for sodium selenite it was both a clearly resolved peak and a symmetrical peak. It also had the added advantage that by using HCl as the electrolyte, the concentration or make up of the electrolyte is not radically altered when the reduced sample is added, the reduced sample being made up of mostly 6M HCl.

The study of the rate of reduction of selenate to selenite was attempted at various temperatures [**Section 2.5.10 Fig's 2.21** to **2.25** inclusive] This section did not turn out as well as expected as the graphs drawn from the reduction had a wide scattering of points and only a general trend was gleaned. To fit a rate curve using the origin computer package, more detailed and accurate readings were needed. The general information taken from this section was that at higher temperatures the reduction of selenate to selenite did occur at a faster rate but any further deducing was impossible from the information.

The effect of having the container closed or open showed that if the container is left open during the reduction step the results are significantly lower than if the container is stoppered during this section. A reasonable assumption is that volatile forms of selenite are formed and are then lost during this boiling stage.

The effect of the organic matrix was also studied. This suggested that having 50μL of the yeast (digested as described in **Section 2.4.1**:D) added to 10mL of the electrolyte increased the Se signal **Fig 2.27**. The analysis of the sample was based on an initial

standard curve showing the linearity of the selenite. Then the sample was added followed by further standard additions [**Section 2.5.13**]. The initial standards were subtracted from the latter and then normal standard addition calculations were employed. These are shown in graphic form in **Fig 2.29** and in *Appendix 2.13* to *2.15*. By this method the mean result was taken as 2437 ppm ± 277 ppm. This is significantly higher then the result from either the XRF method or the H.G.A.A.S. method.

The advantage of this method is the use of no specialised equipment except for the polarographic apparatus. The method is quick. The limit of detection is much lower than the XRF and is down in the ppb range (40ppb). There were some disadvantages to this technique. The apparatus is environmentally dependent, each day the sensitivity can differ radically. The overall results may be the same but the total peak currents can vary considerably. The capillary tube is fragile, easily broken and easily blocked. Based on our work, the results for the percentage of selenium in yeast were significantly higher than those found by the other two methods H.G.A.A.S. or by XRF. However, the temperature for the reduction step was not at the optimum value of 90^0C which was determined subsequently by the H.G.A.A.S. method.

X-ray Fluorescence

The selenium content is very high in the selenium enriched yeast. It is for this reason that it is possible to use the X-ray fluorescence method for the determination of selenium. Once the optimum working conditions have being identified and implemented then a clear and resolved selenium peak can be achieved as shown in **Fig 3.5**. A study of the matrix was carried out using a non-enriched yeast [*Saccharomyces cerevisiae*] as the basis for investigation. The study showed that the matrix did not

interfere with the determination of Se. Once this was confirmed, it was possible to create a standard curve using Se (as sodium selenate) and the non-enriched yeast. This standard curve, developed as described in **Section 3.4.6**, was linear.

The next step was to use this standard curve to see if the enriched yeast behaved exactly as the non-enriched yeast [**Section 3.4.9**]. The reproducibility of the method needed to be tested and verified and this end, several samples were analysed in triplicate and a statistical test done on the results. The mean result was 2033 ppm with a standard deviation of 11.49ppm. The standard deviation is very small indicating that the precision of the analysis is very good. The assumed true answer is 2000ppm but as this is an organic sample, different samples can vary greatly. The value of 2033ppm was taken to be precise for this sample until verified by another source to be otherwise.

To prove the method to be a valid method of determining the selenium content, a further test was carried out. Samples of the non-enriched yeast were spiked with selenate and analysed (**Section 3.4.9**).

This did not work as the amounts needed to be weighed out were so small, that they could not be weighed with the desired accuracy needed to prove the method. An analysis of variance was undertaken (**Section 3.4.10**) and it showed that both the between-sample variance and the within-sample variance fell below the critical value of rejection. This meant that the bulk sample was homogenous.

The result of all these enquires showed the method to be a reliable method for determining selenium in this choice media namely an organic matrix. The other advantage of the X-ray fluorescence method is its quick analysis time and its quick and simple preparation time. Of the three methods discussed in this thesis, the X-ray fluorescence method is by far the quickest method once the initial calibration has been prepared and saved on the Lab-X 3000 benchtop XRF. The method is non-destructive,

which has a double advantage that the exact same sample can then be analysed by another method as a source of validation for that method and as a source to compare the different methods. Apart from the initial cost of the XRF benchtop Lab-X, the running cost of this method is very little. The ease and simplicity of preparation leads to very low setting up time and low running costs.

There are a few drawbacks. As the method is very quick and the sample has no or very little pre-treatment, because the method is so quick a problem with the method is the loss of the lower limit of detection that is seen in other methods. Other methods, which are more costly and far more time consuming, have far better limits of detection. The X-ray Fluorescence method seems to work also because of the high concentration of selenium in the yeast so that at much lower levels (i.e. levels of feed stuff ppb) this method has poor accuracy, precision and resolution.

The combination of all these advantages and disadvantages that makes this an ideal method for routine determination of selenium in Se enriched yeast.

Hydride Generation Atomic Absorption Spectroscopy [H.G.A.A.S.]

The third method under investigation was the H.G.A.A.S. Here again the conditions for optimum detection of selenium were studied and chosen based on the best selenium signal. The effect of the concentration of hydrochloric acid on the selenium peak was looked at and it was found that in pure solutions of sodium selenite, depending on the concentration of HCl used in the analysis, the signal could vary substantially **[Fig 4.3]**. A concentration of 1M HCl was chosen for the reduction step as it gave the best signal to background peak. A standard curve was attempted and created **[Fig 4.4]** giving a linear curve over a wide range from 3ppb to 10ppm. Because this method is so quick

and easy to use, the rate of reduction of selenate to selenite was studied after the failure of the polarographic method in this regard. The rate was followed closely and at various temperatures. The only problem encountered was at the 90^0C temperature with the reduction of SeO_4^{2-} to SeO_3^{2-}, occurred at a rate too fast to be recorded accurately. Within a few minutes at this temperature, the selenite had been reduced to selenium as indicated by the red precipitate which settled on the bottom of the volumetric flask. The rates for the other temperatures were recorded and calculated and are plotted on an Arrhenius plot in **Fig 4.11**. The graph in **Fig 4.11** shows that at lower temperatures the reduction reaction of selenate to selenite in 1M HCl occurs following a first order reaction, but at higher temperatures the reaction either occurs too fast to be recorded and is still first order or more likely it changes to a different rate order. In order to fully understand the reason for this (or to determine the exact rate order) further work is necessary to clarify this aspect, which was not within the ambit of the thesis, are required.

The effect of temperature on the digestion step was studied. Initially 120^0C was used but was deemed too high a temperature and gave high answers (**Section 4.4.4**). A lower temperature of 110^0C was then chosen and has proven very successful. The reason for this could be that at higher temperatures, the water formed from the break down of H_2O_2 is driven off too quickly causing charring of the sample, thereby creating volatile forms of selenium leading to loss of selenium. Also the charred organic material is very difficult to destroy and the undissolved organic material could act to increase the selenium signal as in **Section 2.5.12 Fig 2.27**. At lower temperatures, charring is avoided allowing total digestion of all organic material and giving a true reading of the selenium content.

Appendix 1

Appendix 1.2

NATURAL AMINO ACIDS

Name	Abbreviation	Formula
(+)-Alanine	Ala A	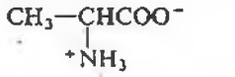
(+)-Arginine[a]	Arg R	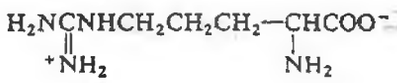
(−)-Asparagine	Asn N	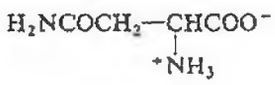
(+)-Aspartic acid	Asp D	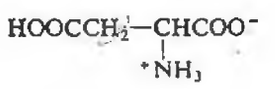
(−)-Cysteine	Cys C	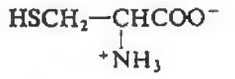
(−)-Cystine	Cys—Cys	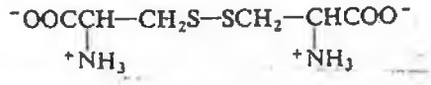
(+)-Glutamic acid	Glu E	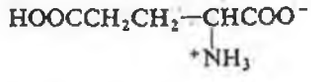
(+)-Glutamine	Gln Q	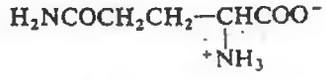
Glycine	Gly G	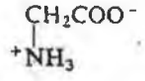
(−)-Histidine[a]	His H	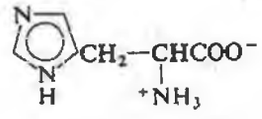

[a]Essential amino acid

NATURAL AMINO ACIDS (*continued*)

Name	Abbreviation	Formula
(−)-Hydroxylysine	Hyl	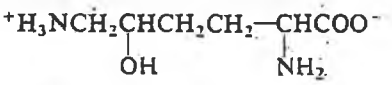
(−)-Hydroxyproline	Hyp	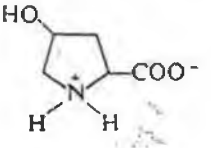
(+)-Isoleucine[e]	Ile I	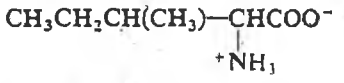
(−)-Leucine[e]	Leu L	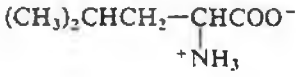
(+)-Lysine[e]	Lys K	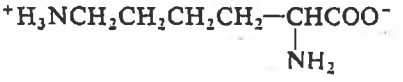
(−)-Methionine[e]	Met M	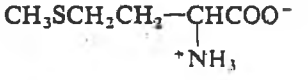
(−)-Phenylalanine[e]	Phe F	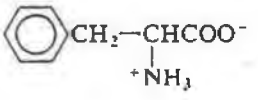
(−)-Proline	Pro P	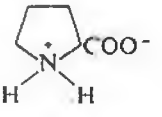
(−)-Serine	Ser S	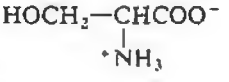
(−)-Threonine[e]	Thr T	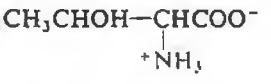
(−)-Tryptophane[e]	Trp W	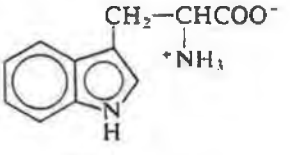
(−)-Tyrosine	Tyr Y	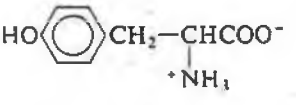
(+)-Valine[e]	Val V	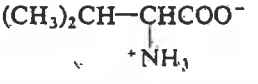

[e]Essential amino acid

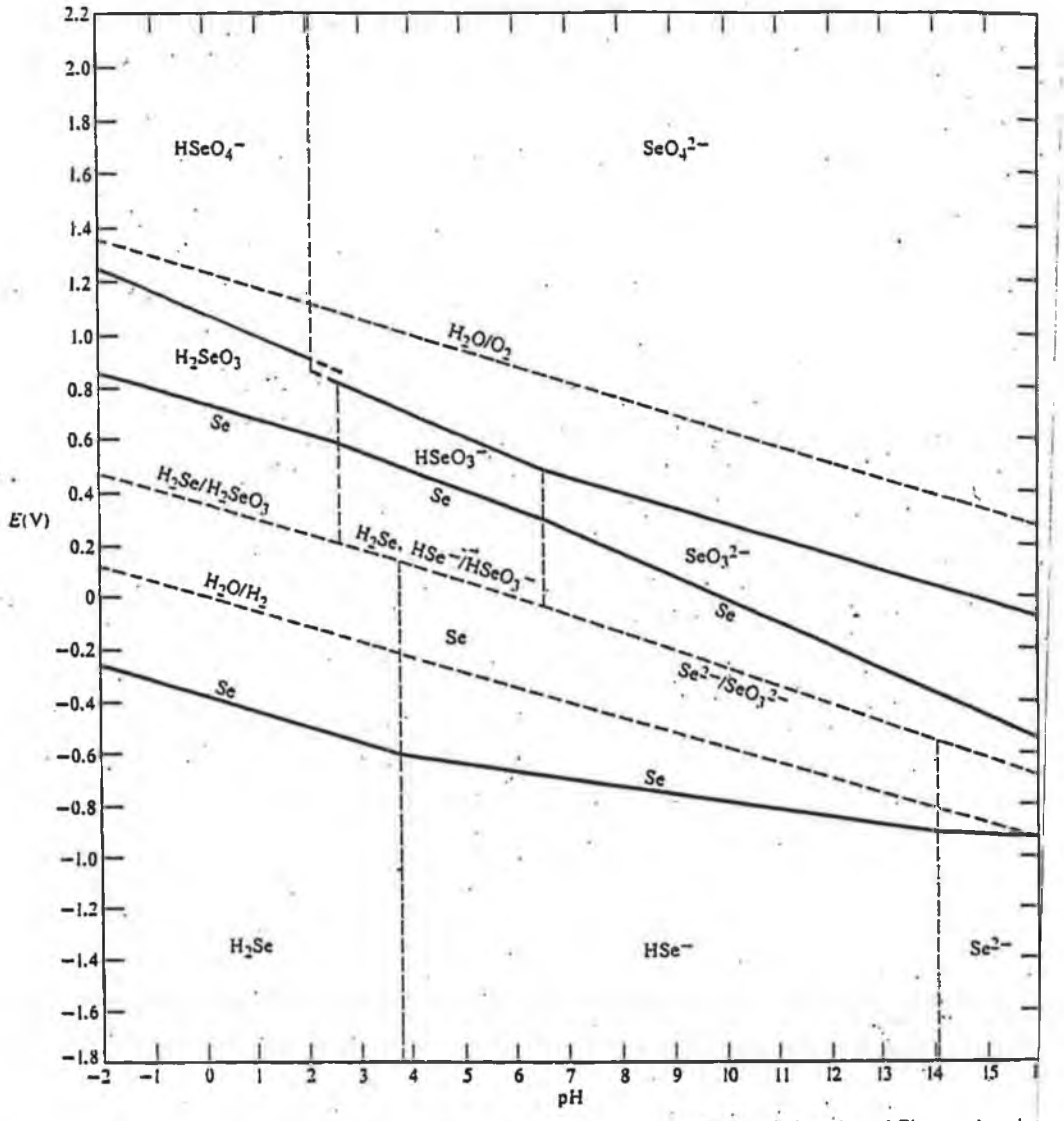

Figure 13.10 Pourbaix diagram for selenium. (Adapted from M. J. N. Pourbaix in *Atlas of Electrochemica Equilibria in Aqueous Solution* (English Translation), Pergamon, New York, 1966.)

$$E_A^0 \quad SO_4^{2-} \xrightarrow{0.17} H_2SO_3 \xrightarrow{0.45} S \xrightarrow{0.14} H_2S$$

$$SeO_4^{2-} \xrightarrow{1.15} H_2SeO_3 \xrightarrow{0.74} Se \xrightarrow{-0.40} H_2Se$$

$$E_B^0 \quad SO_4^{2-} \xrightarrow{-0.91} SO_3^{2-} \xrightarrow{-0.61} S \xrightarrow{-0.48} S^{2-}$$

$$SeO_4^{2-} \xrightarrow{0.05} SeO_3^{2-} \xrightarrow{-0.37} Se \xrightarrow{-0.92} Se^{2-}$$

Appendix 2

Appendix 2

Appendix Table 2.1 Peak Height versus Peak Potential with associated parameter variation

Initial Potential mV	Final Potential mV	Step Duration s	Step Amp. mV	Peak height at -80 mV / nA	Peak height at –480 mV / nA	Peak height at -640 mV / nA
-5	-800	0.2	5	20	15.95	No Peak
-25	-800	0.2	5	520	857	“”
-50	-700	0.4	2	490	664	“”
-75	-700	0.4	2	341	489	“”
-100	-700	0.4	2	No Peak	401	“”
-125	-700	0.4	2	“”	144	“”
-150	-700	0.4	2	“”	10.63	17.363
-200	-700	0.4	2	“”	11.832	13.55
-250	-800	0.4	2	“”	26.472	11.57
-300	-800	0.4	2	“”	125	8.57
-325	-750	0.4	2	“”	189	5.87
-350	750	0.4	2	“”	269	No Peak

Appendix Table 2.2 Statistical data for the calculation of the 95% Confidence interval with equations for mean, standard deviation and coefficient of variance.

Students' t-Table		
ν	**95%**	**99%**
1	12.70615	63.6559
2	4.302656	9.924988
3	3.182449	5.840848
4	2.776451	4.60408
5	2.570578	4.032117
6	2.446914	3.707428
7	2.364623	3.499481
8	2.306006	3.355381
9	2.262159	3.249843
10	2.228139	3.169262
11	2.200986	3.105815
12	2.178813	3.054538
13	2.160368	3.012283
14	2.144789	2.976849
15	2.131451	2.946726

Results					
x_i				Parameter	Value
189			Mean		191
178			Standard Deviation	s	7.54983
188			Number of values	n	9
191			Degrees of Freedom	n–1	8
199			Students t (95% Conf. Level)	t	2.30600
188			Upper Confidence Limit		196.803
204			Lower Confidence Limit		185.196
187					
195					

Calculating the 95% confidence interval.

$$x \pm \frac{t.s}{\sqrt{n}}$$

x = mean
t = t value for n from table
s = Standard Deviation
n = No. of samples

With probability 0.95, x will be within 2.306 of μ = true mean.

Calculating the 99% confidence interval.

With probability 0.99, x will be within 3.355 of μ = true mean.

To get the coefficient of variance =

$$\frac{s}{\bar{x}} \times 100$$

Appendix Table 2.3

Volume / μL of 1 ppm Se (as selenite) added	Concentration of Se in cell / ppb corrected for dilution	Peak Current / nA
20	1.996	2.95
40	3.984	8.397
60	5.964	16.189
80	7.937	25.082
100	9.901	34.154
120	11.858	45.574
140	13.807	59.185
160	15.748	72.180
180	17.682	86.517
200	19.608	99.272
220	21.526	119.0
240	23.438	138.0
260	25.341	153.0

Appendix Table 2.4

Volume / μL of 10ppm Se (as selenite) added	Volume / μL of 50 ppm Se (as selenite) added	Concentration of Se in cell / ppb corrected for dilution	Peak Current / nA
40		39.841	85.636
80		79.365	216
120		118.577	367
160		157.48	516
180		176.817	595
200		196.078	662
220		215.264	749
240		234.375	807
260		253.411	877
280		272.374	953
	10	49.95	128
	20	99.8	352
	30	149.551	559
	40	199.203	747
	50	248.756	937
	60	298.211	1137
	70	347.567	1317
	80	396.825	1466
	90	445.986	1691

Appendix Table 2.5

Volume of Se (as Selenite) added µL	Selenite conc. ppm	Peak Current / nA 1st attempt	Peak Current / nA 2nd Attempt	Peak Current / nA 3rd Attempt
40	10	-56.565	-55.999	-52.775
60	10	-164	-161	-149
80	10	-264	-264	-247
100	10	-365	-359	-352
120	10	-463	-468	-452
140	10	-571	-566	-538

Appendix Table 2.6

Volume of 1M HCl added / µL	Se Peak Current / µA Peak at –545 mV	Se Peak Current / nA Peak at –760 mV
50	-0.593	-8.079
100	-0.635	-8.548
150	-0.660	-9.669
200	-0.625	-10.782
250	-0.505	-14.887
300	-0.484	-15.274
350	-0.656	-10.903
400	-0.644	-9.765
450	-0.663	-47.589
500	-0.625	-9.382

Appendix Table 2.7

Volume of Se (as 10ppm Selenite) added / µL	Conc. of Acid used to make up standard	Scan 1 Peak Current / nA	Scan 2 ***Peak Current / nA***
20	0.1 M HCl	20.454	21.054
40	0.1 M HCl	62.661	63.235
60	0.1 M HCl	110.0	111.0
20	6M HCl	208.0	207.0
80	0.1M HCl	288.0	290.0
100	0.1M HCl	364.0	371.0

Appendix Table 2.8

Volume of Se (as 10ppm Selenite) added / μL	Conc. of acid used to make up the standard	Scan 1 ***Peak Current / nA***	Scan 2 ***Peak Current / nA***
40	0.1M	-36.365	-42.127
60	0.1M	-115	-125
20	6.0M	-212	-208
80	0.1M	-301	-298
100	0.1M	-399	-378
120	0.1M	-492	-466

Appendix Table 2.8a

Volume of Se (as 10ppm Selenite) added / μL	Conc. of acid used to make up the standard	Scan 3 Peak Current / nA
40	0.1M	-50.942
60	0.1M	-136.0
80	0.1M	-227.0
20	6.0M	-332.0
100	0.1M	-413.0
120	0.1M	-498.0

Appendix Table 2.9 Reduction of the selenate sample at room temperature.

Time / mins	Amount added / μL	Peak Current / nA	Current difference per 20μL
0	20	-31.166	0
90	40	-32.469	1.33
100	60	-33.678	1.182
110	80	-35.441	1.763
120	100	-37.295	1.854
130	120	-39.619	2.324
140	140	-43.596	3.977
150	160	-48.225	4.629
160	180	-58.625	10.40
170	200	-71.086	12.461
180	220	-88.998	17.912
190	240	-98.098	9.10
200	260	-104.0	5.902
207	280	-120.0	16.0
215	300	-129.0	9.00

Appendix Table 2.10 40^0C Temperature for reduction. The same parameters as above.

Time / mins	Amount added / μL	Peak Current / nA	Current difference per 20μL
0	20	19.73	0
12	40	22.966	3.203
20	60	23.633	0.667
25	80	28.116	4.483
32	100	39.934	11.818
36	120	47.692	7.758
43	140	56.669	8.977
50	160	63.661	6.992
57	180	72.671	9.01
65	200	79.309	6.638
70	220	84.331	5.022
75	240	123.0	38.669
85	260	149.0	26.0
95	280	157.0	8.0
105	300	168.0	11.0
115	320	188.0	20.0
125	340	218.0	20.0
135	360	278.0	50.0
145	380	335.0	57.0
155	400	425.0	90.0

Appendix Table 2.11 50^0C Temperature for reduction. The same parameters as above.

Time / mins	Amount added / μL	Peak Current / nA	Current difference per 20μL
10	20	4.438	0
20	40	7.281	2.843
30	60	19.077	11.796
40	80	28.930	9.853
50	100	38.552	9.675
60	120	50.527	11.975
70	140	67.71	17.183
80	160	84.71	17.00
90	180	104.663	19.953
100	200	126.56	21.897
120	220	144.785	18.225
130	240	171.814	27.029
155	260	200.314	28.500

Appendix Table 2.12 Using the same parameters as above the experiment was repeated but using the 70^0C temperature for the reduction.

Time / mins	Amount added / µL	Peak Current / nA	Current difference per 20µL
12	50	-93.59	88.41
20	70	-182	123
28	90	-305	123
32	110	-423	118
39	130	-534	112
51	170	-677	123
58	190	-811	134
64	210	-948	137
79	250	-1186	124

Appendix Table 2.13 The temperature was 90^0C the electrolyte 1M HCl The standard was 35ppm Selenate. Reducing agent was 6M HCl.

Time / mins	Amount added / µL	Peak Current / nA	Current difference
7	20	-173	69.2
15	40	-369	130.6
22	60	-526	157.0
30	80	-648	122.0
40	100	-773	125.0
50	120	-899	126.0
60	140	-1001	102.0
70	160	-1059	55.6

Appendix 2.14 Sample calculation for **Analysis of Se enriched yeast**. All other calculations are calculated as such.

Estimation of Se in yeast by modified standard additions

Part1. - Linearity of calibration curve prior to standard additions and estimation of blank current reading.

V= volume of 10 ppm Se as selenite in microlitres
I meas = measured current reading in nano amps.
I corr = current corrected for dilution

Volume of electrolyte = 10 cm3

V	I meas	Corr for I corr
40	77.094	77.40238
60	167	168.002
80	259	261.072
100	355	358.55
120	450	455.4

Slope of standards	4.8582
Intercept of standards	-127.48
Correlation coefficient =	0.999998
Blank current reading	455.5047

Part 2 : Standard addition calculation

V = Total volume of solution added including aliquots added in part 1.
Sample = 20 microlitres of digested and reduced yeast solution.
Std. = 20 microlitres of 10 ppm selenium as selenite
V sub = V - V sample
I sub = I corr less blank current reading

	V	I meas	I corr	V sub	I sub
Sample	140	566	573.924	0	118.4193
Sample. + Std 1	160	657	667.512	20	212.0073
Sample. + Std 2	180	765	778.77	40	323.2653
Sample. + Std 3	200	849	865.98	60	410.4753
Sample. + Std 4	220	904		80	

Slope = 4.93713
Intercept= -23.7787

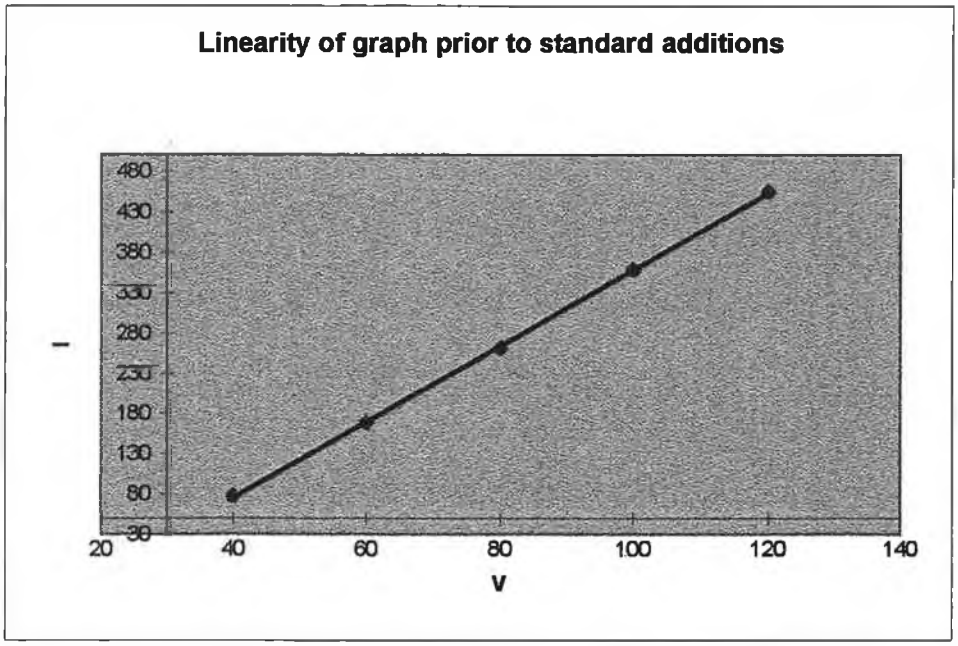
Linearity of graph prior to standard additions
I
480
430
380
330
280
230
180
130
80
30
20
40
60
80
100
120
140
V

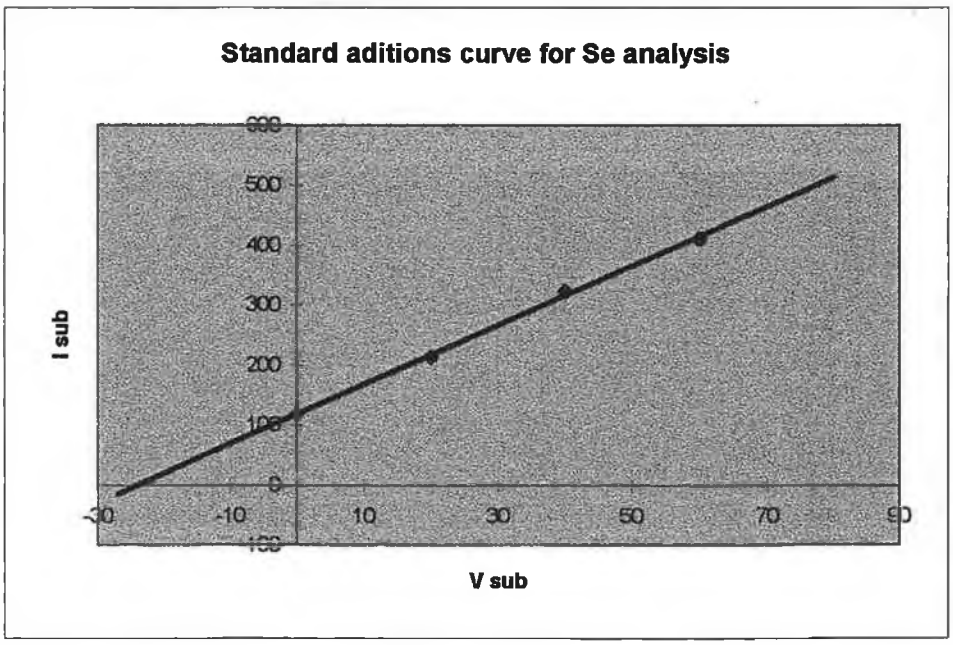
Standard aditions curve for Se analysis
I sub
600
500
400
300
200
100
0
-30
-10
10
30
50
70
90
-100
V sub

Appendix 2.15 Statistical analysis of results from **Analysis of Se enriched yeast**.

Calculation of Mean , Variance and Standard Deviation

Mean $\bar{x} = \sum \frac{x_i}{n}$ **Standard deviation of sample (s) =** $\sqrt{\sum \frac{(x_i - \bar{x})^2}{(n-1)}}$

Variance $\sum \frac{(x_i - \bar{x})^2}{(n-1)}$ **Standard dev. of Mean** $\bar{s} = \frac{s}{\sqrt{n}}$

	Results	**Deviation**	**Square of Deviation**
	x_i	$(x_i - \bar{x})$	$(x_i - \bar{x})^2$
	2378	-59.33333333	3520.444444
	2335	-102.3333333	10472.11111
	2420	-17.33333333	300.4444444
	2556	118.6666667	14081.77778
	2284	-153.3333333	23511.11111
	2760	322.6666667	104113.7778
	2152	-285.3333333	81415.11111
	2950	512.6666667	262827.1111
	2101	-336.3333333	113120.1111
Σ	21936	Σ	613362
n	9	n − 1	8
$\bar{x}$	2437.333333	s^2	76670.25
		s	276.8939328
		$\bar{s}$	92.29797759

Calculations using Excel's Built in Functions

Results
x_i
2378
2335
2420
2556
2284
2760
2152
2950
2101

Parameter	**Value**
s^2	76670.25
s	276.8939

Confidence Limits of the Mean

Confidence Limits = $\bar{x} \pm \frac{st}{\sqrt{n}}$

Students' t-Table

ν	95%	99%
1	12.70615	63.6559
2	4.302656	9.924988
3	3.182449	5.840848
4	2.776451	4.60408
5	2.570578	4.032117
6	2.446914	3.707428
7	2.364623	3.499481
8	2.306006	3.355381
9	2.262159	3.249843
10	2.228139	3.169262
11	2.200986	3.105815
12	2.178813	3.054538
13	2.160368	3.012283
14	2.144789	2.976849
15	2.131451	2.946726

Confidence limits of the mean (P =95%)

Results

x_i
2378
2335
2420
2556
2284
2760
2152
2950
2101

	Parameter	Value
Mean	$\bar{x}$	2437.333
Standard Deviation	s	276.8939
Number of values	n	9
Degrees of Freedom	n–1	8
Students t (95% Conf. Level)	t	2.306006
Upper Confidence Limit		2650.173
Lower Confidence Limit		2224.494

EXP3: Significance Tests

Comparison of an experimental Mean with a Known (True) Value

$$t = \frac{(\bar{x} - \mu)\sqrt{n}}{s}$$

True Value 2000

Results
2378
2335
2420
2556
2284
2760
2152
2950
2101

Parameter	Value
$\bar{x}$	2437.333
s	276.8939
n	9
Calcualted t	4.738276
Tabulated t	2.306006
P =	0.002112

Appendix 3

Appendix Table 3.1a

Channel	Kα	Lα	Lβ	Mα
66	Al			
76		Rb		
78	Si		Rb	
80		Sr		
82			Sr	
86		Y		
88			Y	
90	P	Zr		Pt
94			Zr	Au
96		Nb		
98				Hg
100			Nb	Ti
102	S	Mo		
104				Pb
106			Mo	
108		Tc		Bi
112			Tc	
114		Ru		
116	Cl			
118			Ru	
120		Rh		
126		Pb	Rh	
132	Ar	Ag	Pd	
138		Cd		
140			Ag	
146	K	In		
148			Cd	
152		Sn		
154			In	
160		Sb		
162			Sn	
164	Ca			
168		Te		
170			Sb	
174		I		
178			Te	
182	Sc	Xe		
188			I	
190		Cs		
196			Xe	
198		Ba		
200	Ti			
204			Cs	
206		La		
214		Ce	Ba	
220	V			
224		Pr	La	
232		Nb		
234			Ce	
240	Cr			

Appendix Table 3.1b

Channel	Kα	Lα	Lβ
40		Rh	Ru
42		Pd	Rh
44	Ar	Ag	Pd
46		Cd	Ag
48	K	In	Cd
50		Sn	
52			In
54	Ca		Sn
56		Sb	Sb
58		Te	
60	Sc	I	Te
62		Xe	I
64			
66	Ti	Cs	Xe
68		Ba	Cs
72		La	Ba
74	V	Ce	La
78		Pr	Ce
80	Cr	Pm	
82			Pr
84		Sm	Nd
86		Eu	
88	Mn		Pm
90		Gd	
92		Tb	Sm
94	Fe		
96		Dy	Eu
100		Ho	Gd
102	Co	Er	
104			Tb
106		Tm	
108			Dy
110	Ni	Yb	
112			Ho
114		Lu	
116		Hf	Er
118	Cu		
120		Ta	Tm
124		W	Yb
128	Zn	Re	Lu
132		Os	
134			Hf
136	Ga	Ir	
138			Ta
140		Pt	
142			W
144		Au	
146	Ge		
148		Hg	Re
152		Ti	

154			Os
156	As	Pb	
158			Ir
160		Bi	
164		Po	Pt
166	Se		
168		At	
170			Au
174		Rn	Hg
176	Br		
178		Fr	
180			Ti
182		Ra	
186	Kr	Ac	Pb
192		Th	Bi
196		Pa	
198	Rb		Po
202		U	
206		Np	At
210	Sr		
212		Pu	Rn
216		Am	
218			Fr
222	Y		
226			Ra
232			Ac
234	Zr		
240			Th
246	Nb		

Appendix Table 3.2

Standard Curve for 2g sample and using 4 segments with conditions as in **Section 3.3.12**.

Se Conc / ppm	Fe 60-105	Escape 106-139	Selenium 140-205	Background 206-235
0	1044	516.0	1432	1204
500	1087	552.5	1801	1184
969.5	1194	641.4	2329	1169
1529.5	1297	722.2	2839	1177
1980.8	1406	820.1	3372	1175
2490.7	1479	866.9	3764	1144
2950.3	1536	905.3	4063	1141

Appendix Table 3.3

Standard Curve for 1g sample and 2 segments channels No. 150-175as in **Section 3.3.12**.

Concentration of Se / ppm	Selenium segment 150-175	Background segment 220-230
0	277.3	282.5
500	474.6	275.9
969.5	715.9	273.7
1529.5	989.4	269.6
1980.8	1245	269.1

2490.7	1460	274.0
2950.3	1568	265.3

Appendix Table 3.4

Sample thickness using the Standard Curve for 2g sample channel No. 140-205 as in **Section 3.3.12.**

Sample amount of Se 2000 yeast / grams	Intensity of Se peak / cps 140-205
0.5	1538
0.75	2006
1.0	2439
1.25	2797
1.5	3019
1.75	3265
2.0	3410
3.0	3897
4.0	4098
5.0	4214

Appendix Table 3.5

Sample thickness using the Standard Curve for 2g sample channel No. 150-175 as in **Section 3.3.12.**

Sample amount of Non-enriched yeast / grams	Intensity of Se peak / cps 140-205
0.5	801
1.0	973
1.5	1245
2.0	1458
3.0	1681
4.0	1784
5.0	1886

Appendix Table 3.6

Standard Curve for 1g sample and using 4 segments with conditions as in **Section 3.3.12**

Se Conc / ppm	Fe 60-105	Escape 106-139	Selenium 140-205	Background 206-235
0	776.7	476.3	991.1	767.6
500	808.2	483.1	1256	765.1
969.5	872.2	541.9	1580	755.5
1529.5	926.1	591.9	1899	745.9
1980.8	1035	678.8	2156	749.4
2490.7	1060	715.6	2477	735.0
2950.3	1089	727.0	2688	732.3

Appendix Table 3.7

Standard Curve for 4g sample and using 4 segments with conditions as in **Section 3.3.12**

Se Conc / ppm	Fe 60-105	Escape 106-139	Selenium 140-205	Background 206-235
0	1374	587.8	1838	1683
500	1437	644.4	2294	1614
969.5	1515	732.7	2831	1574
1529.5	1692	885.0	3744	1553
1980.8	1777	940.1	4041	1549

2490.7	1799	984.2	4404	1488
2950.3	1874	1033	4696	1503

Appendix Table 3.8

Data from direct scan of A (Se 2000ppm Enriched yeast) and B (Non-enriched yeast)

KeV	A	B	KeV	A	B	KeV	A	B
1	0	0	3.04	7	4	5	17	9
1.04	0	0	3.08	6	3	5.04	11	12
1.08	0	0	3.12	7	5	5.08	13	7
1.12	0	0	3.16	9	4	5.12	17	8
1.16	0	0	3.2	5	5	5.16	19	12
1.2	0	0	3.24	4	6	5.2	14	14
1.24	0	0	3.28	9	4	5.24	12	10
1.28	0	0	3.32	4	3	5.28	20	8
1.32	0	0	3.36	8	6	5.32	16	14
1.36	1	1	3.4	9	6	5.36	17	11
1.4	3	2	3.44	6	4	5.4	25	12
1.44	4	3	3.48	5	4	5.44	17	17
1.48	4	3	3.52	10	4	5.48	13	12
1.52	3	2	3.56	6	6	5.52	19	9
1.56	3	3	3.6	7	5	5.56	24	13
1.6	3	2	3.64	8	5	5.6	18	16
1.64	4	3	3.68	6	5	5.64	13	12
1.68	3	2	3.72	7	4	5.68	25	9
1.72	3	2	3.76	6	5	5.72	16	17
1.76	5	3	3.8	8	4	5.76	20	10
1.8	3	2	3.84	6	6	5.8	25	13
1.84	3	2	3.88	6	5	5.84	26	17
1.88	5	3	3.92	9	5	5.88	22	18
1.92	5	3	3.96	5	6	5.92	18	15
1.96	4	3	4	4	3	5.96	27	12
2	4	3	4.04	8	5	6	22	18
2.04	6	4	4.08	9	6	6.04	26	17
2.08	5	3	4.12	6	4	6.08	29	20
2.12	6	4	4.16	5	4	6.12	19	13
2.16	6	4	4.2	8	4	6.16	21	15
2.2	4	3	4.24	6	6	6.2	28	20
2.24	5	3	4.28	7	4	6.24	28	20
2.28	7	5	4.32	8	5	6.28	21	14
2.32	9	6	4.36	6	5	6.32	17	12
2.36	6	4	4.4	7	4	6.36	29	19
2.4	5	3	4.44	8	4	6.4	19	13
2.44	7	5	4.48	10	5	6.44	21	14
2.48	5	4	4.52	8	6	6.48	23	16
2.52	6	4	4.56	6	5	6.52	17	12
2.56	7	5	4.6	10	4	6.56	20	14
2.6	5	4	4.64	7	7	6.6	19	13
2.64	6	4	4.68	9	5	6.64	24	17
2.68	5	4	4.72	12	6	6.68	17	12
2.72	4	4	4.76	11	8	6.72	17	12

2.76	7	3	4.8	11	7	6.76	22	14
2.8	4	2	4.84	9	7	6.8	13	8
2.84	5	5	4.88	13	6	6.84	15	10
2.88	7	3	4.92	12	9	6.88	17	12
2.92	7	4	4.96	13	8	6.92	18	13
2.96	5	5				6.96	13	9
3	7	5						

KeV	A	B	KeV	A	B	KeV	A	B
7	10	7	9	11	5	11	40	6
7.04	15	10	9.04	14	6	11.04	40	6
7.08	13	8	9.08	14	6	11.08	51	8
7.12	15	9	9.12	11	4	11.12	37	6
7.16	15	10	9.16	9	4	11.16	43	7
7.2	10	7	9.2	14	5	11.2	44	7
7.24	11	7	9.24	10	4	11.24	51	9
7.28	14	8	9.28	10	4	11.28	40	7
7.32	15	9	9.32	13	5	11.32	30	6
7.36	12	7	9.36	9	4	11.36	52	10
7.4	9	6	9.4	10	4	11.4	32	6
7.44	17	9	9.44	10	4	11.44	39	8
7.48	11	6	9.48	13	5	11.48	47	10
7.52	13	7	9.52	10	4	11.52	46	10
7.56	19	10	9.56	11	4	11.56	35	8
7.6	17	9	9.6	15	6	11.6	30	7
7.64	11	6	9.64	11	3	11.64	43	11
7.68	13	6	9.68	12	4	11.68	33	9
7.72	20	10	9.72	16	5	11.72	37	10
7.76	15	7	9.76	17	5	11.76	42	12
7.8	17	8	9.8	10	3	11.8	27	8
7.84	21	11	9.84	10	3	11.84	30	10
7.88	13	6	9.88	18	5	11.88	38	14
7.92	16	7	9.92	15	4	11.92	46	16
7.96	20	9	9.96	19	5	11.96	22	8
8	23	11	10	22	5	12	20	8
8.04	18	8	10.04	15	4	12.04	37	15
8.08	15	7	10.08	18	4	12.08	23	10
8.12	23	10	10.12	23	5	12.12	23	11
8.16	18	8	10.16	26	5	12.16	28	14
8.2	18	8	10.2	22	4	12.2	21	11
8.24	22	10	10.24	17	4	12.24	23	13
8.28	16	7	10.28	31	6	12.28	21	12
8.32	18	8	10.32	22	4	12.32	26	15
8.36	18	8	10.36	26	4	12.36	21	12
8.4	22	10	10.4	34	6	12.4	21	13
8.44	16	7	10.44	32	5	12.44	27	17
8.48	12	6	10.48	30	5	12.48	16	10
8.52	23	10	10.52	28	5	12.52	20	13
8.56	14	7	10.56	40	6	12.56	24	17
8.6	16	6	10.6	33	5	12.6	25	18
8.64	17	10	10.64	37	6	12.64	19	13

8.68	18	6	10.68	38	7	12.68	16	12
8.72	18	7	10.72	31	5	12.72	24	18
8.76	13	8	10.76	38	6	12.76	19	14
8.8	18	6	10.8	43	7	12.8	22	17
8.84	13	8	10.84	50	8	12.84	24	19
8.88	15	6	10.88	42	7	12.88	16	13
8.92	10	7	10.92	35	6	12.92	18	14
8.96	10	7	10.96	57	9	12.96	18	16
KeV	A	B	KeV	A	B	KeV	A	B
13	19	17	15	22	23	17	24	17
13.04	20	18	15.04	16	17	17.04	32	20
13.08	15	14	15.08	19	19	17.08	13	7
13.12	25	22	15.12	16	17	17.12	11	5
13.16	15	14	15.16	20	22	17.16	8	3
13.2	17	16	15.2	20	21	17.2	7	3
13.24	21	20	15.24	21	22	17.24	3	1
13.28	16	15	15.28	25	27	17.28	1	0
13.32	18	16	15.32	14	15	17.32	0	0
13.36	15	15	15.36	17	18			
13.4	21	21	15.4	20	23			
13.44	16	17	15.44	22	24			
13.48	17	18	15.48	17	18			
13.52	22	23	15.52	14	15			
13.56	14	14	15.56	21	18			
13.6	16	16	15.6	17	23			
13.64	21	22	15.64	14	18			
13.68	24	25	15.68	16	21			
13.72	16	17	15.72	19	23			
13.76	14	14	15.76	20	16			
13.8	23	23	15.8	15	18			
13.84	17	17	15.84	12	20			
13.88	17	17	15.88	22	21			
13.92	22	23	15.92	14	17			
13.96	16	16	15.96	12	13			
14	17	18	16	14	23			
14.04	20	21	16.04	15	14			
14.08	23	24	16.08	20	16			
14.12	13	14	16.12	15	22			
14.16	10	11	16.16	16	16			
14.2	25	27	16.2	16	18			
14.24	14	16	16.24	23	26			
14.28	16	18	16.28	15	18			
14.32	22	23	16.32	17	31			
14.36	22	23	16.36	28	28			
14.4	18	19	16.4	19	34			
14.44	15	16	16.44	24	29			
14.48	21	24	16.48	32	35			
14.52	18	19	16.52	37	39			
14.56	20	22	16.56	25	25			
14.6	22	24	16.6	21	29			

14.64	15	16	16.64	34	44			
14.68	18	19	16.68	38	57			
14.72	22	24	16.72	42	62			
14.76	26	29	16.76	61	70			
14.8	16	17	16.8	43	49			
14.84	13	25	16.84	47	48			
14.88	23	18	16.88	48	47			
14.92	16	24	16.92	53	51			
14.96	17	22	16.96	33	24			

Appendix Table 3.9

Concentration of Se (ppm)	Counts per second (140-205)
0	1435
759.7	2245
1487.3	2917
2364.7	3923
3124.4	4617
3734.3	5297

Appendix Table 3.10

Total counts per channel	Background counts per channel	Total -background	Average	Response Factor
3522	1123	2399		
3514	1126	2388	2390.3	1.17
3513	1129	2384		
3507	1135	2372		
3516	1146	2370	2375.3	1.16
3511	1127	2384		
3609	1154	2455		
3487	1123	2364	2394	1.17
3472	1109	2363		
3513	1131	2382		
3517	1133	2384	2385.3	1.17
3519	1129	2390		
3546	1138	2408		
3497	1127	2370	2386.6	1.17
3516	1134	2382		
3494	1158	2366		
3496	1115	2381	2376	1.17
3497	1116	2381		
3548	1135	2413		
3483	1123	2360	2385	1.17
3497	1115	2382		
3522	1131	2391		
3488	1119	2369	2377.3	1.16
3488	1116	2372		
3545	1133	2412		
3538	1133	2405	2409.3	1.18
3551	1133	2418		
3526	1130	2396		
3487	1126	2361	2380	1.16

3495	1112	2383		

Appendix Table 3.11

Concentration of Se / ppm	Fe (Channel 60-105) / cps	Se (Channel 140-205) / cps
0	1009	1432
759	1174	2222
1487	1310	2935
2365	1477	3865
3124	1624	4598
3734	1760	5278

Appendix 3.12

Preparation of standards using non-enriched yeast.

A series of standards were prepared containing increasing quantities of Se in non-enriched yeast. A sample calculation is given below:

M.wt (Na_2SeO_4) = 369.10 g/mole

% Selenium in Na_2SeO_4 = 41.79%

100g of Na_2SeO_4= 41.79g of Se

$\Rightarrow$ (100/41.79) g Na_2SeO_4= 1g Se

$\Rightarrow$ 2.393g Na_2SeO_4= 1g Selenium.

Preparation of a 750ppm Selenium standard.

This contains 0.75g Se in 1kg of sample but since 2g specimens were used this

$\Rightarrow$0.0015g of Se in 2g of non-enriched yeast.

$\Rightarrow$ 0.0015 x 2.393g of sodium selenate

$\Rightarrow$ 0.00358g of sodium selenate

Calculation of added Se standard

The molecular formula of Sodium Selenate (Na_2SeO_4) $\Rightarrow$ M_r = 188.94

$\Rightarrow$ % Se in Na_2SeO_4 = 41.79%.

The desired concentration of added Se is 500 ppm $\Rightarrow$ 1 mg of Se in a 2g sample

$\Rightarrow$ 2.393 mg of Na_2SeO_4

As this is difficult to weigh precisely, the actual amount (w) weighed out may be slightly different. The exact Se concentration in ppm is calculated using the formula : [Se] = w*500/2.393. For example an addition of 0.0026 g gives 540 ppm Se added.

Appendix 3.13

Statistical tests for comparison of variances and sample means

(Fe tube peak)

	x_i	x_j
	1497	1470
	1516	
	1497	1457
	1484	1501
	1470	1506
Mean($\bar{x}$) =	1492.8	1483.5
Number of values	5	4
df=	4	3
Variance of sample	292.7	565.6667

F- Test for comparison of variances

$$F_{calc} = \frac{s_1^2}{s_2^2}$$

Calculated 1.932582
Tabulated 9.117173

P= 0.307579

t-Test for comparison of two sample means

Pooled variance = $$s^2 = \frac{\{(n_1-1)s_1^2 + (n_2-1)s_2^2\}}{(n_1+n_2-2)}$$

$$t = \frac{(\bar{x}_1 - \bar{x}_2)}{s\sqrt{\left(\frac{1}{n_1} + \frac{1}{n_2}\right)}}$$

Number of degreee of freedom = (n1+n2-2)

Degrees of freedom	7
Pooled variance	409.6857
Pooled std. dev.	20.24069
Calculated t value =	0.684938
Critical t value =	2.364623
P(T<=t) two tail =	0.515415

Statistical tests for comparison of variances and sample means

Se Esc. Peak

	x_i	x_j
	1027	1034
	1065	
	1044	1005
	1038	999
	1031	1020
Mean($\bar{x}$) =	1041	1014.5
Number of values	5	4
df	4	3
Variance of sample	222.5	247

F- Test for comparison of variances

$$F_{calc} = \frac{s_1^2}{s_2^2}$$

Calculated F = 1.110112
Tabulated F = 9.117173

P= 0.485219

t-Test for comparison of two sample means

Pooled variance = $s^2 = \frac{\{(n_1-1)s_1^2 + (n_2-1)s_2^2\}}{(n_1+n_2-2)}$ $\qquad t = \frac{(\bar{x}_1 - \bar{x}_2)}{s\sqrt{\left(\frac{1}{n_1}+\frac{1}{n_2}\right)}}$

Number of degreee of freedom = (n1+n2-2)

Degrees of freedom = 7

Pooled variance 233
Pooled std. dev. 15.26434

Calculated t value = 2.587984

Critical t value (95%)= 2.364623

P(T<=t) two tail = 0.03605

Statistical tests for comparison of variances and sample means

Se K alpha

	x_i	x_j
	3522	3481
	3609	
	3513	3410
	3522	3541
	3494	3472
Mean($\bar{x}$) =	3532	3476
Number of values	5	4
df	4	3
Variance of sample	1983.5	2874

F- Test for comparison of variances

$$Fcalc = \frac{s_1^2}{s_2^2}$$

Calculated 1.448954
Tabulated 9.117173

P= 0.396068

t-Test for comparison of two sample means

Pooled variance = $$s^2 = \frac{\{(n_1-1)s_1^2 + (n_2-1)s_2^2\}}{(n_1+n_2-2)}$$

$$t = \frac{(\bar{x}_1 - \bar{x}_2)}{s\sqrt{\left(\frac{1}{n_1} + \frac{1}{n_2}\right)}}$$

Number of degreee of freedom = (n1+n2-2)

Degrees of freedom = 7

Pooled variance 2365.143
Pooled std. dev. 48.63273

Calculated t value = 1.716537

Critical t value (95%)= 2.364623

P(T<=t) two tail = 0.12977

Statistical tests for comparison of variances and sample means

Background segment

	x_i	x_j
	1123	1124
	1154	
	1131	1128
	1131	1122
	1128	1134
Mean($\bar{x}$) =	1133.4	1127
Number of values	5	4
df	4	3
Variance of sample	143.3	28

F- Test for comparison of variances

$$Fcalc = \frac{s_1^2}{s_2^2}$$

Calculated F = 5.117857
Tabulated F = 9.117173

P= 0.105478

t-Test for comparison of two sample means

Pooled variance = $$s^2 = \frac{\{(n_1-1)s_1^2 + (n_2-1)s_2^2\}}{(n_1+n_2-2)}$$

$$t = \frac{(\bar{x}_1 - \bar{x}_2)}{s\sqrt{\left(\frac{1}{n_1} + \frac{1}{n_2}\right)}}$$

Number of degreee of freedom = (n1+n2-2)

Degrees of freedom = 7

Pooled variance 93.88571
Pooled std. dev. 9.689464

Calculated t value = 0.984632

Critical t value (95%)= 2.364623

P(T<=t) two tail = 0.357606

Appendix 4

Appendix Table 4.1

Molar Concentration of HCl	Mean Absorbance of 10 ppb Se in the various acid concentrations
0	0.002
1	0.2657
2	0.1975
3	0.1913
4	0.1873
5	0.1821
6	0.1364

Appendix Table 4.2.

Concentration of SeO_3^{2-} / ppb	Mean Absorbance
0	0.0005
3	0.0727
6	0.1416
9	0.2065
12	0.2676
15	0.3229

Appendix Table 4.3.

Time / minutes	Experiment 1 Absorbance	Experiment 2 Absorbance	Experiment 3 Absorbance
0	0.0019	0.0011	0.0015
10	0.0607	0.0688	0.0325
20	0.0856	0.11	0.0504
30	0.1111	0.137	0.0652
40	0.1287	0.1498	0.0804
50	0.1383	0.1773	0.0921
60	0.1559	0.1857	0.1037
70	0.1644	0.1932	0.1125
80	0.1752	0.2005	0.1238
90	0.1853	0.2194	0.1317
100	0.1973		0.1438
110	0.2033		0.1491
120	0.2109		0.1729
130	0.2209		0.178

Appendix Table 4.4

Time / minutes	Experiment 1 Absorbance	Experiment 2 Absorbance	Experiment3 Absorbance
0	0.0007	0.0008	0.0014
3	0.0161	0.0191	0.0222
6	0.0435	0.0430	0.045
9	0.0674	0.0725	0.064
12	0.0931	0.0844	0.0814
15	0.1054	0.1014	0.0963
18	0.1232	0.1154	0.11
21	0.1315	0.1274	0.1167
24	0.1486	0.1356	0.1258
27	0.1525	0.1559	0.135
30	0.1567	0.1536	0.1419
35	0.1685	0.1612	0.1498
40	0.1704	0.1656	0.1615

45	0.1775	0.1785	0.1734
50	0.1705	0.1798	0.1719
55		0.1916	0.1825
60			0.1726
75	0.1698	0.2156	0.2142

Appendix Table 4.5

Time / minutes	Experiment 1 Absorbance	Experiment 2 Absorbance	Experiment 3 Absorbance
0	0.0005	0.0005	0.0006
2	0.0305	0.0939	0.0375
4	0.0613	0.0883	0.0753
6	0.086	0.1228	0.1042
8	0.1101	0.1486	0.1321
10	0.1281	0.1789	0.1513
12	0.1429	0.1961	0.1648
14	0.1492	0.1915	0.1783
16	0.1617	0.2042	0.1894
18	0.1732	0.2792	0.1926
25	0.1860	0.2058	0.2024

Appendix Table 4.6

Time / minutes	Experiment 1 Absorbance	Experiment 2 Absorbance	Experiment 3 Absorbance
0	0.0005	0.0055	0.0056
1		0.0733	0.0828
1.33	0.0713		
2		0.1106	0.1108
3		0.1378	0.1375
4		0.1629	0.1576
4.5	0.1495		
5		0.1821	0.1924
6			0.2039
7		0.2004	0.2066
7.75	0.1987		
8		0.2004	0.2092
9		0.2035	0.214
10		0.2101	0.2105
10.8	0.1942		
13.86	0.2068		
17.25	0.1987		
20.88	0.1981		
21.4		0.2043	
24			0.2069

Appendix Table 4.7

Time / minutes	Experiment 1 Absorbance	Experiment 2 Absorbance	Experiment 3 Absorbance
0	0.0067	0.0024	0.0057
1			0.0569
1.92		0.0611	
2.83	0.1413		
4			0.2192
4.83		0.1462	
6.08	0.2369		

6.83			0.2439
8.42		0.2273	
8.83	0.2422		
9.58			0.2588
11.83		0.2267	
12.25	0.2259		
13.67			0.2593
15.25		0.2004	
16.00	0.1674		
16.75			0.2686
18.67		0.1436	
18.75			0.2767
19.27	0.0931		
21.92			0.2823
25.25	0		0.2919
29.42			0.2858

Digested at 150^0C 50μL of the sample to $100cm^3$ theoretically gives 5ppb

Appendix Table 4.8

Sample	0.0705	0.0809
Sample + 2.5ppb	0.2166	0.2098
Sample + 5ppb	0.1638	0.1638
Sample +7.5ppb	0.2129	0.2172
Sample + 10ppb	0.2485	0.2535

100μL of the sample to $100cm^3$ theoretically gives 10ppb

Appendix Table 4.9

Sample	0.1788	0.1410
Sample + 2.5ppb	0.2133	0.2122
Sample + 5ppb	0.2350	0.2363
Sample +7.5ppb	0.2650	0.2711
Sample + 10ppb	0.2969	0.2971

200μL of the sample to $100cm^3$ theoretically gives 20ppb

Appendix Table 4.10

Sample	0.3003	0.3078
Sample + 5ppb	0.3792	0.3805
Sample + 10ppb	0.4474	0.4480
Sample +15ppb	0.5020	0.5029
Sample + 25ppb	0.6531	0.6550

150μL of the sample to 100cm^3 theoretically gives 15ppb

Appendix Table 4.11

Sample	0.1620	0.1602
Sample + 5ppb	0.2427	0.2423
Sample + 10ppb	0.3203	0.3200
Sample +15ppb	0.3850	0.3852
Sample + 20ppb	0.4484	0.4485

Digested at 120^{0}C 200μL of the sample to 100cm^3 theoretically gives 20ppb

Appendix Table 4.12

Sample	0.2807	0.2775
Sample + 5ppb	0.3579	0.3535
Sample + 10ppb	0.4334	0.4318
Sample +15ppb	0.5011	0.5015
Sample + 20ppb	0.5668	0.5602

Digested at 110^{0}C 150μL of the sample to 100cm^3 theoretically gives 15ppb added SeO_3^{2-} was added.

Saved as hydr008.org

Appendix Table 4.13

Sample A	0.2238
Sample + 5ppb	0.3101
Sample + 10ppb	0.3828
Sample + 20ppb	0.5234

Digested at 110^{0}C 150μL of the sample to 100cm^3 theoretically gives 15ppb added SeO_3^{2-} was added.

Saved as hydr009.org

Appendix Table 4.14

Sample B	0.2324
Sample + 5ppb	0.3194
Sample + 10ppb	0.3978
Sample + 15ppb	0.4705
Sample + 20ppb	0.5537

Digested at 110^{0}C 150μL of the sample to 100cm^3 theoretically gives 15ppb added SeO_3^{2-} was added.

Saved as hydr010.org

Appendix Table 4.15

Sample C	0.2358
Sample + 5ppb	0.3252
Sample + 10ppb	0.4052
Sample + 15ppb	0.4704
Sample + 20ppb	0.5515

Digested at 110^{0}C 150μL of the sample to 100cm^3 theoretically gives 15ppb added SeO_3^{2-} was added.

Saved as hydr011.org

Appendix Table 4.16

Sample D	0.243
Sample + 5ppb	0.321
Sample + 10ppb	0.4072
Sample + 12.5ppb	0.4447
Sample + 15ppb	0.4765
Sample + 17.5ppb	0.5007
Sample + 20ppb	0.5384

Digested at 110^{0}C 200μL of the sample to 100cm^3 theoretically gives 20ppb added SeO_3^{2-} was added.

Saved as hydr012.org

Appendix Table 4.17

Sample E	0.2658
Sample + 10ppb	0.4075
Sample + 12.5ppb	0.4456
Sample + 15ppb	0.4762
Sample + 17.5ppb	0.5001
Sample + 20ppb	0.537

Digested at 110^{0}C 200μL of the sample to 100cm^3 theoretically gives 20ppb added SeO_3^{2-} was added.

Saved as hydr013.org **Appendix Table 4.18**

Sample F	0.3355
Sample + 5ppb	0.4097
Sample + 10ppb	0.4971
Sample + 12.5ppb	0.5375
Sample + 15ppb	0.5750

Digested at 110^{0}C 200μL of the sample to 100cm^3 theoretically gives 20ppb added SeO_3^{2-} was added. Saved as hydr014.org

Appendix Table 4.19

Sample F	0.3281
Sample + 5ppb	0.4139
Sample + 10ppb	0.4993
Sample + 12.5ppb	0.5343
Sample + 15ppb	0.5741

Digested at 110^{0}C 150μL of the sample to 100cm^3 theoretically gives 15ppb added SeO_4^{2-} was added. Saved as hydr016.org

Appendix Table 4.20

Spiked Sample A	0.2602
Sample + 5ppb	0.3588
Sample + 10ppb	0.439
Sample + 12.5ppb	0.481
Sample + 15ppb	0.5249

Digested at 110^{0}C 150μL of the sample to 100cm^3 theoretically gives 15ppb added SeO_3^{2-} was added. Saved as hydr017.org

Appendix Table 4.21

Spiked Sample B	0.2526
Sample + 5ppb	0.3355
Sample + 10ppb	0.4125
Sample + 12.5ppb	0.455
Sample + 15ppb	0.4889

Digested at 110^{0}C 150μL of the sample to 100cm^3 theoretically gives 15ppb added SeO_3^{2-} was added. Saved as hydr018.org

Appendix Table 4.22

Spiked Sample C	0.2509
Sample + 5ppb	0.3347
Sample + 10ppb	0.411
Sample + 12.5ppb	0.4548
Sample + 15ppb	0.4889

Digested at 110^0C 150μL of the sample to $100cm^3$ theoretically gives 15ppb added SeO_3^{2-} was added. Saved as hydr019.org

Appendix Table 4.23

Spiked Sample D	0.2538
Sample + 5ppb	0.3387
Sample + 7.5ppb	0.3811
Sample + 10ppb	0.4211
Sample + 12.5ppb	0.4725
Sample + 15ppb	0.5084

Digested at 110^0C 150μL of the sample to $100cm^3$ theoretically gives 15ppb added SeO_3^{2-} was added. Saved as hydr020.org

Appendix Table 4.24

Spiked Sample E	0.2387
Sample + 5ppb	0.3066
Sample + 7.5ppb	0.352
Sample + 10ppb	0.3905
Sample + 12.5ppb	0.4239
Sample + 15ppb	0.4546

Digested at 110^0C 150μL of the sample to $100cm^3$ theoretically gives 15ppb added SeO_3^{2-} was added. Saved as hydr021.org

Appendix Table 4.25

Spiked Sample F	0.269
Sample + 3ppb	0.3339
Sample + 6ppb	0.3863
Sample + 9ppb	0.4407
Sample + 12ppb	0.4923
Sample + 15ppb	0.5465

Bibliography

A

Adeloju, S. B.; Bond, A. M.; Briggs, M. H.; Huges, H. C. *Analytical Chemistry* **1983,** *55*, 2076-2082.

Adrian, W. J. *Analyst* **1973,** *98*.

Allaway, W.H. (1973). Selenium in the food chain. *Cornell Vet.* **63**:151

Allaway, W.H. (1978). Prespectives on trace elements in soil and human health. In Trace Substances in Environmental Health,XII, D.D. Hemphill, ed. Columbia: University of Missouri Press.

Andrews, E. D., Hartley W. H., and Grant A. B. (1968). Selenium-responsive diseases of animals in New Zealand. *N. Z. Vet. J.* **16**:3-17.

Arthur, D. (1972). Selenium content of Canadain foods. *Can. Inst. Food Sci. Technol.* **5**:165.

Auger, P. , Paris, 1926.

Awasthi, Y. C., Beutler E., and Srivatava S. K. (1975). Purification and properties of erythrocyte glutathione peroxidase. *J. Biol. Chem.* **250**:5144-5149.

Aydin. H., and G.H. Tan. *Analyst*, **1991**, 116, 941-945.

Aydin, H.; Yahaya, A. H. *Analyst* **1992,** *117*, 43-45.

Aydin. H., and G. H. Tan. *Analyst*, **1991**, 116, 941-945.

B

Beer, A.(1852). *Ann. Physik.* **86**,78.

Bell, M. C., Bacon J. A., Bratton G. R., and Wilkinson J. E. (1978). Effects of dietary selenium and lead on selected tissues of chicks. Pp. 604-607 in *Trace Element Metabolism in Man and Animals*, 3, Kirchgessner E. M., ed Weihenstephan: Arbeitskreis fur Tierernahrungsforschung.

bin Ahmad. R., J. Hill and R.J. Magee. (1983) *Analyst*, , **108**, 835-839.

Bisbjerg, B., Jochumsen. P., and Rasbech. N.O. (1970). Selenium content in organs, milk, and fodder of the cow. *Nord. Veterinaermed.* **22**:532.

Black, R. S., Tripp M. J., Whanger P. D., and Weswig P. H. (1978). Selenium proteins in ovine tissues. III. Distribution of selenium and glutathione peroxidase in tissue cytosols. *Bioinorg. Chem.* 161-172.

Black, W. G., Ulberg L. C., Kidder H. E., Sinvi J., McNutt S. H., and Casida L. E. (1953). Inflammatory response of the bovine endometrium. *Am. J. Vet. Res.* **14**:179.

Bock, Rudolf. (1979) *A handbook of decomposition methods in analytical chemistry.* International Textbook Co. Glasgow

Bouguer, P. (1729). Essai d'Optique sur la gradation de la lumiere. Paris.

Boyne, R., and Arthur J. R. (1979). Alterations of neutrophil function in selenium deficient cattle. *J. Comp. Pathol.* **89**(1):151-158.

Brown, D. G., and Burk R. F. (1973). Selenium retention in tissues and sperm of rats fed a torula yeast diet. *J. Nutr.* **103**:102.

Bruttel, P.A., Schafer J. Metrohm Publication: *Sample preparation techniques in voltammetric trace analysis.*

Buchanan-Smith, J. G., Nelson E. C., and Tillman A. D. (1969). Effect of vitamin E and selenium deficiencies on lysosomeal and cytoplasmic enzymes in sheep tissues. *J. Nutr.* **99**:387-394.

Burhop. (1952).*The Auger Effect*; University Press: Cambridge,

Burk, R. F., Nishiki K., Lawrence R. A., and Chance B. (1978). Peroxide removal by selenium-dependent and selenium-independent peroxidases in hemoglobin-free perfused rat liver. *J. Biol. Chem.* **253**: 43-46.

Burk, R. F., Pearson W. N., Wood II, R. P., and Viteri F. (1967). Blood selenium levels and in vitro red blood cell uptake of ^{75}Se in kwashiorkor. *Am. J. Clin. Nutr.* **20**:723-733.

C

Callahan, C. J. (1969). Post parturient infection of dairy cattle. *J. Am. Vet. Med. Assoc.* **155**:1963-1964.

Calvin, H. I. (1978). Selective incorporation of selenium –75 into a polypeptide of the rat sperm tail. *J. Exp. Zool.* **204**:445-452.

Calvin, H. I., Wallace E., and Cooper G. W. (1981). The role of selenium in the organisation of the mitochondrial helix in rodent spermatozoa. Pp. 319-324 in *Selenium in Biology and Medicine*, J. E. Spallholz, J. L. Martin, and H. E. Ganther, eds. Westport, Conn.: AVI.

Chance, B., Boveris A., Nakase Y., and Sies H. (1978). Hydroperoxidase metabolism: An overview. Pp. 95-106 in Functions of Glutathione in Liver and Kidney, H. Sies and Wendel, eds. Berlin: Springer-Verlag.

Chau, a. J. P. R. Y. K. *Anal. Chim. Acta.* **1965,** *33*, 36.

Chen, J. R., and Anderson J. M. (1979) Legionnaire's Disease: Concentration of selenium and other elements. *Science* **206**:1426-1427.

Christian, G. D. *Anal. Chem.* **1969,** *41*, 24A.

Cotton, F. A. and Wilkinson W. (1988) Advanced Inorganic Chemistry Fifth Edition. John Wiley & Sons. Chichester.

Conrad, H. R., and Moxon A. L. (1979). Transfer of dietary selenium to milk. *J. Dairy Sci.* **62**:404.

Cousins, F. B., and Cairney I. M. (1961). Some aspects of selenium metabolism in sheep. *Aust. J. Agric. Res.* **12**:927.

Cowgill, U. M. (1976) Selenium and human fertility. Pp. 300-315 *in Proc. Symp. Selenium-Tellurium in the Environment*. Pittsburgh: Industrial Health Foundation.

D

Dalton, E. F., and A. J. Malanoski. (1971). *At. Absorption. Newslett.* **10**,92.

Danger, F. P. a. F., C. (1841), *Compt. Rend. 12*, 1089.

Davis, C. W. *Canad. J. Res.* **(1938),** *16B.*

Dedina, J., and I. Rubeska. (1980). *Spectrochim. Acta.* 35B, 119. Pp73 of Welz.

Diplock, A.T., Caygill C. P. J., Jeffrey E. H., and Thomas C. (1973). The nature of the acid volatile selenium in the liver of the male rat. *Biochem. J.* **134**:283.

Douglas, B., McDaniel, D.H., and Alexander J.J. (1985) Concepts and Models of Inorganic Chemistry Second Edition. John Wiley & Sons. New York.

Duane, W.; Hunt, F. L. *Phys. Rev.* **1915,** *6*, 166.

E

Ebdon, L., (1982). *An Introduction to Atomic Absorption Spectroscopy*. Heyden, London.

Ehlig, C.F., Allaway. W. H., Cary. E.E., and Kubota. J. (1968). Differences among plant species in selenium accumulation from soils low in available selenium. *Agron.J.* **60**:43.

Elleouet, C.; Quentel, F.; Madec, C. (1996), *Water Rtesearch* **30**, 909-914.

F

Fernando. A. R., and J.A. Plambeck. ***Analyst***,1992, 117, 39-42.

Filipovic-Kovacevic, Z., I. Kruhak, B. Borovnjak-Zlataric and S. Milardovic. (1996), *Analytical Letters*, **29**, 3, 451-461.

Flohé, L., Loschen G., Gunzler W. A., and Eichele. E. (1972). Glutathione peroxidase. V. The kinetic mechanism. *Hoppe-Seyler'r Z. Physiol. Chem.* **353**:987-999.

Florence. T.M., ***Analyst***.1992,117,551-553

Fostrom, J. W., Zakowski J. J., and Tappel A. L. (1978) Identification of the catalytic site of rat liver glutathione peroxidase as selenocysteine. *Biochemistry*. **17**:2639-2644.

Franke, K. W., and Moxon A. L. (1936) A comparison of the minimam fatal doses of selenium, tellurium, arsenic, and vanadium. *J. Pharmacol. Exp. Ther.* **58**:454-459.

Frost, D. V. (1973).*Paper delivered at the 66th Annual Meeting of the Air Pollution Control Association,* Chicago

G

Ganapathy, S. N., Joyner. B. T., Sawyer. D. R., and Hafner. K. M. (1977). Selenium content of selected foods. In Proceedings of the 3rd International Symposium of Trace Element Metabolism in Man and Animals, *M. Kirchgessener, ed., Freising*, Germany.

Ganther, H. E. (1978) Metabolism of hydrogen selenide and methylated selenides. Pp.2-107 in *Advances in Nutritional Research*, H. H. Draper, ed. New York: Plenum Press.
Ganther, H. E., and Baumann C. A. (1962a) Selenium metabolism. II. Modifying effects of sulphate. *J. Nutr.* 77:408.

Ganther, H. E., Goudie D. G., Sunde M. L., Kopecky M. J., Wagner P., Oh S. –H., and Hoekstra W. G. (1972). Selenium: Relation to decreased toxicity of methylmercury added to diets containing tuna. *Science* **175**: 1122-1124.

Gardner, S. (1973) Selenium in animal feed. Proposed food additive regulation. *Fed. Reg.* **38**:10458-10460.

Gasiewicz, T. A., and Smith J. C. (1978). The metabolism of selenite by intact rat erythrocytes in vitro. *Chem. Biol. Interact.* **21**:299

Glover, J. R. (1967) Selenium in human urine: A tentative maximum allowance concentration for industrial and rural populations. *Ann. Occup. Hyg.* **10**:3-14.

Godwin, K. O., and Fuss C. N. (1972). The entry of selenium into rabbit protein following the administration of $Na_2{}^{75}SeO_3$. *Aust. J. Biol. Sci.* **25**:865.

Godwin, K. O., Partick E. J., and Fuss C. N. (1978). Adverse effects of copper, and to a lesser extent iron, when administered to selenium-deficient rats. Pp. 185-187 in *Trace Element Metabolism in Man and Animals*, 3, Kirchgessner E. M., ed Weihenstephan: Arbeitskreis fur Tierernahrungsforschung.

Green, J. M. (1996),*Analytical Chemistry 68*, 305A - 309A.

Greenwood. N.N. and Earnshaw. A., Chemistry of the elements Second Ed. pp 880-919 Peragon Press, Oxford. (1997).

Griffin, A. C. (1979) Role of selenium in the chemoprevention of cancer. *Adv. Cancer Res.* **29**:419-442.

Groce, A. W., Miller. E. R., Hitchcock. J. P, Ullrey. D. E., and Magee. W.T. (1973a). Selenium balance in the pig as affected by selenium source and vitamin E. *J. Anim. Sci.* **37**:942.

Guang Lan and Wong and Sin (1994) *Talanta*,

H

Hafeman, D. G., Sunde R. A., and Hoekstra W. G. (1974). Effect of dietary selenium on erythrocyte and liver glutathione peroxidase in the rat. *J. Nutr.* **104**: 580-587.

Hamdy, A. H., Pounden W. D., Trapp A. L., Bell D. A., and Lagace A. (1963). Effect on lambs of selenium administered to pregnant ewes. *J. Am. Vet. Med. Assoc.* 143-749.

Handreck, K. A., and Godwin. K. D. (1970). Distribution in sheep of selenium derived from ^{75}Se- labelled ruminal pellets. *Aust. J. Agr. Res.* **21**:78.

Hartley, W. J., and Grant A. B. (1961). A review of selenium responsive diseases of New Zealand livestock. *Fed. Proc.* **20**:679-688.

Hewett, C.N. *Instrumental Analysis of Pollutants*. Publisheed by Elsevier Applied Science.

Heyrovsty, J and Zuman P. (1968) Practical Polarography. Academic Press London and New York.

Hill, C. H., (1974) Reversal of selenium toxicity in chicks by mercury, copper and cadmium. *J. Nutr.* **104**:593.

Hoekstra, W.G. (1975). Biolchemical function of selenium and its relation to vitamin E. *Fed. Proc.* **34**:2083.

Hoffman, I., Jenkins. K. J., Merganger. J.C., and Pigden. W. J. (1973). Muscle and kidney selenium levels in calves and lambs raised in various parts of Canada: Relationship to selenium concentrations in plants and possibly human intakes. *Can. J. Anim. Sci.* **53**:61.

Hogue, D. E. (1958). Vitamin E, selenium and other factors related to nutritional muscular dystrophy in lambs. Pp. 32-39 in *Proc. Cornell Nutr. Conf. for Feed Manufacturers*, Ithaca, New York.

Holak, W. (1969). *Anal. Chem.* 41,1712.

Hoover, W. L.; Reagor, J. C.; Garner, J. C. (1969) *J. Assoc. Off. Anal. Chemists. 52.*

Hopkins, L. L., Jr., and Majaj A. S. (1967). Selenium inhuman nutrition. Pp. 203-214 in *Selenium in Biomedicine: A Symposium*, O. O. Muth, ed. Westport, Conn: AVI.

Hsieh, H. S., and Ganther H. E. (1975). Acid-volatile selenium formation catalysed by glutathione reductase. *Biochemistry* **14**:1632.

Human, H. G., A. Strasheim, and L. R. P. Butler. (1969), *IAASC*, Sheffield. FI.

I

Imhoff, D., and Andreesen J. R. (1979). Nicotinic acid hydroxylase from *Clostridium barkeri*: Selenium-dependent formation of active enzymes. FEMS *Microbiol. Lett.* **5**: 155-158.

Ishiyama. T., and T. Tanaka. (1996), *Anal. Chem.* **68**,3789-3792.

J

Jacobs, M. M., and Griffin A. C. (1979) Effects of selenium on chemical carcinogenesis: Comparative effects of antioxidants. *Biol. Trace Element Res.* **1**:1-13.

Jaffe, W. G. (1976) Effect of selenium intake in humans and in rats. Pp. 188-193 in *Proc. Symp. Selenium-Tellurium in the Environment.* Pittsburgh: Industrial Health Foundation.
Jaffe, W. G., and Mondragon M. C. (1969) Adaptation of rats to selenium intake. *J. Nutr.* **97**:431-436.

Jaffe, W. G., Ruphael M. D., Mondragon M. C., and Ojeda A. (1972a) Clinical and biochemical studies on school children from a seleniferous zone. *Arch. Latinoamer. Nutr.* **922**:595-611.

Jaquess, P. A., Smalley D. L., and Layne J. S. (1980) Enhanced growth of *Legionella pneumophila* in the presence of selenium. *J. Am. Med. Assoc.* **244**:27.

Johnson, C. M. (1975). Selenium in soils and plants: contrasts in conditions providing safe and adequate amounts of selenium in the food chain. P. 165 in *Trace Elements in Soil-Plant-Animals Systems*, D. J. D. Nicholas and A. R. Egan, eds. New York: Academic Press.

Jenkins, K.J. , M. Hidiroglou, J.M. Wauthy, and J.E. Proulx. (1974) Prevention of nutritional muscular dystrophy in calves and lambs by selenium and vitamin E additions to the maternal mineral supplement. *Can. J. Anim. Sci.* **54**:49

Jenkins, R.; DeVries, J. L. (1970). *Practical X-ray Spectrometry*, 2nd ed.; Springer-Verlag: New York,

Jenkins, R. (1988). *X-ray Fluorescence Spectrometry*; Wiley & Sons.: New York,

Julien, W. E., and Murray F. A. (1977). Effect of selenium and selenium with vitamin E on in vitro motility of bovine spermatozoa. P. 174 in *Proc. Am. Soc. Anim. Sci. 69th Annual Meeting*. Madison: University of Wisconsin.

K

Kelleher, W.; Johnson, M. (1961), J. *Anal. Chem. 33*, 1429.

Kelly. M. P. (1995) *The production and characterisation of selenium enriched Saccharomyces cerevisiae.* Thesis University College Galway.

Kendall, O. K. (1960). Non-specific diarrhoea in white disease areas--Probable cause and treatment. *Calif. Vet.* **14**:39.

Kerdel-Vegas, F. (1966) The depilatory and cytotoxic action of "Coco de Mono" (Lecythis ollaria) and its relationship to chronic selenosis. *Econ. Bot.* **20**:187-195.

Kiermeier, F., and Wigand. W. (1969). Selengehalt von Miech and Milchpulver. *Z. Leensm.-Unters.-Forsch.* **139**:205.

Kos, V. Veber, M and Hudnik, V. (1998) *Determination of selenium in soil by hydride generation A.A.S.* Fresenius J Anal. Chem **360**:225-229

Kuchel, R. E., and Buckley. R. A. (1969). The provision of selenium to sheep by means of heavy pellets. *Aust. J. Agric. Res.* **20**:1099-1107.

L

Lakin, H. W., and Davidson, D. F. (1967). The relation of the geochemistry of selenium to its occurrence in soils. P. 27 in *Selenium in Biomedicine: A Symposium*, O. H. Muth, ed. Westport, Conn.: AVI

Lakin, H.W. (1961). Geochemistry of selenium in relation to agriculture. In Selenium in Agriculture. *U. S. Department of Agriculture, Agric. Handb.* 200. Washington, D.C.: U.S. Government Printing Office.

Lambert, H.(1760). Photometria, sive de mesura et gradibus luminis colorum et umbrae.

Landsford, M., E. M. McPherson, and M. J. Fishman. (1974). *At. Absorption Newslett.* 13,103.

Latshaw, J. D., and Osman M. (1975) Distribution of selenium in egg white and yolk after feeding natural and synthetic selenium compounds. *Poult. Sci.* **54**:1244.

Lawrence, R. A., Sunde R. A., Schwartz G. L., and Hoekstra. W. G. (1974). Glutathione peroxidase activity in rat lens and other tissues in relation to dietary selenium intake. *Exp. Eye Res.* **18**: 563-569.

Levander, O.A. (1976a). Selenium in foods. Pp. 26-53 in Proc. Symp. Selenium-Tellurium in the environment. Pittsburgh: Industrial Health Foundation.

Levander, O.A. (1983). Considerations in the design of selenium bioavailability studies. *Fed. Proc.* In press.

Levander, O. A., Sutherland B., Morris V. C., and King J. C. (1981). Selenium balance in young men during selenium depletion and retention. *Am. J. Clin. Nutr.* **34**:2662-2669.

Levine, R. J., and Oslon R. E. (1970). Blood selenium in Thai children with protein-calorie malnutrition. *Proc. Soc. Exp. Biol. Med.* **134**:1030-1034.

Little, C., and O'Brien. P. J. (1968). An intracellular GSH-peroxidase with a lipid peroxidase substrate. *Biochem. Biophy. Res. Commun.* **31**:145-150.

M

Manning (1971), *Atomic Absorption Newsletter 10*, 86.

Mattsson, G.; Nyholn, L.; Olin, A. (1994),*Journal of Electroanalytical Chemistry 377*, 149-162.

Mattsson, G.; Nyholm, L.; Olin, A.; Ornemark, U. *Talanta* **1995,** *42*, 817-825.

McConnell K. P., Burton R. M., Kute T., and Higgins P. J. (1979b) Selenoproteins from rats testis cytosol. *Biochim. Biophy. Acta* **588**:113.

McConnell, K. P., and Portman O. W. (1952b) Toxicity of dimethyl selenidse in the rat and mouse. *Proc. Soc. Exp. Biol. Med.* **79**:230.

McDaniel, M., A. D. Shendrikur, K. D. Reiszner, and P. W. West. (1976). *Anal. Chem.* **48**,2240.

McKeehan, W. L., Hamilton W. G., and Ham R. G. (1976). Selenium is an essential trace nutrient for growth of WI-38 diploid human fibroblasts. *Proc. Natl. Acad. Sci.* **73**:2023-2027.

McKenzie, R. L., Rea H. M., Thomson C. D., and Robinson M. F. (1978). Selenium concentration and glutathione peroxidase activity in blood of New Zealand infants and children. *Am. J. Clin. Nutr.* **31**:1413-1418.

Meites, Louis. (1965) Polarograhic Techniques Second edition. Interscience Publishers. A Division of the John Wiley & Sons, Chichester.

Meyer, A., Ch. Hofer, G. Tolg, S. Raptis, and G. Knapp. (1979). *Z. Anal. Chem.* **196**,337.

Miller,D., Soares, Jr. J.H., Bauersfelf, Jr. P., and Cuppett. S.L. (1972). Comparative selenium retention by chicks fed sodium selenite, selenomethionine, fish meal and fish solubles. *Poult. Sci*. **51**:1669.

Miller J.C. and Miller J.N. (1984) Statistics for analytical chemistry. Ellis Horwood series in Analytical Chemistry Series Editors Dr. R. A. Chalmers and Dr. M. Masson. John Wiley & Sons. Chichester.

Millar, K. R., Sheppard. A. D. (1972). Tocopherol and selenium levels in human and cow milk. *N. Z. J. Sci*. **15**:1.

Millon, E. (1864), *J. Pharm. Chim 3*, 191.

Money, D. F. L. (1970) Vitamin E and Selenium deficiencies and their possible aetiological role in the sudden death infants syndrome. *N. Z. Med. J.* **21**:32-34.

Money, D. F. L. (1978) Vitamin E, selenium, iron, and vitamin A content of livers from sudden infant death syndrome cases and control children: Interrelationships and possible significance. *N. Z. J. Sci*. **21**:41-55.

Morris, V. C., and Levander. O. A. (1970). Selenium content of foods. *J. Nutr.* **100**:1383.

Mosier, E. A., Julien W. E., and Palmquist D. L. (1978). Response of noenatal calves to selenium supplementation. *J. Dairy Sci*. **61**:Supl. 1, p. 183.

Moxon, A.L., Olson, O.A., and W.V. Searight. (1939). Selenium in rocks, soils and plants. *Tech. Rull. 2.S.D. Agri. Exp. Stn.*, Brookings.

Muth, O.H., 1955. White muscle disease (myopathy) in lambs and calves. I. Occurrence and nature of the disease under Oregon conditions. *J. Am. Vet. Med. Assoc.* **126**:355-361.

Muth, O. H. (1963). White muscle disease, a selenium-responsive myopathy. *J. Am. Med. Assoc.* **142**:272-277.

Muth, O. H., Oldfield J. E., Remmert L. F., and Schubert J. R. (1958). Effects of selenium and vitamin E on white muscle disease. *Science* **128**:466-469.

N

National Research Council (NRC) (1971). Selenium in Nutrition. Agricultural Board, *Committee on Animal Nutrition*. Washington, D. C. National Academy of Sciences.

National Research Council (NRC) (1976a). Nutrient Requirements of Beef Cattle, 5th rev. ed. Board on Agriculture and Renewable Resources, *Committee on Animal Nutrition*. Washington, D. C. National Academy of Sciences.

National Research Council (NRC)(1976b). Selenium. Assembly of Life Sciences, Committee on medical and Biologic Effects of Environmental Pollutants. Washington, D.C. National Academy of Sciences.

National Cancer Institute. (1979) Bioassay of selenium sulphide for possible carcinogenicity. *Tech. Rep.* **197**, DHEW Pub. No. (NIH) 79-1750. Bethesda, Md.: U.S. Department of Health, Education, and Welfare. 135pp.

Noguchi, T., Cantor A. H. and Scott. M. L. (1973a). Mode of action of selenium and vitamin E in prevention of exudative diathesis in chicks. *J. Nutr.* **103**:1502-1511.

O

Oh, S. –H., Ganther H. E., and Hoekstra W. G. (1974). Selenium as a component of glutathione peroxidase isolated from ovine erythrocytes. *Biochemistry* **13**:1825.

Oh, S. –H., Pope A. L., and Hoekstra W. G. (1976a). Dietary selenium requirement of sheep fed a practical-type diet as assessed by tissue glutathione peroxidase and other criteria. *J. Anim. Sci.* **42**:984.

Oh, S. –H., Sunde R. A., Pope A. L., and Hoekstra. W. G. (1976b). Glutathione peroxidase response to selenium intake in lambs fed a torula yeast-based, artificial milk. *J. Anim. Sci.* **42**:977.

Olsen, O. E. (1969) *J. Assoc. Off. Anal. Chemists.* ***52.***

Olson O. E., Novacek E. J., Whitehead E. I., and Palmer I. S. (1970) Investigations on selenium in wheat. *Phytochemistry* **9**: 1181.

Olson, O. E., and Palmer I. S. (1976) Selenoamino acids in tissues of rats administered inorganic selenium. *Metabolism* **25**:299.

Omaye, S. T., and Tappel A. L. (1974). Effect of dietary selenium on gluthathione peroxidase in the chick. *J. Nutr.* **104**: 747-753.

Osman, M., and Latshaw J. D. (1976). Biological potency of selenium from sodium selenite, selenomethionine and selenocysteine in the chick. *Poult. Sci.* **55**:987.

P

Palmer, I. S., Arnold R. L., and Carlson C. W. (1973) Toxicity of various selenium derivatives to chick embryos. *Poult. Sci.* **52**:1841-1846.

Parizek, J., Kalouskova J., Babicky A., Benes J., and Pavlik L. (1974). Interaction of selenium with mercury, cadmium and other toxic metals. Pp. 119-131 in *Trace Element Metabolism in Animals*, 2, Hoekstra W. G., Suttie J. W., Ganther H. E., and Mertz W., eds. Baltimore: University Park Press.

Pecsok, R. l. (1976) Modern methods of chemical analysis Second Edition. John Wiley & Sons New York.

Pedersen, N.D., Whanger P. D., Weswig P. H., and Muth O. H. (1972). Selenium binding proteins in tissues of normal and selenium responsive myopathic lambs. *Bioinorg. Chem.* **2**:33-45.

Peterson, P. J., and Bulter G. W. (1962). The uptake and assimilation of selenite by higher plants. *Aust. J. Biol. Sci.* **15**:126.

Pollock, E. N., and S. J. West. (1973). *At. Absorption. Newslett.* **12**,6.

Potin-Gautier, M.; Seby, F.; Astruc, M. (1995), *Fresenius Journal of Analytical Chemistry 351*, 443-448.

Prasada Rao. T., M.Anbu, M.L.P. Reddy, C.S.P. Iyer and A.D. Damodaran. (1996), *Analytical Letters*, **29**, 14, 2563-2571.

Prasad. P.V.A., j. Arunachalam, and S. Ganadharan. (1994) *Electroanalysis*., **6**, 589-592.

Pratt, W. (1978). A study of the effect of in vitro supplementation of sodium selenite on the metabolism of bovine sperm. *M. S. thesis*. Ohio State University, Columbus.

Q

R

Reilly C., Selenium in Food and Health, (1996) Blackie, London

Reilly .T., Watson A. (1987) Polarography and other Voltammetric Methods. Editor was James A.M. Published for Analytical Chemistry by Open Learning by John Wiley & Sons Chichester.

Riley, T.; Tomlinson, C. (1987) *Principles of electroanalytical methods.*; John Wiley & Sons.: Chichester,.

Rhead, W. J., Cary E. E., Allaway W. H., Saltzstein S. L., and Schrauzer G. N. (1972) The vitamin E and selenium status of infants and the sudden infant death syndrome. *Bioinorg. Chem.* **1**:289-294.

Robertson, D. S. F. (1970) Selenium, a possible teratogen? *Lancet* **1**:518.

Robinson, M. F., Rea H. M., Freiend G. M., Stewart R. D. H., Scow P. C., Thomson and C. D. (1978a). On supplementing the selenium intake of New Zealanders.2. Prolonged metabolic experiments with daily supplements of selenomethioniine, selenite and fish. *Br. J. Nutr.* **39**:589.

Rojas. C.L., S.B. de Maroto, P. Valenta. ***Fresenius J. Anal. Chem***. 1994, 348, 775-776

Rosenfeld I., and Beath. O.A. (1964). Selenium. Seobotany, Biochemistry, Toxicity and Nutrition. New York: Academic Press. 411pp.

Rotruck, J. T., Hoekstra W. G., and Pope A. L. (1971). Glucose-dependent protection by dietary selenium against haemolysis of rat erythrocytes in vitro. *Nature (London), New Biol.* **231**: 223-224.

Rotruck, J. T., Pope. A. L., Baumann. C. A., Hoekstra. W. G, and Paulson. G. D. (1969). Effect of long-term feeding of selenized salt to ewes and their lambs. *J. Anim. Sci.* **29**:170.

Rotruck, J. T., Pope A. L., Ganther H. E., and Hoekstra W. G. (1972a). Prevention of oxidative damage to rat erythrocytes by dietary selenium. *J. Nutr.* **102**:689-696.

Rubeska, I., and B. Moldan. (1971). *Atomic absorption Spectrophotometry*. Illiffe Books. Prague.

S

Sakurai, H., and Tsuchiya. K. (1975). A tentative recommendation for maximum daily intake of selenium. *Environ. Physiol. Biochem.* **5**:107-118.

Schafer, P. A. B. a. J. *Sample preparation techniques in voltammetric trace analysis.*

Schingoethe, D. J., Parsons J. G., Ludens F. C., Turker W. L., and Shane K. J. (1978). Vitamin E status of dairy cows fed stored feeds continuously during the summer. *J. Dairy Sci.* **61**:1582-1589

Schmidt, F. J., and J. L. Royer. (1973). *Anal. Letters* **6**,17.

Schrauzer, G. N., and White D. A. (1978). Selenium in human nutrition: dietary intakes and effects of supplementation. *Bioinorg. Chem.* **8**:303-318.

Schroeder, H.A., Frost. D.V., and Balassa. J.J. (1970). Essential trace metals in man: Selenium. *J. Chron. Dis.* **23**:227-243.

Schubert, J.R., Muth, O.H., and Oldfield, J.E., and L.F. Remmert. (1961). Experimental results with selenium in white muscle disease of lambs and calves. *Fed. Proc.* **20**:689-694.

Schwarz, K., and Foltz C. M. (1957). Selenium as an integral part of factor 3 against dietary necrotic liver degeneration. *J. Am. Chem. Soc.* **79**:3292-3293.

Seby, F.; Potin-Gautier, M.; Castetbon, A.; Astruc, M. (1995), *Analusis 23*, 510-515.

Segerson, E. C., Murray F. A., Moxon A. L., Redman D. R., and Conrad H. R. (1977). Selenium and vitamin E: Role in fertilisation of the bovine ova. *J. Dairy Sci.* **60**:1001-1005.

Shamberger, R. J. (1971) Is selenium a teratogen? *Lancet* **2**:1316.

Shamberger R.J., Biochemistry of Selenium (1983) Plenum Press, New York.

Shrift, A. (1969). Aspects of selenium metabolism in higher plants. *Anny. Rev. Plant Physiol.* **20**:475.

Shrift, A. (1973). Metabolism of selenium by plants and microorganisms. P. 763 in Organic Selenium Compounds: Their Chemistry and biology, D.L. Klayman and W.H.H. Gunther, eds. New York: Wiley-Interscience.

Sies, H., Gerstenecker C., Menzel H., and Flohé L. (1972). Oxidation in the NADP system and release of GSSG from hemoglobin-free perfused rat liver during peroxidatic oxidation of glutathione by hydroperoxides. *FEBS Lett.* **27**:171-175.

Sies, H., and Summer K. –H. (1975). Hydroperoxidase-metabolising systems in rat liver. *Eur. J. Biochem.* **57**:503-512.

Smeaton, W. A. (1965) *Chemistry in Britain*, *1*, 353.

Smith, M. I., Westfall B. B., and Stochlman, Jr. E. F. (1937) The elimination of selenium and its distribution in the tissues. *U. S. Public Health Rep.* **52**:1171-1177.

Stowe, H. D. (1980). Effects of copper pretreatment upon toxicity of selenium in ponies. *Am. J. Vet. Res.* **41**:1925.

Stowe, H. D., and Brady P. S. (1978). Effect of copper pretreatment on selenium toxicity in ponies. *Fed. Proc.* **37**:324 (Abstr.).

T

Tabourg, T. (1908), *Ann. Chim. Phys. 15.*

Thompson, K. C., and D. R. Thomerson, (1974). *Analyst* **99**,595.

Thomson, C. D., Burton C. E., and Robinson M. R. (1978a). On supplementing the selenium intake of New Zealanders. 1. Short experiments with large doses of selenite or selenomethionine. *Br. J. Nutr.* **39**: 579.

Thorn, J., Robertson. J., Buss. D. H., and Bunton. N. G. (1978). Trace nutrients. Selenium in British foods. *Br. J. Nutr.* **39**: 391.

Toepfer, E. W.; Boutwell, P. W. (1930), *Ind. Eng. Chem. Anal.Ed* ***2.***

Trinder, N., Hall R. J., and Renton C. P. (1973). The relationship between intake of selenium and vitamin E on the incidence of retained placentae in dairy cows. *Vet. Rec.* **93**:641-645.

Trinder, N., Woodhouse C. D., and Renton C. P. (1969). The effect of vitamin E and selenium on the incidence of retained placentae in dairy cows. *Vet. Rec.* **85**:550-553.

U

U.S. Department of Health, Education, and Welfare. Drinking Water Standards. *Public Health Serv. Publ.* **956**.

U.S. Department of Health, Education, and Welfare, Food, and Drug Administration. (1974). Food additives: Selenium in animal feed. *Fed. Reg.* **39**(5):1355.

U.S. Department of Health, Education, and Welfare, Food, and Drug Administration. (1979). 21 CFR Pt. 573. Food additives permitted in feed and drinking ware of animals: Selenium. *Fed. Reg.* **44**(19):5392.

U.S. Department of Health and Human Services, Food and Drug Administration. (1981a). 21 CFR Pt. 573. Food additives permitted in feed and drinking water of animals: Selenium. *Fed. Reg.* **46**(167):43415.

U.S. Department of Health and Human Services, Food and Drug Administration. (1981b). 21 CFR Pt. 573. Food additives permitted in feed and drinking water of animals: Selenium. *Fed. Reg.* **46**(193):49115.

U.S. Department of Health and Human Services, Food and Drug Administration. (1982). 21 CFR Pt. 573. Food additives permitted in feed and drinking water of animals: Selenium. *Fed. Reg.* **47**(108):24292.

V

Van den Berg. C. M. G. and S.H. Khan. ***Analyst***, 1991, 116, 585-588.

Van Houweling, C. D. (1979) Selenium in animal feeds. *J. Am. Vet. Med. Assoc.* **175**:298-300.

Van Soest, P. J. (1965). Symposium on factors influencing voluntary intake of herbage by ruminants: Voluntary intake in relation to chemical composition and digestibility. *J. Anim. Sci.* **24**:834.

Vega. M., C. M. G. van den Berg. ***Anal. Chem.*** 1997, 69, 874-881.

W

Wallach, J. D. (1978) Cystic fibrosis: A proposal of etiology and pathogenesis. Workshop on Model Systems for the Study of Cystic Fibrosis. Bethesada, Md: National Institutes of Health.

Wei Guang Lan, Ming Keong Wong and Yoke Min Sin, ***Talanta*** 1994, 41, 1, 53-58.

Welch, R. M.; Allaway, W. H. (1972), *Anal. Chem. **44**.*

Welz, B. (1985). *Atomic Absorption Spectrometry*. 2 Ed. VCH Verlagsgesellschaft. Germany.

Whanger, P. D., Pedersen N.D., and Weswig P. H. (1973). Selenium proteins in ovine tissues. II. Spectral properties of a 10,000 molecular weight selenium protein. *Biochem. Biophys. Res. Commun.* **53**:1031-1035.

Whanger, P. D., Weswig P. H, Schumitz J. A., and Oldfield J. E. (1978b). Effects of various methods of selenium administration on white muscle disease, gultathione peroxidase and plasma enzymes activities in sheep. *J. Anima. Sci.* **47**:1157-1166.

Wu, A. S., Oldfield J. E., Shull L. R., and Cheeke P. R. (1979). Specific effect of selenium deficiency on rat sperm. *Biol. Reprod.* **20**:793-798.

Wu, A. S., Oldfield J. E., Whanger P. D., and Weswig P. H. (1973). Effect of selenium, vitamin E, and antioxidants on testicular functions in rats. *Biol. Reprod.* **8**:625-629.

X

Y

Yang, G. Q., Wang S., Zhou R., and Sun S. (1983) Endemic selenium intoxication of man in China. *Am. J. Clin. Nutr.* In press.

Yarrington, J. T., Whitehair C. K., and Corwin R. M. (1973). Vitamin E-selenium deficiency and its influence on avain malarial infection in the duck. *J. Nutr.* **103**:231-241.

Z